

GEOLOGICA ULTRAIECTINA

Mededelingen van de
Faculteit Aardwetenschappen
Universiteit Utrecht

No. 246

Organic geochemical reconstruction of
palaeo-environmental conditions during
the deposition of Pliocene sapropels in
the eastern Mediterranean Sea



Diana Menzel

GEOLOGICA ULTRAIECTINA

Mededelingen van de
Faculteit Aardwetenschappen
Universiteit Utrecht

No. 246

**Organic geochemical reconstruction of
palaeo-environmental conditions during
the deposition of Pliocene sapropels in
the eastern Mediterranean Sea**

Diana Menzel

**Organic geochemical reconstruction of
palaeo-environmental conditions during
the deposition of Pliocene sapropels in
the eastern Mediterranean Sea**

Organisch geochemische reconstructie van
palaeomilieu condities tijdens de afzetting van Pliocene
sapropelen in de oostelijke Middellandse Zee

(met een samenvatting in het Nederlands)

Organisch geochemische Rekonstruktion friiherer
Umweltbedingungen wahrend der Ablagerung von Pliocene
Sapropelen im 6stlichen Mittelmeer

(mit einer Zusammenfassung in deutscher Sprache)

Proefschrift

ter verkrijging van de graad van doctor
aan de Universiteit Utrecht
op gezag van de Rector Magnificus, Prof. Dr. W.H. Gispen,
ingevolge het besluit van het College voor Promoties
in het openbaar te verdedigen
op vrijdag 1 oktober 2004 des middags te 12.45 uur

door

Diana Menzel

geboren op 2 april 1968 te Woldegk, Duitsland

Promotoren: Prof. Dr. Ir. I.S. Sinninghe Damste
Department of Marine Biogeochemistry and Toxicology
Royal Netherlands Institute for Sea Research
Den Burg, Texel, The Netherlands

Prof. Dr. J.W. de Leeuw
Royal Netherlands Institute for Sea Research
Den Burg, Texel, The Netherlands

Co-promotor: Dr. P.F. van Bergen
Shell Global Solutions International
Amsterdam, The Netherlands

Cover illustration: the Mediterranean and Black Sea, obtained from CIBRA at http://cibra.unipv.it/cibra_edu_mediterraneo_uk.html.

The research described in this thesis was carried out at the Department of Geochemistry, Faculty of Geosciences, Utrecht University, Budapestlaan 4, PO Box 80021, 3508 TA Utrecht, The Netherlands, and the Department of Marine Biogeochemistry and Toxicology, Royal Netherlands Institute for Sea Research (NIOZ), Landsdiep 4, 1790 AB Den Burg, Texel, The Netherlands.

This work was financially supported by the Institute of Paleoenvironments and Paleoclimate Utrecht (IPPU).

Printer: Grafisch bedrijfFebodruk BV, Enschede, The Netherlands

ISBN 90-5744-107-1

Für meinen Vater

Table of contents

Chapter 1	General introduction	1
Chapter 2	Development of photic zone euxinia in the eastern Mediterranean Basin during deposition of Pliocene sapropels	13
Chapter 3	A newly discovered fossil carotenoid in Pliocene sapropels of the eastern Mediterranean Sea	25
Chapter 4	Reconstruction of changes in export productivity during Pliocene sapropel deposition: a biomarker approach	33
Chapter 5	Membrane tetraether lipids of planktonic Crenarchaeota in Pliocene sapropels of the eastern Mediterranean Sea	49
Chapter 6	Higher plant vegetation changes during Pliocene sapropel formation	65
Chapter 7	The molecular composition of kerogen in Pliocene Mediterranean sapropels and associated homogeneous calcareous oozes	79
References		99
Summary		117
Samenvatting in het Nederlands (summary in Dutch)		121
Zusammenfassung (summary in German)		125
Dankwoord (acknowledgements)		129
Curriculum Vitae		131

Chapter 1

General introduction

The modern Mediterranean Sea: climate and general circulation

The Mediterranean is a region of transition between the sub-oceanic, cool temperate zone of Europe, and the high-pressure, arid subtropics of North Africa straddling the pressure systems of the Atlantic and the monsoon climates of the Indian subcontinent and East Africa. The Mediterranean Sea is a semi-enclosed sea and an almost isolated oceanic system. The Mediterranean climate is basically characterized by hot dry summers and mild wet winters, accompanied by strong winds (Allen, 2001). Today, evaporation in the eastern basin exceeds precipitation and river-runoff. The negative water balance is compensated by the inflow of Atlantic waters through the Straits of Gibraltar. Atlantic surface waters flowing eastwards through the Mediterranean are warmed by solar radiation and the resulting evaporation causes a steady increase in salinity and density. As a result, deep water formation and therefore oxygenation in the Mediterranean takes place in the Gulf of Lion (northwestern basin) and in the Adriatic and Aegean Sea (northeastern basin). This occurs when the surface water cooling during winter results in highest densities. In the easternmost Mediterranean the high salinities combined with the winter cooling results in the formation of Levantine Intermediate Water (LIW) between (150/200 m) and 600 m, which flows westwards into the western Mediterranean and ultimately leaves through the Straits of Gibraltar (Wiist, 1961) (Fig. 1.1).

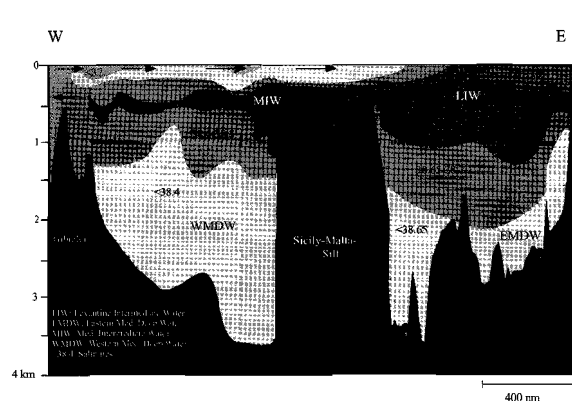


Figure 1.1 Hydrographic section through the Mediterranean Sea (after Wiist, 1961 and Vergnaud-Grazzini *et al.*, 1977) giving the major water masses and their salinities. MIW = Mediterranean Intermediate Water, LIW = Levantine Intermediate Water, EMDW = Eastern Mediterranean Deep Water, WMDW = Western Mediterranean Deep Water.

The formation of the Eastern Mediterranean Deep Water (EMDW), originating from the Adriatic and Aegean Sea, the Western Mediterranean Deep Water (WMDW), originating

from the Gulf of Lion, and primarily Levantine Intermediate Water (UW) ensures that the basins remain well ventilated. This anti-estuarine circulation pattern makes the Mediterranean a nutrient desert: it receives nutrient-depleted surface waters and the nutrients received from rivers to the Atlantic are exported with its deeper water. This has a strong negative influence on the biological productivity in the Mediterranean resulting in deposition of sediments poor in organic matter (OM) $\ll 0.5\%$ organic carbon) (Fig. 1.2).

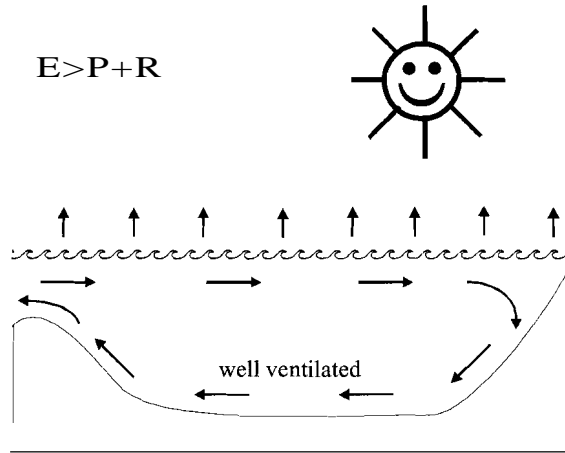


Figure 1.2 Anti-estuarine circulation pattern of the modern Mediterranean Sea. E = evaporation, P = precipitation, R = river runoff.

Climate change in the Mediterranean region and its impact on hydrography

Eccentricity, obliquity and precession influence the incoming solar radiation to the Earth and are thus important factors affecting global climate. Together they are responsible for 'Milankovitch cycles' (Fig. 1.3).

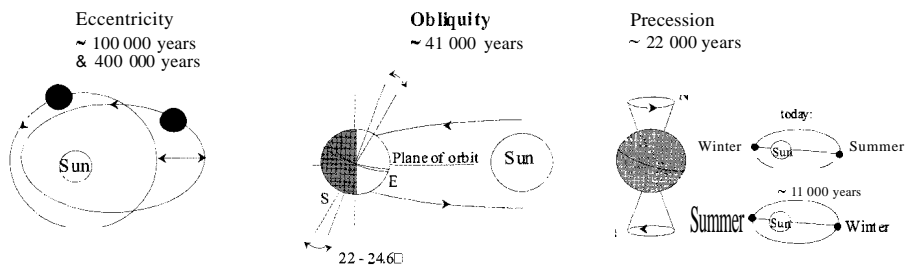


Figure 1.3 The Milankovitch cycles which influence global climate: Eccentricity, Obliquity and Precession.

The *eccentricity* cycle is caused by variations in the shape of the earth's orbit around the sun. The shape of the Earth's orbit changes between maximum eccentricity (strong ellipse) and minimum eccentricity (near a circular orbit) with periods of 100,000 and 400,000 years. The gradual change in the angle of the Earth's rotation axis relative to the perpendicular of the plane of the Earth's orbit is called *obliquity*. This angle changes from 22.5 to 24.5 degrees and back over a period of 41,000 years. The obliquity cycle predominantly affects the distribution of sunlight between the high polar latitudes and the tropics. The *precession* cycle is related to the wobble in the Earth's rotational axis relative to the plane of the Earth's orbit around the sun. The precession cycle manifests itself in the insolation onto the Earth's surface in a period of 21,000 years governing the seasonal distribution of insolation. its impact depends on the degree of eccentricity of the orbit. Whereas in a perfect circular orbit the precession cycle would have no impact, maximum eccentricity results in maximum impact of the precession cycle. During precession minima, perihelion (i.e. when the Earth is closest to the sun) falls within Northern Hemisphere summer causing maximum insolation. Consequently, aphelion (i.e. when the Earth is farthest from the sun) falls in winter, reducing insolation. This results in the seasonal insolation contrast to be considerably higher during a precession minimum.

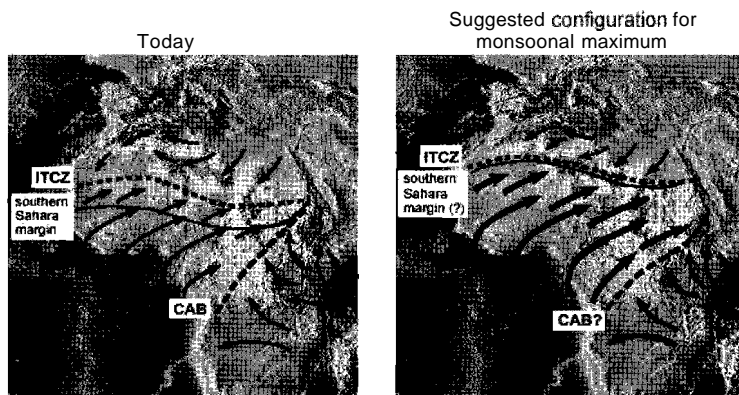


Figure 1.4 Rough location of the Intertropical Convergence Zone (ITCZ), the Congo Air Boundary (CAB), and the southern margin of the Sahara Dessert, for the present-day and in an artist's interpretation for the monsoonal maximum for the time around the boreal summer, when the sun reaches its northernmost position (www.soes.soton.ac.uk/staff/ejr/ejrhome.htm).

Higher summer insolation enhances atmospheric pressure difference between the land and sea by the large temperature contrast between the relatively cold ocean and the relatively warm continent. As a consequence, the monsoon inflow into low-latitude Africa, which has a westerly component is amplified and this results in enhanced transport of moisture from the Atlantic to the African continent. In addition, the Sahara interior heats up faster leading to a northwards shift of the Intertropical Convergence Zone (ITCZ). In addition, a periodical northwards penetration of the African summer monsoon front (northern boundary is

represented by the ITCZ) into the north and central Saharan watershed irrespective to the extent of northwards ITCZ penetration, is related to eccentricity-, obliquity- and precession controlled insolation maxima causing enhanced precipitation rates over the northern part of the African continent (Rohling *et al.*, 2002; Larrasoana *et al.*, 2003) (Fig. 1.4). The substantially increased rainfall results in enhanced soil moisture and vegetation cover that inhibit dust production and increase the delivery of fresh water into the Mediterranean Sea. The river Nile is responsible for the largest part of the increased run-off from the North African continent affecting in particular the easternmost part of the Mediterranean Sea (e.g. Adamson *et al.*, 1980; Rossignol-Strick *et al.*, 1982; Rossignol-Strick, 1985; Rohling, 1991, 1994). However, at many places on the North-African continent, large lakes developed and impressive fossil river systems of the northern African continent also playing an important role in freshwater discharges into the Mediterranean during times of organic carbon rich sediments (Rohling *et al.*, 2002; Larrasoana *et al.*, 2003). This enhanced freshwater supply influenced the Mediterranean oceanography to a large extent. The more humid climate conditions inhibited the salinity-dependent formation of LIW in the Cyprus-Rhodes area. Under these conditions deep-water formation relied on winter cooling only. Because of the reduced salinity/density of newly formed deep water, this water could no longer ventilate the deeper parts of the basin (e.g. Cita *et al.*, 1977, 1982; Calvert, 1983, Mangini and Schlosser, 1983). As a result, the eastern Mediterranean became 'stagnant' downwards from 300/400 m depth. After some time bottom waters became oxygen-depleted and OM-rich sediments ("sapropels") were deposited (Fig. 1.5).

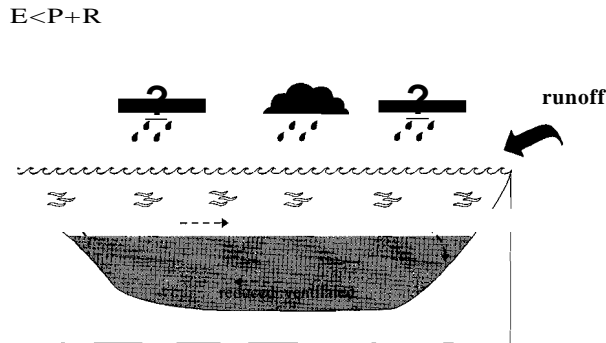


Figure 1.5 Illustration of the sluggish anti-estuarine circulation pattern during sapropel deposition in the eastern Mediterranean Basin. E = evaporation, P = precipitation, R = river runoff.

Sapropel formation

Sapropels are defined as discrete layers, greater than 1 cm in thickness, set in open pelagic sediment and containing greater than 2% organic carbon by weight (Kidd *et al.*, 1978). They contain more than average amounts of pyrite and benthic fauna indicative of low bottom water oxygen concentrations (sometimes benthic fauna is completely absent) and

notably high concentrations of elements such as Sand Ba (e.g. Kullenberg, 1952; Olausson, 1961; Vergnaud-Grazzini *et al.*, 1977). Initially, in 1947/48 sapropels were recovered in abundance mainly from the eastern Mediterranean Sea in 1947/48 (Kullenberg, 1952). These showed a prominent cyclic bedding characterized by brown to blackish coloured organic-rich sapropels from the Neogene to the Quaternary (e.g. Cita *et al.*, 1982; Vergnaud-Grazzini, 1985; Rohling, 1994). Drilling of deep-water post Messinian sedimentary sequences in the Mediterranean Sea has shown the occurrence of organic-rich sapropels and sapropel-like sediments extending from the Levantine Basin westwards into the Alboran basin (Rullkotter *et al.*, 1995, Murat, 1999). The large differences in organic carbon content of sapropels recovered in the eastern and western Mediterranean Sea can be explained by ventilation of oxygen-rich Atlantic waters via the Straits of Gibraltar into the western Mediterranean basin. In the eastern Mediterranean Sea and the Tyrrhenian Sea (easternmost part of the western Mediterranean Sea), sapropel deposition began in the early Pliocene (e.g. Olausson, 1961; Kidd *et al.*, 1978; Emeis *et al.*, 1991). In the Alboran Sea (westernmost Mediterranean Sea) and therefore basin-wide onset of sapropel formation occurred later, in the early Pleistocene (Bouloubassi *et al.*, 1999). Very organic-rich sapropels were deposited during the middle Pliocene, and sapropel formation became less frequent with the onset of glaciations in the Northern Hemisphere (ca. 2.4 Ma). These sapropels layers range in total organic carbon content between 2-30% TOC (Emeis *et al.*, 1996) and are intercalated by homogeneous calcareous ooze containing < 0.1 % TOC (e.g. Calvert, 1983; Calvert and Pedersen, 1992).

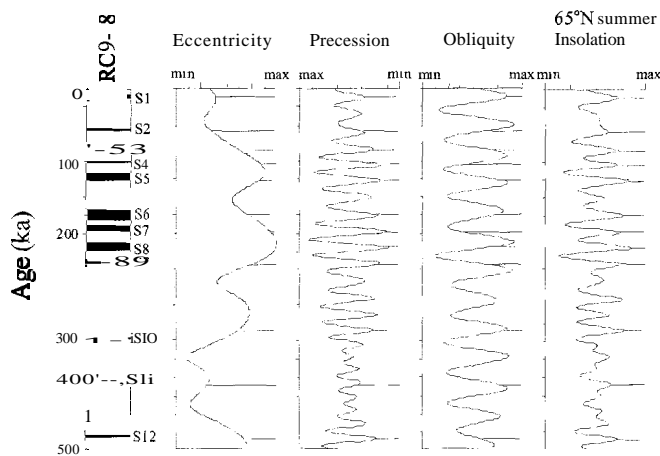


Figure 1.6 Astronomical calibration of late Pleistocene sapropels to astronomical curves of eccentricity, obliquity, precession and isolation (65°N summer insolation) (from RiiGen, 1991).

Integrated stratigraphic studies have convincingly demonstrated that these sedimentary cycles reflect astronomically induced variations in the regional Mediterranean climate. These cycles are controlled by wet-dry oscillations, whereby the sapropels are related to precession minima, i.e. insolation maxima (Fig. 1.6) (e.g. Rossignol-Strick *et al.*, 1982; Rossignol-Strick, 1985; Prell and Kutzbach, 1987; Hilgen, 1991; Rohling, 1991).

These resulted in a relatively humid part of the climate cycle as indicated by lower aeolian (Saharan) dust supply, i.e. decreased Ti/Al ratios (e.g. Nijenhuis and de Lange, 2000; Wehausen and Brumsack, 2000). Further evidence is provided from changes in clay minerals, which showed cyclic variations between two groups of clay minerals. Palyorskite and kaolinite showed maximum abundance at times of aridity on the African continent, enabling them to be transported as wind-blown dust. Smectite dominates at periods of abundant rainfall, which coincides with sapropel formation (e.g. Foucault and Melieres, 2000). Enhanced fresh water input would have diluted surface waters leading to a more sluggish (but not necessarily ceased) circulation of the intermediate (Mediterranean Intermediate Water) and deeper waters associated with high amounts of nutrients into the Mediterranean Basin (Boyle and Lea, 1989).

Based on the above, two models have been proposed to explain the enrichment in organic carbon during sapropel events. In general, two types of models have been proposed or the combination of both: (1) a Stagnation Model that explains the elevated TOC levels of sapropels by enhanced OM preservation under oxygen-deficient deep-water conditions (e.g. Demaison and Moore, 1980); (2) a Productivity Model that links the occurrence of sapropels to increased marine biological production in the photic zone (e.g. Calvert, 1983, Pedersen and Calvert, 1990, Calvert and Pedersen, 1992). The Stagnation Model explains anoxic bottom conditions by increasing density stratification of the water column caused by a strong low-salinity surface layer which ultimately inhibits convective overturning and ventilation of the deeper water column (e.g. Shaw and Evans, 1984). A primary cause of sapropel deposition resulting from increase in biological productivity within the photic zone as evidenced by the recognition of OM fluxes to the sea floor in today's eastern Mediterranean Sea, would not be sufficient to produce sapropels, even if extensive water column stratification and complete bottom-water anoxia would occur (e.g. Calvert, 1983; Lourens *et al.*, 1992; van Os *et al.*, 1994). A third model combining both, increased productivity and decreased deep-water formation has also been proposed (Rohling and Gieskes, 1989, Rohling, 1991). In this model, shoaling of the pycnocline to a depth within the euphotic layer would lead to increased nutrient availability to the lower euphotic layer. This would enable the development of a deep chlorophyll maximum below the pycnocline and a concomitant increase in the downwards flux of OM from the euphotic zone (export production). According to this model, shoaling of the pycnocline could have occurred in response to an enhanced freshwater flux to the surface layer of the Mediterranean in conjunction with a continuous anti-estuarine circulation pattern.

Biomarkers as palaeoenvironmental proxies

Depending on the depositional conditions in the environment only 0.1 to 1% of biologically derived OM is preserved in most present-day oceanic settings (Calvert and Pedersen, 1992). The composition of sedimentary OM is substantially different from its precursor, biomass, because major differences exist in the rate of biodegradation between biomolecules. Bacteria mineralize polysaccharides and proteins, which represent the bulk of

biomass in most organisms, very efficiently during diagenetic processes and are thus selectively removed during transport through the water column or in top layers of sediments. As a consequence, other biochemicals, such as certain low- and high-molecular weight compounds occurring in cell walls and membranes, and aromatic biomacromolecules, such as lignin, are selectively preserved and thus enhanced in sedimentary OM (Tegelaar *et al.*, 1989).

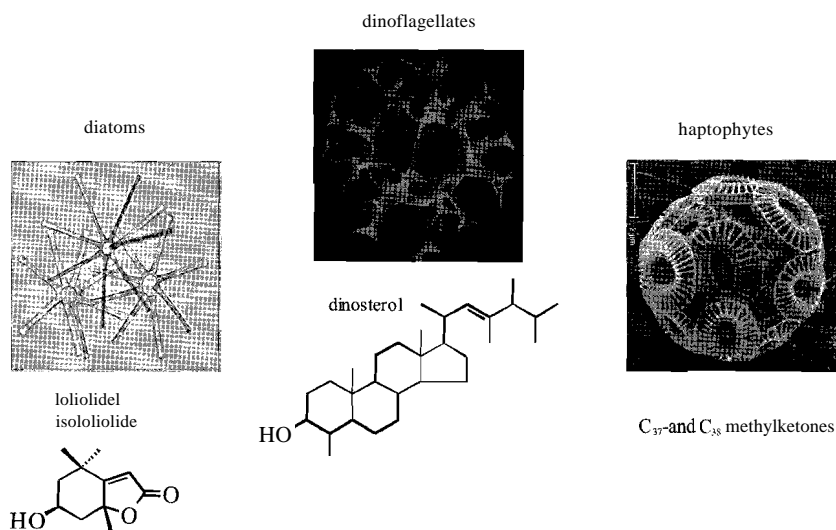


Figure 1.7 Lipid biomarker of different marine phytoplankton classes.

Organic compounds whose basic carbon skeleton suggests an unambiguous link with known, contemporary biochemicals are defined as "biological markers" or "biomarkers" although terms as "molecular fossils" are also used (Eglinton *et al.*, 1964; Eglinton and Calvin, 1967; Mackenzie, 1984) (see Fig. 1.7 for some typical examples). Molecular fossils, such as lipid biomarkers, in sediments can provide information on the presence of specific organisms and, therefore, supply valuable insights in palaeoenvironmental conditions during deposition (e.g. de Leeuw *et al.*, 1995). In Pliocene/Pleistocene sapropels of the Mediterranean Sea different lipid biomarker studies were applied to reconstruct sea surface temperature (SST). These studies used the $U_{37}^{K'}$ index of the di- and tri-unsaturated C₃₇ methylketones (e.g. Emeis *et al.*, 1998; Rinna *et al.*, 2002; Bouloubassi *et al.*, 1999) derived from marine haptophyte algae (Brassell *et al.*, 1986; Volkman *et al.*, 1980; Marlowe *et al.*, 1984a; Marlowe *et al.*, 1984b). Another biomarker is Isorenieratene. This is a specific aromatic carotenoid of anaerobic, photolithotrophic green sulphur bacteria requiring sulfide and light. Thus, this biomarker can indicate the shallowing of the chemocline into the photic zone (e.g. Repeta, 1993, Sinninghe Damste *et al.*, 1993a) (Fig. 1.8). The presence of diagenetic derivatives of isorenieratene in Pliocene sapropels revealed the first evidence of basin-wide water column euxinia over substantial periods in the eastern Mediterranean Sea (Passier *et al.*, 1999a). Other biomarkers, specific for marine algae, were analysed to indicate

the floral diversity during deposition of Pliocene sapropels (e.g. Bosch *et al.*, 1998; Bouloubassi *et al.*, 1999; Rinna *et al.*, 2002). For example, haptophyte-derived long-chain methylketones and C₂₈ - C₃₂ alkanediols- and keto-ols, reflecting eustigmatophytes were reported (Volkman *et al.*, 1992). Loliolides and isololiolides that are anoxic degradation products of fucoxanthin, the major carotenoid found in diatoms (Klok *et al.*, 1984) and to some extent in dinoflagellates and haptophytes (Jeffrey and Vesk, 1997), and dinosterol, reflecting dinoflagellates, also occur in sapropels. Changes in terrestrial input during sapropel deposition were studied using long-chain fatty acids, alcohols and alkanes (Rinna *et al.*, 2002), biomarkers derived from higher land plant cuticular waxes (e.g. Eglinton and Hamilton, 1967).

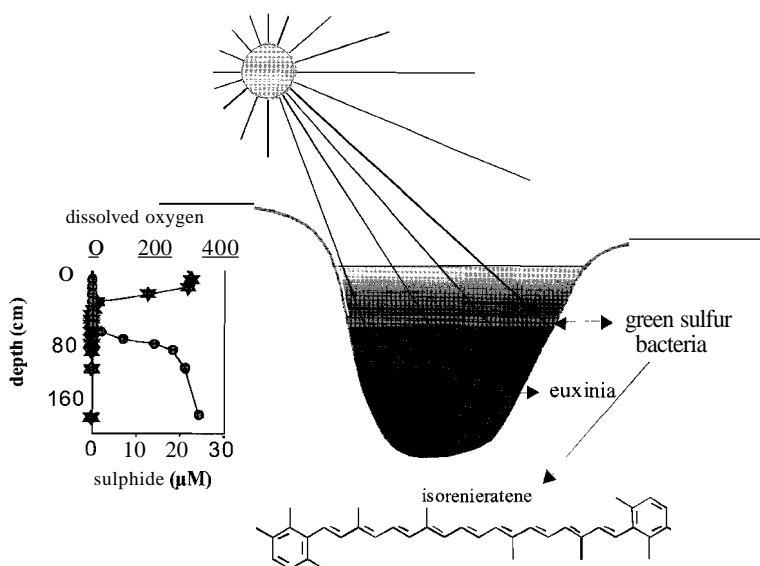


Figure 1.8 Illustration of photic zone euxinia, i.e. shoaling of the chemocline up to the photic zone of the water column.

Scope and framework of this thesis

Ocean Drilling Program (ODP) Leg 160 covered a transect of drill sites in the eastern Mediterranean Sea during March-April 1995 to investigate the tectonic and palaeoceanographic history of the area. Astronomical tuning of precession-controlled sapropel cycles recognized in the land-based sections Vrica and Singa (Italy), correspond chronically with the marine sedimentary records (Lourens *et al.*, 1996). Sapropels recovered from three eastern Mediterranean Sea drill sites [ODP Sites 964D-IOH-1 (110-103 cm), 969E-6H-6 (40-26 cm) and 967C-8H-4 (130-114 cm) (Fig. 1.9)] could unambiguously be correlated to each other and to a sapropel event of 2.943 Ma in the land-based Vrica and Singa sections (Lourens *et al.*, 1996). These late Pliocene sapropels are particularly suitable

Chapter 2 reveals that photic zone euxinia (i.e. the presence of free sulfide present in the photic zone, typically shallower than 100 m) occurred widespread over the entire eastern Mediterranean basin during Pliocene sapropel deposition. This finding is based on the presence of isorenieratene, a carotenoid biosynthesized by anaerobic, photolithotrophic-living Chlorobiaceae, in the sapropels. This carotenoid first appeared at Site 967, closest located to the river Nile and extended, with higher abundances, towards the western Site 964. This might be related to the input of fresh water and associated nutrients from the river Nile, triggering primary productivity in the Levantine basin. The subsequently enhanced export production and thus oxygen depletion in the deep water resulted in widespread anoxia. Spatial and temporal variations in isorenieratene abundances probably reflected fluctuations of the chemocline in the water column during sapropel formation. In **Chapter 3**, an "unknown purple carotenoid" is studied which is also abundant in these Pliocene sapropels. Accumulation rates of this "unknown purple carotenoid" showed a similar profile as found for isorenieratene. Two different candidates of carotenoids are considered (i) spheroidenone, a carotenoid related to various purple non-sulphur bacteria and (ii) thiothece-474, a minor carotenoid produced by the purple sulphur bacterium *Thiocystis gelatinosa*. In case thiothece-474 is the main source, the presence of this carotenoid would indicate severe water column euxinia, as purple sulphur bacteria need more light than Chlorobiaceae. **Chapter 4** shows changes in the relative distribution of the major phytoplankton classes using marine biomarkers of the haptophytes, diatoms, dinoflagellates and eustigmatophytes during Pliocene sapropel formation. At Site 967, diatoms increased in abundance relative to other phytoplankton classes at the onset of sapropel formation, indicating the enhanced supply of nutrients from the river Nile, which is in agreement with the early development of photic zone euxinia first in the most eastern Mediterranean Sea (Chapter 2). Biomarker contents differed substantially between the homogeneous intervals and sapropels, resulting partly from different redox conditions during deposition. Whereas terrestrial biomarkers, like long-chain n-alkanes and n-alcohols dominated in the homogeneous calcareous intervals, marine biomarkers were the major compounds in the sapropels. Enhanced export productivity resulted in increased export production and consequently led to oxygen depletion in the pore waters and water column. In **Chapter 5**, a newly established sea surface temperature (SST) proxy, called TEX₈₆, based on membrane lipids derived from planktonic crenarchaeota, was compared with values obtained from the most common SST proxy in palaeoceanography, the $U_{37}^{K'}$ - based on alkenones. Whereas the $U_{37}^{K'}$ -based SST estimates in the homogeneous intervals and sapropels, remained almost the same, the SST estimates showed a substantial cooling of 10-12°C during Pliocene sapropel formation. Similarities with respect to low TEX₈₆-based SST estimates were found in the contemporary euxinic Black Sea. The large drop in TEX₈₆-based SST in all sapropels is associated with the shoaling of the chemocline resulting in planktonic crenarchaeota occupying a different ecological niche. In **Chapter 6**, long-chain n-alkanes (C₂₇-C₃₃) were analysed for their stable carbon isotopic composition. Since they are derived from higher land plants, they record the effect of changes in aridity/humidity on the vegetation of the North African continent. Based on a two-end member mixing model the contribution of C₄ plants to the wax lipids increased up to 20% in the sapropels at all sites. This unexpected shift from C₃ to C₄ plant vegetation is

resulting from an increase in the overall plant coverage of the Mediterranean borderlands as response of the wetter climate during sapropel deposition leading to the change of formerly barren desert areas into C₄ grass-dominated savannahs. **Chapter 7** focuses on the differences in composition of the macromolecular OM using Rock-Eval and analytical pyrolysis in combination with palynology. The kerogen pyrolysates of homogeneous intervals consisted of a mixture of resistant marine and terrestrial macromolecular OM, which resisted aerobic decomposition during their deposition. The kerogen pyrolysates of the sapropels originated predominantly from marine macromolecular OM with only a minor terrestrial contribution, resulting from enhanced preservation conditions leading to increased preservation of labile OM in the sapropels.

Chapter 2

Development of photic zone euxinia in the eastern Mediterranean Basin during deposition of Pliocene sapropels

Diana Menzel, Ellen C. Hopmans, Pim F. van Bergen, Jan W. de Leeuw and Jaap S. Sinninghe Damste

Published in *Marine Geology* 189 (2002) 215-226

ABSTRACT

Carotenoids were analysed in ca. 1-cm thick subsamples of three laterally time-equivalent sapropels from a west-east transect of the eastern Mediterranean basin to study euxinic periods during Pliocene sapropel formation. The amount of intact isorenieratene (summed *all-trans* and *cis* isomers), ranged from non-detectable at the base and top of a sapropel up to 140 µg/g sediment in the central parts. Isorenieratene accumulation rates at the central and western site are remarkably similar and increase sharply to levels of up to 3.0 mg m⁻² yr⁻¹ in the central part of the sapropel and then drop to low levels. This pattern indicates an expansion of euxinic conditions reaching into the photic zone, followed by deepening of the chemocline during deposition of this Pliocene sapropel. The sapropel from the easternmost site of the basin, which contains less organic carbon, shows much lower isorenieratene accumulation rates and even absence of isorenieratene in the central part of the sapropel. *BalAl* ratios indicate enhanced palaeoproductivity during sapropel formation, supporting previously proposed models, according to which increased productivity is the driving force for the generation of euxinic conditions.

INTRODUCTION

Organic-matter-rich sediments, although atypical, are nonetheless widespread in marine environments ranging in age from the Devonian to the present day. This type of sediment was formed in a wide variety of depositional settings and under different palaeoenvironmental conditions (e.g. Arthur and Sageman, 1994). However, the precise processes that have caused the high organic matter burial are often unclear. Cores taken during Ocean Drilling Program (ODP) Leg 160 at three sites (Fig. 2.1) in the eastern Mediterranean basin revealed episodic, laminated intervals with high organic carbon contents ($C_{org} > 2\%$ TOC), so-called sapropels (Erneis *et al.*, 1996). These include Pliocene showing variations in organic matter deposition strongly correlated to the precession cyclicity of the Earth's orbit (e.g. Rossignol-Strick, 1983, 1995; Lourens *et al.*, 1996). Some of these sapropels have extraordinarily high amounts of organic matter ($C_{org} > 26\%$ TOC;

Emeis *et al.*, 1996). Scientific controversy remains with regard to the mechanisms and factors governing sapropel formation; the two main causes being either climate-related enhanced organic matter productivity and/or increased preservation due to oxygen depletion of the bottom waters (e.g. Canfield, 1994; Bouloubassi *et al.*, 1999; Calvert and Fontugne, 2001). Previous geochemical studies explained the formation of sapropels by climate-induced, large-scale fluvial input by the Nile river causing water column stratification and, consequently oxygen depletion in the water column (e.g. Rossignol-Strick *et al.*, 1982; Rossignol-Strick, 1995). Nijenhuis *et al.* (1999, 2000) shed new light on the deep-water circulation pattern based on trace metal enrichments and K/Al and Mg/Al ratios indicating that bottom water currents were not restricted during Pliocene sapropel formation. Primary productivity appears an essential factor based on high barium contents in the sapropels supporting an association with enhanced bioproductivity during these episodes (e.g. Wehausen and Brumsack, 1999; Nijenhuis and de Lange, 2000).

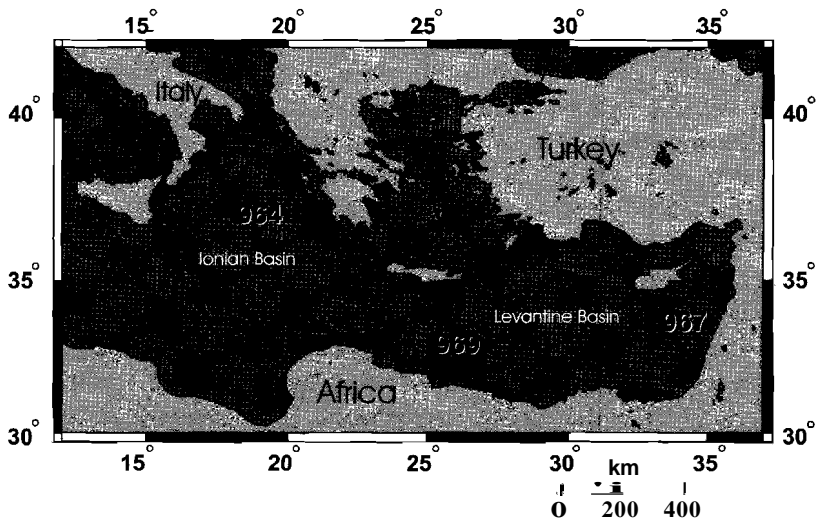


Figure 2.1 Map of the eastern Mediterranean showing the locations of the ODP drilling Sites 964, 969 and 967 (after Emeis *et al.*, 1996).

Recent studies on individual samples of Pliocene sapropels revealed evidence of photic zone euxinia, based on the presence of isorenieratene derivatives (Bosch *et al.*, 1998; Passier *et al.*, 1999a). Isorenieratene is the characteristic pigment biosynthesised by anaerobic, photolithotrophic Chlorobiaceae (Liaaen-Jensen, 1978). These green sulphur bacteria live at the chemocline performing anoxygenic photosynthesis requiring sulphide and light. Thus, the presence of isorenieratene in sediments indicates the past penetration of the sulphide-containing bottom water into the photic zone.

At present, the stratified, euxinic, Black Sea has a H_2S chemocline at a depth of 90-150 m (Repeta *et al.*, 1989), where the obligate photoanaerobes grow under very low light conditions (e.g. $<0.5 \mu E$; Takahashi and Ichimura, 1970; Bergstein *et al.*, 1979; Overmann *et*

al., 1992). Variations in isorenieratene contents were reported to be due to seasonal and interannual depth fluctuations of the chemocline, observed in Holocene sediments (Repeta, 1993; Sinninghe Damste *et al.*, 1993a). Chemocline oscillations are explained by temporal changes in the balance of riverine and Mediterranean inflow to the basin, which can have a significant impact on the intensity of anoxygenic phototrophic activity (Bryantsev *et al.*, 1988; Murray, 1991).

In this paper we report isorenieratene contents in three lateral time-equivalent Pliocene sapropels (2.943 Ma; Lourens *et al.*, 1996) of the eastern Mediterranean basin using liquid chromatography-mass spectrometry (LC-MS) to obtain temporal and spatial insights into the development of photic zone euxinia throughout the basin. Our data indicate permanent photic zone euxinia at the central and western site during sapropel deposition. In contrast, the eastern site shows a deepening of the chemocline at time of maximum organic carbon burial probably caused by the strong increase of the discharge of fresh, less dense water of the Nile during the period of maximum humidity of the Mediterranean climate.

MATERIAL AND METHODS

Sample description

Core samples were taken during ODP Leg 160 in the eastern Mediterranean basin. Three time-equivalent sapropels (2.943 Ma; Lourens *et al.*, 1996) were sub-sampled from cores obtained at Sites 964 (Ionian Basin), 969 (Mediterranean Ridge) and 967 (Eratosthenes Seamount; Fig. 2.1). Astronomical time scale calibrations of Mediterranean land sections have been performed on Pliocene sediments (Lourens *et al.*, 1996). Correlation of the sapropel layers in these land sections with the distribution of sapropels in the ODP cores at Sites 964, 969 and 967 revealed unambiguously that the three investigated sapropels represent the same sapropel event (pers. commun. Lourens *et al.*, 1997; Passier *et al.*, 1999a; Nijenhuis and de Lange, 2000). Total organic carbon (TOC) and trace metal contents were reported previously and showed distinct differences between these sapropels (Nijenhuis *et al.*, 1998).

Extraction and fractionation

Freeze-dried and ground sediment samples of 0.1 to 3 g were ultrasonically extracted with acetone (3x, 3 min) to optimise carotenoid yield. Samples were centrifuged at 3000 rpm for 5 min. The supernatants were decanted, combined and concentrated using rotary vacuum evaporation. The extract was subsequently dried under a gentle flow of nitrogen. This residue was re-dissolved in dichloromethane and applied to a silica column, where isorenieratene and other non-polar carotenoids were subsequently eluted with dichloromethane.

High performance liquid chromatography-mass spectrometry (LC-MS)

Carotenoid fractions (Fig. 2.2) were analysed on a HP 1100 series LC-MS instrument equipped with an auto-injector, photodiode array detector and mass detector. Separation was achieved on a HP XDB-C 18 column (2.1 x 120 mm, 5 μ m) maintained at 30°C, with a

gradient from methanol/water (4:1, v/v) to acetone/methanol/water (19:1:1, v/v/v) in 50 min. The flow rate was 60 ml/min. Detection was achieved by in-line UV-detection and atmospheric pressure positive ion chemical ionisation mass spectrometry (APCI-MS) of the eluent. Conditions for APCI-MS were as follows: nebuliser pressure was 60 psi, vaporiser temperature was 325°C, drying gas (N₂) was delivered at 7 l/min at 350°C, capillary voltage was -3 kV and the corona discharge was set at 6 μA. Compounds were identified based on their retention times, UV-spectra (250-750 nm) and APCI-mass spectra (*m/z* 100-1000). Isorenieratene was quantified based on UV response by comparing the peak area at 454 nm to the peak area at 454 nm of known amounts of an authentic B-carotene standard (Aldrich). Isorenieratene and B-carotene have identical UV spectra and extinction coefficients (Britton, 1995) allowing B-carotene to be used as an external standard for isorenieratene.

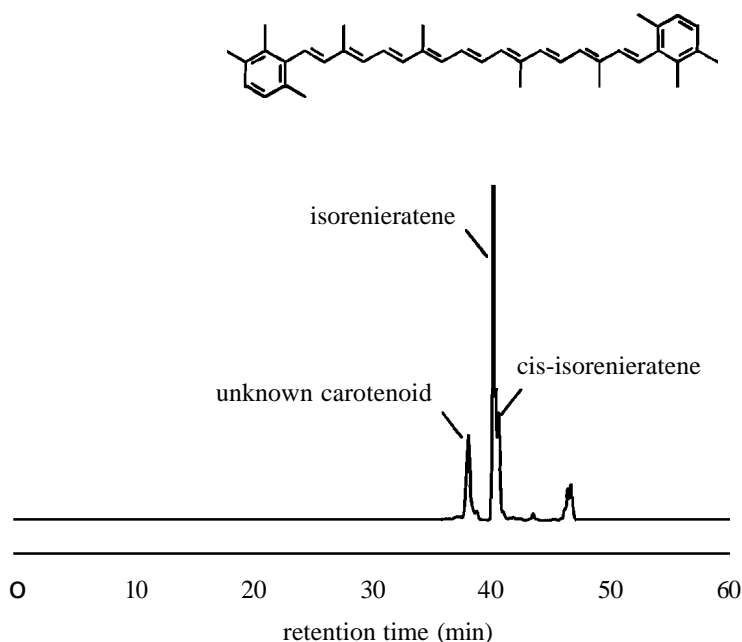


Figure 2.2 UV chromatogram at 454 nm of the isorenieratene containing fraction of 967-CH8-4, 118.5-120 em.

RESULTS

Isorenieratene contents varied within and between sapropels (Table 2.1; Fig. 2.3A-C). The isorenieratene profile of Site 964 generally followed the total organic carbon (TOC) profile through the complete sapropel with the highest content of isorenieratene (140 μg/g) being measured in the central part of the sapropel (Fig. 2.3A). Isorenieratene contents at Site 969 (Fig. 2.3B) showed a profile similar to that of Site 964. The highest content of ca. 100 μg/g was measured close to the central part of the sapropel. In contrast, Site 967 showed a

different isorenieratene content profile. Isorenieratene was absent in the sapropel centre (Fig. 2.3C) and the maximum content of 17.5 $\mu\text{g/g}$ occurred at the base of the sapropel. Contents of isorenieratene measured in Holocene sediments of the world's largest stratified anoxic basin, the Black Sea ranged from non-detectable to $>70 \mu\text{g/gdw}$ (Repeta, 1993).

Table 2.1 Subsamples of the ODP site, core sample and interval with TOC content and isorenieratene concentration.

ODP 964D-IOH-1 interval				ODP 969E-6H-6 interval				ODP 967C-8H-4 interval			
(em)	(%)*	($\mu\text{g/g}$ sediment)	($\mu\text{g/g}$ TOC)	(em)	(%)*	($\mu\text{g/g}$ sediment)	($\mu\text{g/g}$ TOC)	(em)	(%)*	($\mu\text{g/g}$ sediment)	($\mu\text{g/g}$ TOC)
103.5-104	10.1	16.0	158.8	23-26	0.8	0.2	30.7	111-114	0.2	0	5.9
104.5-105	18.4	97.9	531.8	26-27	3.7	11.7	319.1	114-115	1.4	0.3	19.0
105.5-106	16.4	138.6	842.5	27-28	6.1	15.5	254.3	115-116.5	3.3	0.6	18.1
106.5-107	24.9	100.3	402.1	29-30	11.5	8.4	73.5	116.5-117.5	4.1	1.3	31.1
107.5-108	20.7	49.0	236.4	31-32	26.6	43.2	162	118.5-120	8.9	3.4	38.6
108.5-109	7.2	6.7	93.8	33-34	26.6	65.6	247	121.5-122.5	10.3	0	0.02
109.5-110	1.9	0	0	35-36	25.9	98.7	380.7	123.5-125	15.4	0	0
				37-38	19.8	25.4	128.1	127-128	10.3	17.5	170.7
				39-40	3.1	0.3	9.2	128-130	4.1	4.4	108.8
				40-43	0.1	0	0	130-134	0.2	0	11.8

* from Nijenhuis et al. (1998)

Table 2.2 Characteristics of the three lateral time-equivalent Pliocene sapropels

Core, section, interval (em)	964D-IOH-1, 103-110	969E-6H-6, 26-40	967C-8H-4, 114-130
Maximum of TOC (%)	24.9	26.6	15.4
Thickness of the sapropel (em)	7	14	16
Sedimentation rate (em kyr^{-1}) ^a	1 ^b	2 ^b	2.28 ^b
Water depth (m)	3660	2201	2553
Depth	80.2	50.7	72.2

^a assuming a constant sedimentation rate

^b assuming sapropel duration of 7000 years

^c mbsf: metres below seafloor

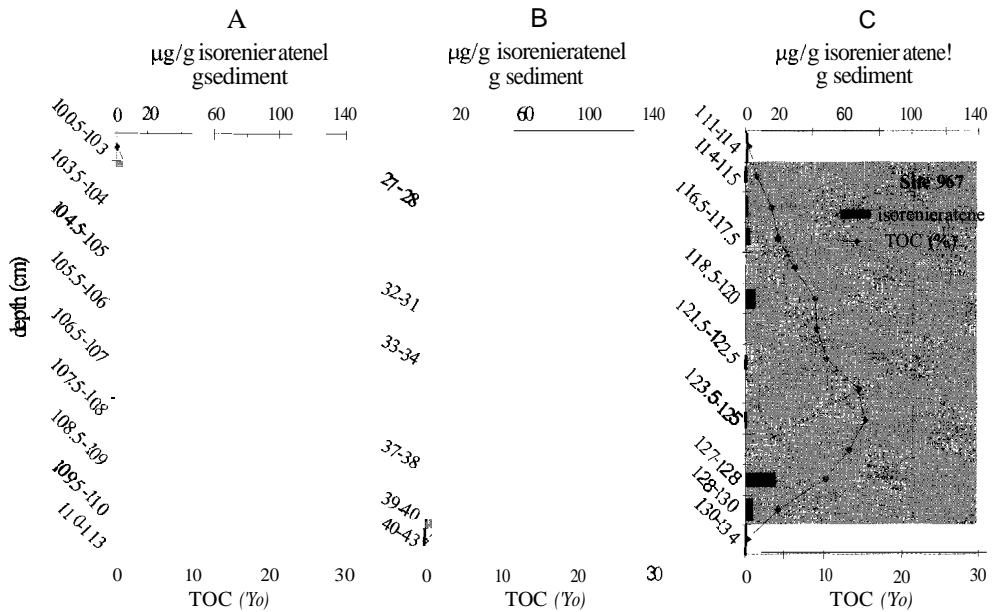


Figure 2.3 Isorenieratene contents and TOC contents measured in subsamples plotted against depth of sapropels (A) 964, (B) 969 and (C) 967. Light grey shaded regions represent the sapropel. White regions represent the homogeneous calcareous ooze.

DISCUSSION

Sapropel chronology

Many studies have investigated the chronology of sapropels with one major question in mind: is a sapropel deposited synchronously throughout the basin or are there differences in the onset and duration of sapropel formation depending on the location within the basin (e.g. shallow vs. deep water, east vs. west; Troelstra *et al.*, 1991; Strohle and Krom, 1997; Mercone *et al.*, 2000)? Such studies are complicated by the fact that only the most recent sapropel (S1) can be dated by ^{14}C analysis. A further complication is that the S1 sapropel is often severely affected by post-depositional oxidation (e.g. de Lange *et al.*, 1989; Thomson *et al.*, 1993) resulting in almost complete removal of organic carbon from the top of the sapropel. The original thickness of the sapropel can only be assessed by high-resolution inorganic geochemical studies (i.e. BajAI and MniAI profiles; van Santvoort *et al.*, 1996; Thomson *et al.*, 1999). A variety of S1 sapropels from different locations and water depths investigated by radiocarbon dating revealed discrepancies in sapropel timing records ranging from depth-progressive development and vice versa to synchronous onset (e.g. Troelstra *et al.*, 1991; Fontugne *et al.*, 1994; Strohle and Krom, 1997). A recent study of the eastern Mediterranean Sea sapropel S1 at different locations using accelerator mass spectrometry

radiocarbon dating in combination with Ba/Al ratios revealed an average sapropel duration of ca. 4000 years with differences between sites of approx. 700 years (i.e. by only 20 %; Mercone *et al.*, 2000).

The investigated Pliocene sapropels differ in sapropel thickness by a factor of ca. 2 (Table 2.2). Comparison of TOC and Ba/Al profiles of these sapropels indicate that post-depositional oxidation has not affected the top of the sapropels (Nijenhuis and de Lange, 2000) and is, thus, not the cause for these differences in thickness. Calculations, based on astronomical tuning and the thickness of the sapropels assuming constant sedimentation rates would result in sapropel duration of 3300 years at Site 964 and approx. 7000 years at Site 969 and 967. This difference is much higher than observed for the S1 sapropel (Mercone *et al.*, 2000) and seems unrealistic. Nijenhuis *et al.* (1999, 2000) has suggested continued bottom water circulation for the Pliocene sapropels based on trace metal enrichments and transport of Mg-rich chlorite and K-rich illite from the Adriatic and Aegean Sea into the Ionian basin. This model would be more consistent with more synchronous deposition of sapropels at the three different sites. Therefore, we feel it is more likely to attribute the difference in thickness of the sapropels to differences in sedimentation rate. These may be caused by the higher flux of detrital matter at sites closer to the Nile River and differences in preservation of carbonate (higher in the eastern sites; Nijenhuis and de Lange, 2000). Furthermore, sedimentation rates for the sapropel S1 can vary more than a factor 2 (Mercone *et al.*, 2000) observed here for the Pliocene sapropels. To obtain temporal and spatial insights into the development of photic zone euxinia throughout the basin, it is, therefore, realistic to assume synchronous sapropel deposition at the three different sites studied.

Isorenieratene accumulation rates

Isorenieratene contents were transformed to isorenieratene accumulation rates assuming (i) a synchronous start and end of sapropel formation at the three locations, (ii) a duration of sapropel formation of approx. 7000 years (Nijenhuis and de Lange, 2000) and (iii) a constant sedimentation rate within the sapropel (Table 2.2). This transformation was undertaken to compensate for "dilution" effects and to compare these accumulation rates with rates of primary production at the three sites. The calculated accumulation rate profiles of isorenieratene at Sites 964 and 969 are similar in intensity (Fig. 2.4A). Changes in isorenieratene accumulation rates are explained by variations in the level of anoxygenic photosynthesis by green sulphur bacteria in response to the shoaling and deepening of the chemocline (Repeta, 1993; Sinninghe Damste *et al.*, 1993a). Photic zone euxinia was significantly more than in the most eastern part (Fig. 2.4A). Site 967 showed an initial increase in isorenieratene accumulation rate at the base of the sapropel to a maximum value of only 0.3 mg m⁻² yr⁻¹ followed by a drop to zero at the sapropel centre. At the top of the sapropel, accumulation rates increased slightly again (Fig. 2.4A). Maximum accumulation rates for this site are, however, only 10% of those reached at Sites 964 and 969.

Based on these calculated isorenieratene accumulation rates, photic zone euxinia first appeared in the Levantine basin (Site 967) and continued to develop more strongly towards the Ionian basin (Site 964). The strongly reduced isorenieratene accumulation rates at Site 967, located closer to the mouth of the Nile, at the time of maximum isorenieratene accumulation

rates at Sites 969 and 964 is remarkable. This observation implies a deepening of the chemocline below the photic zone, most probably due to a large increase in the run-off of fresh, less dense water from the Nile. This interpretation is consistent with the fact that Site 967 also shows the highest sediment accumulation rate (Table 2.2), most probably due to fluvial delivery of mineral matter.

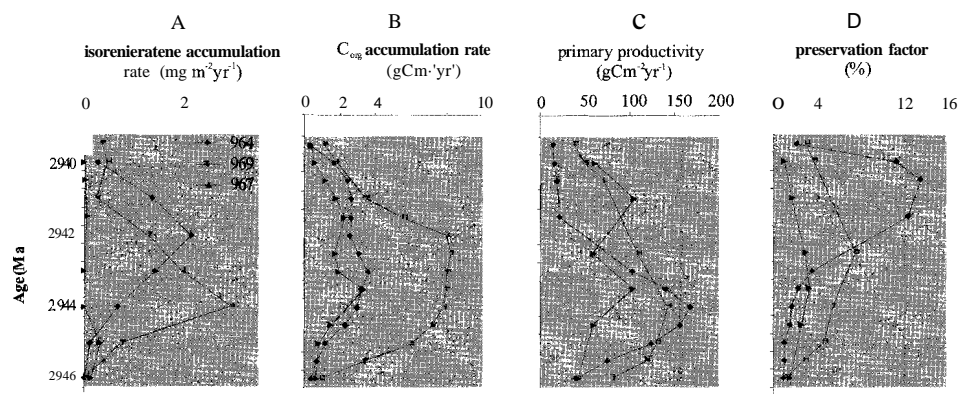


Figure 2.4 Comparison of the accumulation rates (A and B), PP (C), PF (D) among sapropel Sites 964, 969 and 967.

A isorenieratene accumulation rate (AR_i):

$$AR_i [\text{mg m}^{-2} \text{yr}^{-1}] = \text{isorenieratene concentration} \times \text{sediment rate} [\text{cm kyr}^{-1}] \times \text{dry density} [\text{g cm}^{-3}] / 100.$$

B C_{org} accumulation rate (AR_{Corg}):

$$AR_{C_{org}} [\text{gCm}^{-2} \text{yr}^{-1}] = C_{org} [\text{wt}\%] \times \text{sediment rate} [\text{cm kyr}^{-1}] \times \text{dry density} [\text{g cm}^{-3}] / 100.$$

C primary productivity (PP) after Dymond *et al.* (1992):

$$Ba_{(bio)} [\mu\text{g/g}] = Ba_{(total)} - (AI \times Ba_{Aluminosilicate})$$

$$FbioBa [\mu\text{g cm}^{-2} \text{yr}^{-1}] = (Ba_{bio} \cdot aoc) / (0.2091 \log(MAR) - 0.213)$$

(B_{bio}-acc cm⁻² kyr⁻¹) ~ accumulation of barium in sediments after correcting for aluminosilicate barium

MAR cm⁻² yr⁻¹ ~ mass accumulation rate of the sediments; after Francois *et al.* (1995):

$$EP [\text{gC m}^{-2} \text{yr}^{-1}] = 1.95(FbioBa) / 41$$

after Eppley and Peterson, (1979):

$$PP [\text{gC m}^{-2} \text{yr}^{-1}] = (EP \cdot \text{new production}) / 0.0025$$

(EP = new production)

D preservation factor (PF)

$$PF [\%] = (AR_{C_{org}} / PP) \times 100$$

Because the H₂O content for the sapropel at Site 969 was not determined, an estimated dry density of 1.5 g cm⁻³, similar to Site 964, was used for all AR calculations. Light grey shaded regions represent the sapropel. White regions represent the homogenous calcareous ooze.

Organic carbon accumulation rates, primary productivity and preservation factor

To assess if photic zone euxinia played a significant role in the burial of organic matter in the sapropels, C_{org} accumulation rates, estimated primary productivity and the estimated preservation factor were calculated from published data (Nijenhuis and de Lange, 2000) with the same assumptions as listed for the calculations of isorenieratene accumulation rates. Calculation of the C_{org} accumulation rates revealed a two-fold higher rate for the sapropel at Site 969, when compared to those at Sites 964 and 967 (Fig. 2AB).

Barium is believed to be a good indicator for primary productivity (PP) of marine organic matter because it is removed by organic particles from the photic zone (Bishop,

1989; Dehairs *et al.*, 1987). The export production (EP) was calculated from Ba data (Nijenhuis and de Lange, 2000) using equations proposed by Francois *et al.* (1995) and Dymond *et al.* (1992) assuming a detrital *Ba/Al* ratio of 0.0019 (40 % on average; van as *et al.*, 1994). Primary productivity was estimated from EP values using the equation established by Eppley and Peterson (1979). Euxinic conditions may lead to reduced formation and relatively poor preservation of barite (Dymond *et al.*, 1992; Falkner *et al.*, 1993; Francois *et al.*, 1995), which implies that the estimated PP is a minimum value.

Enhanced PP during sapropel formation is noted at Site 967 with two maxima of ca. 100 gC m⁻² yr⁻¹ (Fig. 2AC). Sites 969 and 964 showed more or less similar estimated PP, reaching maximum values just before the central part of the sapropel of 140 gC m⁻² yr⁻¹ and 160 gC m⁻² yr⁻¹, respectively (Fig. 2AC). In the upper part of the sapropel at Site 969 estimated PP decreases slowly, ultimately reaching estimated PP values similar to those of homogenous, calcareous ooze. In contrast, estimated PP at Site 964 decreased sharply and at two third of the sapropel estimated PP levels are back to background levels.

The average PP of the present-day Mediterranean is 26 gC m⁻² yr⁻¹. This is slightly higher than the background levels of ca. 20 gC m⁻² yr⁻¹ in the Pliocene, because of the present excessive anthropogenic nutrient input into the Mediterranean (Bethoux, 1989). The present-day Black Sea has PP values of about 210 gC m⁻² yr⁻¹ (Karl and Knauer, 1991), similar to PP values estimated for the three time-equivalent sapropels of the Pliocene. PP values during Pliocene sapropel deposition show an approx. 5 to 10-fold increase. In addition to the input of nutrients from the Nile and other rivers (Rossignol-Strick, 1983), the substantial increase in primary production may have been caused partially by the release of labile phosphorous from deep-basin under anoxic bottom water conditions (van Cappellen and Ingall, 1994). Phosphorous regeneration has been reported in Holocene Mediterranean sapropel S1 leading to higher C: P ratios (Slomp *et al.*, 2002). An up to a factor of four higher C: P ratio has been measured for the central part of the Pliocene sapropel (2.943 Ma) at Site 969, indicating an even more significant recycling of phosphorous, caused by the enhanced C_{org} burial (Slomp *et al.*, 2003).

The preservation factors (PFs, defined as the fraction of primary production preserved in the sediments) in the sapropels of Sites 967 and 969 show an average value of 2% and 4%, respectively (Fig. 2AD). This is slightly less than the PF of 5% reported for the stratified, euxinic Black Sea (Arthur *et al.*, 1994). In the lower section of the sapropel from Site 964 there is a relatively low PF of ca. 2%. In strong contrast, the upper section shows significantly enhanced PFs of up to 13%, which is caused by the much lower estimated primary production in this section (Fig. 2AC). It is known that barite dissolves at depth when pore water sulphate levels draw down to low levels by sulphide production (e.g. Brumsack, 1986; Torres, *et al.*, 1996; Gingele *et al.*, 1999). However, pore water analysis indicated no depletion of sulphate based on $\delta^{34}\text{S}_{\text{pyr}}$ in these sapropels. This relates to the increase of sulphate upon depth owing to the dissolution of the underlying evaporites (Emeis, *et al.*, 1996; Passier, *et al.*, 1999c). Albeit, Ba remobilisation in the upper part cannot be completely discounted. However, it is difficult to understand why this process would not have affected the other two sapropels.

With the new data it is now possible to address two major questions related to photic zone euxinia: (i) is the estimated PP during sapropel formation high enough to cause euxinic conditions in the complete water column and (ii) how did photic zone euxinia affect preservation of organic matter; in other words did it promote sapropel formation?

The first question has already been discussed thoroughly by Passier *et al.* (1999a) based on sedimentary barium and C_{org} accumulation rate calculations, which implied increased primary productivity during sapropel formation. Trace metal budgets indicated, however, that continued circulation (as opposed to stagnant water conditions) was required to supply enough trace metals to account for the higher trace metal accumulation rates in the sapropels. Despite continued circulation, which also resulted in the delivery of oxygen to the basin, calculations indicated that the downward flux of organic matter was high enough to consume all the delivered oxygen (Passier *et al.*, 1999a).

Our detailed isorenieratene accumulation and PP rate profiles (Fig. 2.4A,C) show no significant relationship. This is probably due to the fact that the position of the chemocline is also governed by other factors. For example, the significantly increased fresh water transport of the Nile River probably deepened the chemocline in the Levantine basin (Site 967). With respect to the second question, numerous studies have investigated whether anoxic conditions lead to increased preservation of organic matter (e.g. Demaison and Moore, 1980; Pedersen and Calvert, 1990; Arthur and Dean, 1998). Water-column anoxia often coincides with organic matter deposition on the seafloor in ancient and present-day sediments (e.g. Mediterranean Sea, Black Sea, Cariaco basin), but is not the only factor for deposition (e.g. Cowie *et al.*, 1999). There are other factors, which also affect increased organic matter preservation (e.g. sediment accumulation rate, sources of organic matter, water depth, bacterial grazing, adsorption, geopolymerization; Canfield, 1994). Based on isorenieratene measurements in unit II sediments of the presently euxinic Black Sea, Sinninghe Damste *et al.* (1993a) found that the top of the chemocline was within the photic zone during deposition of subunit IIb, but was below the photic zone during deposition of subunit IIa. Pyrite framboid size distributions (Wilkin *et al.*, 1997) and $\delta^{34}S$ values of pyrite (Calvert *et al.*, 1996) are interpreted to indicate the presence of euxinic waters during the entire period of deposition of unit II (Lyons, 1997). The content and accumulation rate of organic matter, and its degree of preservation (as evidenced by slightly lower hydrogen indices) decreased in subunit IIa (Arthur and Dean, 1998). This was interpreted to result from an erosion of the chemocline, possibly as a consequence of the cooler and drier climate during deposition of subunit IIa leading to a salinity increase of surface waters and a consequent weakened stratification. A decrease in overturn rate of nutrients and consequent lower surface-water productivity would lead to a deepening of the chemocline. These data show that there may be a tight coupling between the depth of chemocline and organic carbon accumulation in the sediment.

The isorenieratene accumulation rate and PF profiles in the sapropels show no direct correlation (Fig. 2.4A,D). Site 967 shows a maximum preservation in the central part of the sapropel, while the chemocline has deepened below the photic zone (Fig. 4A,D). Site 969 shows an approximately two-fold higher preservation factor compared to Site 967. Shoaling of the chemocline into the photic zone is clearly indicated by the large increase in the

accumulation rate of isorenieratene (Fig. 2.4A), but the increase in PF lagged slightly behind. The delay in the occurrence of photic zone euxinia at Site 964 may explain the high PF of organic matter in the upper part of the sapropel (Fig. 2AD; Table 2.2), again lagging slightly behind. However, as discussed above, the estimated factors at this site may be overestimated due to barite dissolution.

CONCLUSIONS

Based on measurements of isorenieratene, photic zone euxinia was widespread during deposition of time-equivalent sapropels at three locations in the eastern Mediterranean basin, resulting in improved organic matter preservation. The H₂S chemocline first appeared at the Levantine basin (east) and extended into the Ionian basin (west). Variations in isorenieratene content reflect fluctuations of the chemocline in the water column. The absence of isorenieratene in some parts of the sapropel at the eastern site is probably due to a deepening of the chemocline resulting from the increased delivery of fresh water from the Nile. Photic zone euxinia was most probably triggered by the large-scale input of nutrients from the Nile and other rivers leading to enhanced primary productivity and consequently high sedimentation OM fluxes, which in turn played an important role in causing anoxia and deposition of sapropels (Fig. 2.5).

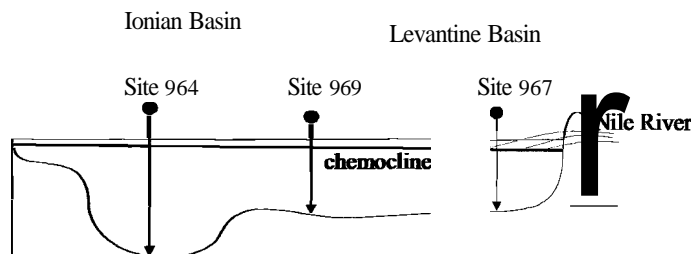


Figure 2.5 East-west gradient of the palaeochemocline based on isorenieratene data of three time-equivalent Pliocene sapropels indicating the large-scale river runoff causing the deepening of the chemocline at Site 967.

ACKNOWLEDGEMENTS

We thank the Ocean Drilling Program for samples and G. Nobbe for analytical assistance. We also would like to thank Drs. G.J. de Lange, R. Haese, I. Poole and I. Nijenhuis for helpful discussions and the journal referees for their remarks.

Chapter 3

A newly discovered fossil carotenoid in Pliocene sapropels of the eastern Mediterranean Sea

Diana Menzel, Ellen C. Hopmans, Stefan Schouten and Jaap S. Sinninghe Damste

ABSTRACT

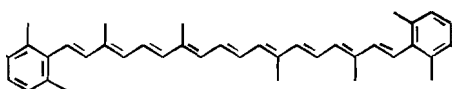
Analyses by high performance liquid chromatography-mass spectrometry (LC-MS) of three time-equivalent late Pliocene sapropels (2.943 Ma) of the eastern Mediterranean Basin revealed the presence of two intact fossil carotenoids. In a previous study we reported the presence of isorenieratene, the characteristic pigment of the green sulfur bacteria, indicating that sulphide-rich bottom waters reached the photic zone for a substantial period during sapropel deposition in the entire eastern Mediterranean Basin. In addition to isorenieratene, a novel unknown carotenoid was found, which showed temporal and spatial differences in relative abundances between the three sites. Highest relative abundances of the unknown carotenoid were measured at Site 967, located closest to the Nile, and coincided with changes in isorenieratene abundances. Based on its molecular weight, mass spectrum, and its UV/VIS absorption maximum this unknown pigment reflects either (i) spheroidenone (derived from nonsulfur purple bacteria) or (ii) thiothece-474 (derived from sulfur purple bacteria). Further research will focus on the elucidation of this "unknown purple carotenoid".

INTRODUCTION

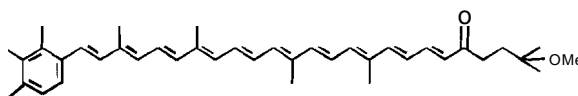
Photosynthesis is the process by which electromagnetic radiation in the form of photon flow is transformed into chemical energy and is either oxygenic or anoxygenic, depending on whether there is release of oxygen. For example with green plants, algae, cyanobacteria, there is release of oxygen whilst in a number of bacterial photosynthetic processes there is not. Anoxygenic phototrophic bacteria require electron donors that are more reduced than water. This leads to extraordinary versatility, as these organisms are able to use many compounds, such as sulfide, and other reduced sulfur compounds, hydrogen and a wide range of organic molecules, and even reduced iron (Sasikala and Ramana, 1995). The photosynthetic pigments of these bacteria are bacteriochlorophylls (Bchls) *a*, *b*, *c*, *d*, *e* and *g*, as well as a variety of carotenoids (Eraso and Kaplan, 2001).

Based on many characteristics, including 16S rRNA and pigment analysis, the anoxygenic phototrophic bacteria have been classified into two major groups, purple and green bacteria (Sasikala and Ramana, 1995). Green bacteria are subdivided into two subgroups, the green nonsulfur bacteria and green sulfur bacteria. They contain mostly Bchl *c*, *d* or *e* and very little Bchl *a*, as well as carotenoids, such as chlorobactene and

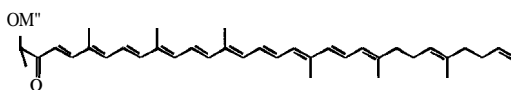
isorenieratene. Isorenieratene (I, see Fig. 3.1 for structures) is a characteristic carotenoid of the brown-coloured strain of the green sulfur bacteria, Chlorobiaceae (Liaaen-Jensen, 1978), which are obligate photoanaerobes growing under very low light conditions (e.g. <0.5 Takahashi and Ichimura, 1970; Bergstein *et al.*, 1979; Overmann *et al.*, 1992). The purple bacteria are subdivided into two subgroups, the purple sulfur bacteria, which encompass the families Chromatiaceae and Ectothiorhodospiraceae, and the purple nonsulfur bacteria with the family of the Rhodospirillaceae. This grouping is based on the ability, or inability, to use elemental sulfur as an electron donor for phototrophic carbon dioxide assimilation (Imhoff *et al.*, 1984). Purple sulfur bacteria preferentially oxidize sulfide, thiosulfate or sulfur facultatively chemoautotrophic (de Wit and van Gernerden, 1987; and Pfennig, 1986), whereas organic substrates are only poorly oxidized if at all. This is the major difference with the purple nonsulfur bacteria, of which nearly all species are facultatively chemoorganotrophic using different organic compounds as carbon source serving as respiratory substrates. The main photopigments in purple bacteria are Bchl *a* or *b*, and carotenoids, e.g. spirilloxanthin, alternative spirilloxanthins (spheroidene and spheroidenone), okenone (II) or the rhodopinal series (Eraso and Kaplan, 2001).



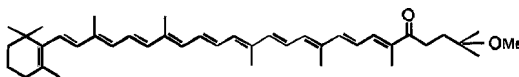
I - isorenieratene



II - okenone



III - spheroidenone



IV - thiothece-474

Figure 3.1 Structures of carotenoids discussed in the text.

Fossil photopigments in sediments can be used as chemical markers for the presence of these photosynthetic sulfur bacteria in past depositional environments (Sinninghe Damste and Koopmans, 1997). For example, Chromatiaceae have been mostly reported in different environmental settings, such as stratified lakes (Pfennig *et al.*, 1968), sewage lagoons and estuaries (Pfennig and Triiper, 1989), and shallow coastal lagoons and marine sediments

(Matheron and Baulaigue, 1972; Caumette, 1986; Pfennig, 1989). In contrast, compared Ectothiorhodospiraceae which live under hypersaline and alkaline conditions (Triiper and Imhoff, 1981; Blankenship *et al.*, 1995). The presence of isorenieratene and its derivatives representing Chlorobiaceae was reported in the present-day euxinic Black Sea water column (Repeta *et al.*, 1989) and sediments (Repeta, 1993; Sinninghe Damste *et al.*, 1993a) as well as in many older organic-rich sediments (e.g. Passier *et al.*, 1999a; van Kaam-Peters *et al.*, 1997; Summons and Powell, 1986; Koopmans *et al.*, 1996) indicating the (past) penetration of sulphide-containing bottom waters into the photic zone. Isorenieratene and its derivatives are, therefore, palaeoenvironmental indicators for "photic zone euxinia" (Repeta, 1993; Sinninghe Damste *et al.*, 1993a). In much the same way, carotenoids of purple sulfur bacteria can be used. For example, okenone has been found in lake sediments (Hartgers *et al.*, 2000; Schaeffer *et al.*, 1997) and in sediments of a stratified Norwegian fjord (Smittenberg *et al.*, 2004).

The development of photic zone euxinia in the eastern Mediterranean Sea during the late Pliocene was recently studied based on the distribution of intact isorenieratene in three time-equivalent sapropels (Menzel *et al.*, 2002). Besides isorenieratene, a newly discovered fossil carotenoid, previously also identified in the S5 sapropel of the eastern Mediterranean Sea (Hopmans *et al.*, 2003), was also present. Here we identify this "carotenoid" as either (i) spheroidenone (III), a carotenoid related to various species of the family Rhodospirillaceae or (ii) thiothece-474 (IV), a minor carotenoid produced in *Thiocystis geiatinosa*, and discuss the palaeo-ecological implications of this finding.

MATERIAL AND METHODS

Samples

Core samples were taken during ODP Leg 160 in the eastern Mediterranean Basin. Three time-equivalent sapropels (2.943 Ma; Lourens *et al.*, 1996) were sub-sampled from cores obtained at Sites 964 (Ionian Basin), 969 (Mediterranean Ridge) and 967, spanning an east-west transect of the eastern Mediterranean Basin (Eratosthenes Seamount; see Menzel *et al.*, 2002). Astronomical time scale calibrations of Mediterranean land sections have been performed on Pliocene sediments (Lourens *et al.*, 1996). Correlation of the sapropel layers in these land sections with the distribution of sapropels in the ODP cores at Sites 964, 969 and 967 revealed unambiguously that the three investigated sapropels represent the same sapropel event (e.g. Lourens *et al.*, 1996; Passier *et al.*, 1999a; Nijenhuis and de Lange, 2000). Total organic carbon (TOC) contents were reported previously and showed distinct differences between these sapropels.

Extraction and fractionation

Freeze-dried and ground sediment samples of 0.1 to 3 g were ultrasonically extracted with acetone (3x, 3 min) to optimise carotenoid yield. Samples were centrifuged at 3000 rpm for 5 min. The supernatants were decanted, combined and concentrated using rotary vacuum evaporation. The extract was subsequently dried under a gentle flow of nitrogen. This residue

was re-dissolved in dichloromethane and applied to a silica column, where non-polar carotenoids were subsequently eluted with dichloromethane.

High performance liquid chromatography-mass spectrometry (LC-MS)

Carotenoid fractions were analysed by LC-MS as described previously (Menzel *et al.*, 2002). Detection was achieved by in-line UV/VIS-detection and atmospheric pressure positive ion chemical ionisation mass spectrometry (APCI-MS) of the eluent. Relative abundances of the "unknown purple carotenoid" were estimated using the UVNIS response of the peak area at 482 nm (UVNIS absorption maximum of the unknown carotenoid).

RESULTS

In addition to isorenieratene (I) (Menzel *et al.*, 2002), the apolar carotenoid fractions of the Pliocene sapropels often contain an earlier eluting unknown carotenoid (Fig. 3.2a).

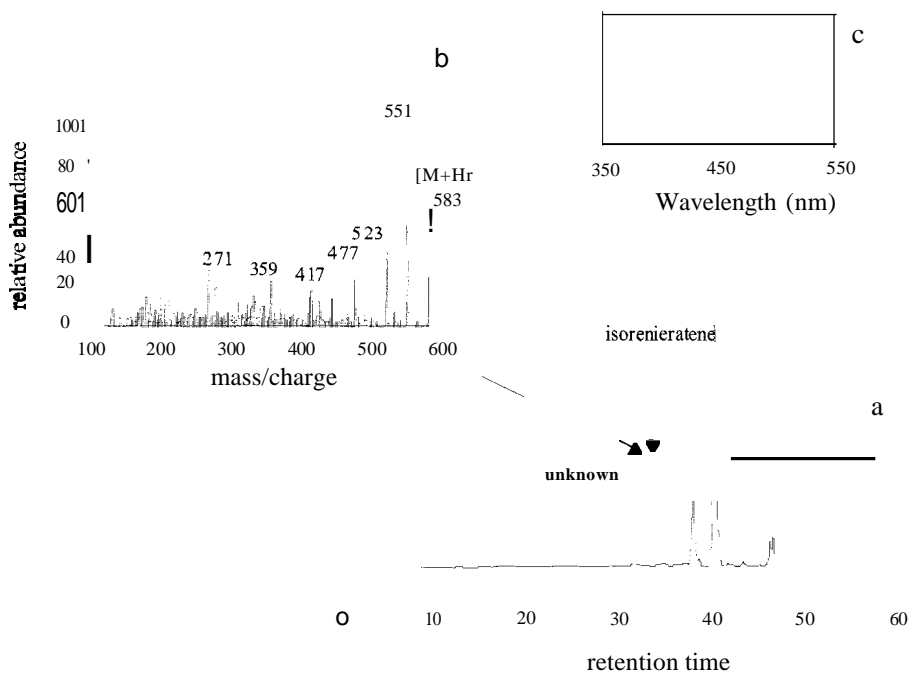


Figure 3.2 (a) UV chromatogram at 454 nm of the carotenoid fraction of Site 967-CH8-4, 118.5-120 cm showing the presence of isorenieratene and the "unknown purple carotenoid", (b) and (c) mass and UV spectrum of the "unknown purple carotenoid", respectively.

The APCI mass spectrum of this compound was dominated by an ion at m/z 583 (representing $[M+Ht]$), suggesting a molecular weight of 582 (Fig. 3.2b). Two major fragments were observed at m/z 551 and m/z 523, respectively. The first fragment, 32 Da

lower relative to the protonated molecule, may represent loss of a methoxy functionality. A second fragment at m/z 523, which is 18 Da lower, suggests a further loss of an alcohol, aldehyde or keton functional group as water. Its UVNIS spectrum showed an absorption band with a maximum at 482 nm (Fig. 3.2c). Comparison with literature data indicated that this carotenoid is either (i) spheroidenone (III) or (ii) thiothece-474 (IV) as these have molecular weights of 582 Da, possess functional groups that could lead to the observed fragments in the APCI mass spectrum, and similar absorption maxima (Pfennig *et al.*, 1968), (Andrews and Liaaen-Jensen, 1972), (Staub, 1987). Unfortunately, authentic standards of these components were not available to check if relative retention time data could be used to discriminate between these two possibilities. Small amounts of this carotenoid were isolated by repetitive preparative HPLC to further elucidate its structure, but ^1H NMR studies of the isolate indicated that the carotenoid had become oxidized during the isolation process. Therefore, we are at present not able to further identify this carotenoid.

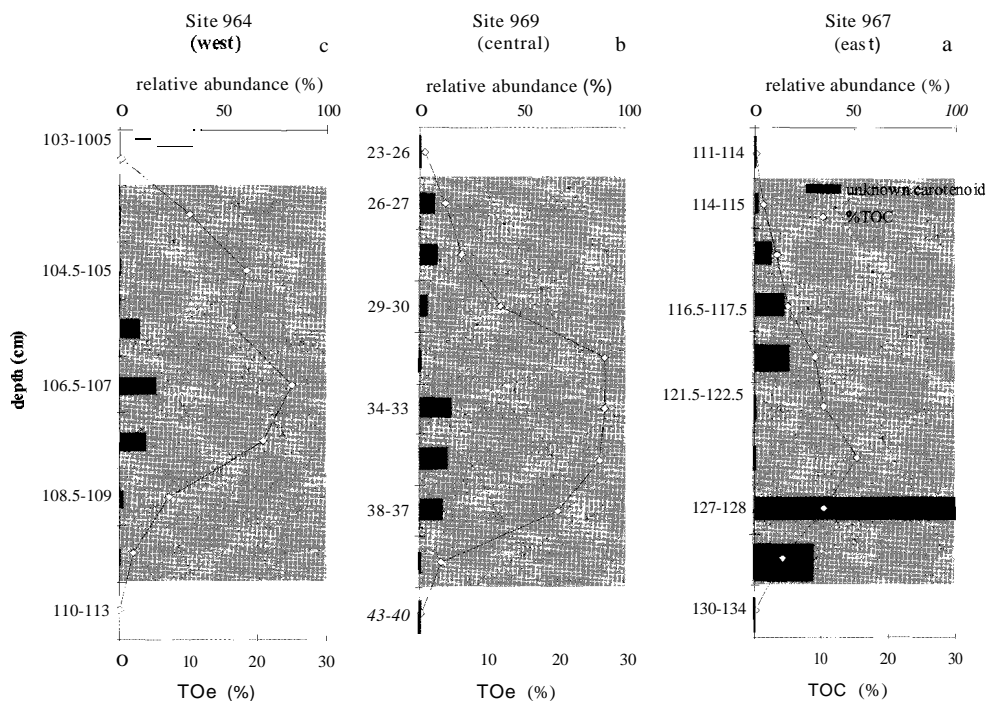


Figure 3.3 Relative abundances of the "unknown purple carotenoid" in sub-samples plotted against depth of sapropels (a) Site 967, (b) Site 969 and (c) Site 964 and total organic carbon (TOC) (*data from Nijenhuis *et al.*, 1998). Light grey shaded regions represent the sapropel and white regions represent the homogeneous calcareous ooze.

The peak area of the unknown carotenoid was in few sub-samples of the sapropels as large as the peak area of isorenieratene. Thus, the unknown carotenoid is an important fossil bacterial pigment in addition to isorenieratene preserved in the late Pliocene sapropels. Abundances of this carotenoid varied within and between the three sapropels (Fig. 3.3). In the

homogeneous, calcareous intervals below and above the sapropels it was absent at all three sites. In the lower part of sapropel at Site 967 (closest to the mouth of the Nile), the highest relative abundances of the unknown carotenoid ranged between 30 to 100 % (Fig. 3.3a). This carotenoid was absent in the central part of the sapropel parting the top of the sapropel its relative abundance declined upwards to about 15%. Site 969 (central eastern Mediterranean) showed at the base of the sapropel low relative abundances of about 10% with increasing values towards the central part of the sapropel of about 15% and remained unchanged in relative abundances in the top of the sapropel of about 7% (Fig. 3.3b). At Site 964 (western eastern Mediterranean), the carotenoid only occurs in relatively abundances (ca. 15%) in the central part of the sapropel (Fig. 3.3c).

DISCUSSION

Possible biological origin for the unknown carotenoid

Spheroidenone (III) and thiothece-474 (IV) are proposed as the two candidates for the structure of the "unknown purple carotenoid". Spheroidenone has been described as end product of the carotenoid biosynthesis pathway of various species of the family Rhodospirillaceae (purple nonsulfur bacteria). Thiothece-474 is a minor carotenoid (ca. 1%) of the species *Thiocystis gelatinosa*, family belonging to the Chromatiaceae (purple sulfur bacteria) (Andrews and Liaaen-Jensen, 1972). *Thiocystis gelatinosa* is generally characterised by okenone as the major pigment (e.g. Pfennig *et al.*, 1968). Thus, the carotenoid represents the fossil remains of a purple photosynthetic bacteria, either a purple sulfur bacteria or a purple nonsulfur bacteria. Based on the abundance of spheroidenone among photosynthetic bacteria, compared to thiothece-474 and the absence of okenone, spheroidenone seems the most likely candidate for the carotenoid found in the late Pliocene sapropels. However, work to confirm the structure identification is ongoing.

Fossil photopigments of anaerobic, green and purple photosynthetic bacteria are common components of meromictic lakes (Lami *et al.*, 2000) and have been used to reconstruct the palaeo-environmental history of different lakes (e.g. Brown *et al.*, 1984; Ryves *et al.*, 1996; Lami *et al.*, 2000). Spheroidenone was used as indicator of the development of transparency in meromictic lakes and therefore, its trophic state (e.g. Brown *et al.*, 1984; Ryves *et al.*, 1996; Lami *et al.*, 2000). For instance, changes in palaeoenvironmental conditions during the Holocene of the small, shallow, eutrophic Lake Candia (N. Italy) revealed enhanced accumulation rates of algal and anaerobic photosynthetic bacterial pigments indicating more intense microbial mineralisation and consequently oxygen depletion (Ryves *et al.*, 1996; Lami *et al.*, 2000).

Palaeo-ecological implications

With respect to the light intensity, green bacteria require in general less light, based on the chlorosomes as light harvesting units, which are unique among all phototrophic organisms in that they require only about one-fourth of the light intensity of the purple bacteria in order to grow at comparable growth rates (Biebl and Pfennig, 1978). Therefore,

the green sulfur bacteria populations regularly occur below the layers of all other phototrophs, where light penetration is severely hampered (Blankenship *et al.*, 1995; Pfenning, 1978) and are closest to the sulfide zone (Fig. 3.4).

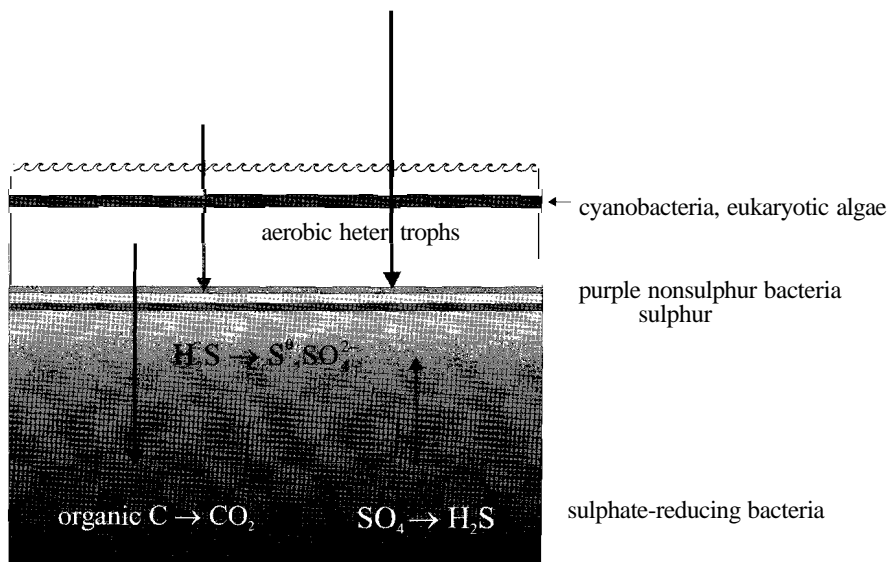


Figure 3.4 mustration of a water ecosystem involving oxygenic and anoxygenic photosynthesis in the upper water column and sulphate reduction activities near the bottom of the water column.

In previous studies of the eastern Mediterranean Sea, the presence of isorenieratene revealed sulfide-rich water up into the photic zone in the entire basin during Pliocene sapropel deposition (Passier *et al.*, 1999a). Sulfide was formed as an end product of the dissimilatory sulphate reduction of sulphate-reducing bacteria due to anoxic degradation of organic matter (e.g. Passier and de Lange, 1998), which have been caused by enhanced primary productivity leading to high sedimentation rates of OM and consequently oxygen depletion in the pore waters and water column up to the photic zone (e.g. Nijenhuis and de Lange, 2000; Passier *et al.*, 1999a; Menzel *et al.*, 2003). Variation of isorenieratene abundances at the three different sites reflected fluctuation of the chemocline in the water column during sapropel deposition (Menzel *et al.*, 2002). The H_2S chemocline first appeared at the Levantine basin (east) and extended with higher abundances into the Ionian Basin (west). Abundances of the "carotenoid likely derived from Rhodospirillaceae" showed highest relative at Site 967, located closest to the Nile and decreased towards the Ionian basin (Site 964). These bacteria were more abundant at Site 967, compared with Sites 969 and 964 (Fig. 4.5). Rhodospirillaceae are facultative anaerobes possessing the adaptive capacity to grow anaerobically in the light (photosynthetically) and aerobically in darkness by oxidative phosphorylation using organic compounds as electron donor (Saunders, 1978). It is the great ability of this group to practice photoheterotrophy using a wide range of carbon sources, that likely accounts for their competitive success in nature (Brock, 2000) explaining their true

omnipresence (Eraso and Kaplan, 2001). Based on the wide range of physiological adaptations of these Rhodospirillaceae, the palaeo-ecological implication of the presence of these bacteria is uncertain but probably related to the temporal occurrence of shallow photic zone anoxia (i.e. even more shallow than indicated by the presence of the Chlorobiaceae).

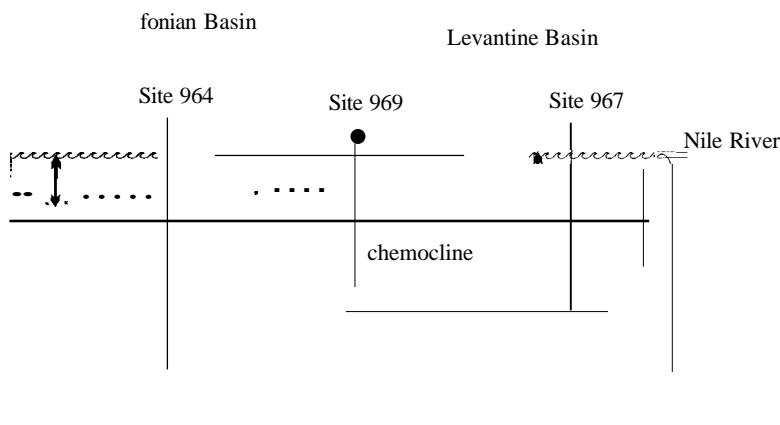


Figure 3.5 Illustration of the east-west gradient of the palaeochemocline based on isorenieratene (see Menzel *et al.*, 2002) and "unknown purple carotenoid" (dotted line) data of the three time-equivalent Pliocene sapropels abundances.

CONCLUSIONS

A novel sedimentary carotenoid was tentatively identified in sapropel sediments. It is likely derived from photosynthetic purple nonsulfur bacteria, i.e. Rhodospirillaceae. Based on the wide range of physiological adaptations of these Rhodospirillaceae, the palaeo-ecological implication of the presence of these bacteria is uncertain but probably related to the temporal occurrence of shallow photic zone anoxia, (i.e. even more shallow than indicated by the presence of pigments of the Chlorobiaceae).

ACKNOWLEDGEMENTS

We would like to thank Anja Reitz for analytical help and IPPU for funding a Ph.D. position.

Chapter 4

Reconstruction of changes in export productivity during Pliocene sapropel deposition: a biomarker approach

Diana Menzel, Pim F. van Bergen, Stefan Schouten and Jaap S. Sinninghe Damste

Published in *Palaeogeography, Palaeoclimatology, Palaeoecology* 190 (2003) 273-287

ABSTRACT

Biomarkers (alkenones, loliolide/isololiolide, dinosterol and C₃₀ 1,15-diol/keto-ol) representative of four major classes of marine primary producers (haptophytes, diatoms, dinoflagellates, eustigmatophytes, respectively) were studied for changes in phytoplankton export production before, during and after deposition of a Pliocene, TOC-rich (up to 27%) sapropel (2.943 Ma) from three sites of an east-west transect spanning the entire eastern Mediterranean basin. Biomarker contents showed substantial differences between non-sapropelic and sapropelic sediments. In non-sapropelic sediments, small contents are observed, reflecting extensive oxic degradation in oxic pore waters during deposition. In the sapropels, biomarker accumulation rates (ARs) showed a substantial increase from the base to the centre, likely resulting from increased biological productivity since bottom waters were continuously anoxic and preservation conditions are similar. The diatom biomarker, loliolide/isololiolide became distinctly more abundant in the sapropels indicating that the eastern Mediterranean basin was enriched in nutrients. This caused enhanced export production by the major phytoplankton classes leading to periods of sapropel deposition. Alkenone-based SST reconstructions indicated that this change in phytoplankton composition was not influenced by changes in sea surface temperature, but was mainly nutrient-controlled. Compound-specific $\delta^{13}\text{C}$ measurements did not provide additional evidence for substantially increased primary production rates: $\delta^{13}\text{C}$ values of C_{37:2} alkenones and loliolide/isololiolide showed a slight negative shift instead of the anticipated positive shift. This was probably caused by the enrichment of dissolved inorganic carbon in the upper water column, caused by enhanced recycling of respired CO₂ due to the shallow chemocline.

INTRODUCTION

Since the discovery of sapropels, i.e. sediments rich in organic matter, in the Mediterranean seabed there has been extensive research on their origin, but the exact mechanism of their formation is still not well understood. Sapropels are characterized by carbonate-poor and organic-rich (up to 30% TOC) material interspersed between organic-poor (<0.3% TOC) nannofossil and foraminiferal marl ooze (Calvert *et al.*, 1992). Benthic

foraminifera are generally rare in sapropels, or even absent, due to suboxic/anoxic conditions of the bottom waters (e.g. Lourens *et al.*, 1996). Sapropels occur in regular intervals in the eastern Mediterranean basin (Emeis *et al.*, 1996) showing a mainly precession-controlled correlation (Lourens *et al.*, 1996). Minima of the Earth's cycle precession are characterized by the intensification of the African monsoon leading to increased precipitation over the Mediterranean region as a whole and consequently an increase in river discharges and nutrients (e.g. Rossignol-Strick, 1985; Rohling, 1994). These river-borne nutrients most probably led to enhanced biological productivity causing increased export production of organic matter (OM) to the seafloor. Evidence for enhanced productivity is derived from substantial barite enrichments in sapropels (Wehausen and Brunsack, 1999; Passier *et al.*, 1999c; Nijenhuis and de Lange, 2000; Rinna *et al.*, 2002). As a consequence of increased export production, oxygen depletion and bottom water anoxia occurred, which in turn resulted in increased preservation of settling OM. Sapropel formation is thus both a consequence of increased productivity and improved preservation of OM.

In contrast to Pleistocene sapropels, which generally have total organic carbon (TOC) contents of less than 10% and often below 3%, Pliocene sapropels are characterised by extreme enrichments in TOC (up to 30%; Nijenhuis *et al.*, 1998; Passier *et al.*, 1999a; Rinna *et al.*, 2002). This seems to point to an even larger change in climatic and environmental conditions during the "sapropel mode" of the Mediterranean. Passier *et al.* (1999a) described a model for Pliocene sapropel deposition under continued deep-water circulation, based on trace metal data and organic geochemical evidence for photic zone euxinia (i.e. the presence of sulphide in the photic zone). Detailed studies of isorenieratene, a biomarker for photic zone euxinia (Repeta, 1993; Sinninghe Damste *et al.*, 1993a), revealed an early development of euxinia in the Levantine basin most probably caused by the large-scale nutrient input from the Nile that subsequently spread towards the Ionian basin (Menzel *et al.*, 2002).

The dominance of siliceous or organic-walled plankton over calcareous species at times of sapropel formation suggests that the phytoplankton composition of the Mediterranean Sea might have varied substantially (van Os *et al.*, 1994; Nijenhuis *et al.*, 1996). Studies on late Quaternary Mediterranean sapropels reported enhanced diatom production and inferred their contribution to the organic-rich nature of the sapropels (Kemp *et al.*, 1999). However, to date little information is known about the composition and distribution of the major primary producers during sapropel formation, especially in cases where siliceous and calcareous skeletons have dissolved, as is often the case in sapropels with a high TOC content. In such cases, lipid biomarkers can provide valuable insights into the changes in phytoplankton composition.

In the current paper four biomarkers, characteristic of different phytoplankton taxa, occurring in three time-equivalent Pliocene sapropels (2.943 Ma; Lourens *et al.*, 1996) from an east-west transect spanning the entire eastern Mediterranean basin were used to reconstruct changes in phytoplankton export production before, during and after sapropel formation. The extraordinarily high organic matter content (up to 27% TOC), in these Pliocene sapropels was predominately of marine origin and terrestrial OM contribution was insignificant (Bosch *et al.*, 1998). Results of this study show that loliolide/isololiolide, a biomarker of diatoms previously reported from sediments underlying highly productive

surface waters (e.g. ten Haven *et al.*, 1987b; Repeta, 1989), become distinctly more abundant in the sapropels, compared with biomarkers of haptophytes, eustigmatophytes and dinoflagellates. In addition, measurements of C_{37:2} alkenones and loliolide/isololiolide were used as a tool to assess changes in biological productivity during sapropel formation since during extensive periods of enhanced productivity, the isotopic fractionation (ϵ_p) between DIC and phytoplanktonic biomass can be reduced (Laws *et al.*, 1995).

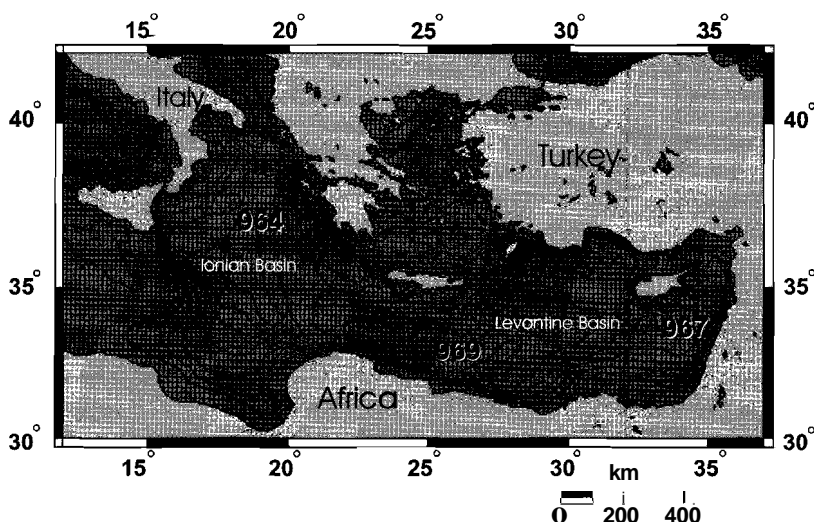


Figure 4.1 Location of the ODP drilling sites.

MATERIAL AND METHODS

Samples

Core samples were taken during ODP Leg 160 in the eastern Mediterranean basin (Erneis *et al.*, 1996). Site 967C-8H-4, 111-134 cm (Eratosthenes Seamount) and Site 969E-6H-6, 23-43 cm (Mediterranean Ridge) are located in the Levantine basin. Site 964D-IOH-1, 100.5 -113 cm is located in the Ionian basin (Fig. 4.1). The detailed chronology for these cores obtained by astronomical tuning enabled us to select three laterally equivalent sapropels with an age of 2.943 Ma (see Lourens *et al.*, 1996 for details). Each sapropel was subsampled in 0.5, 1 and 1.5 cm slices above, through and below the sapropel. Total organic carbon (TOC) was reported previously and showed distinct differences between these sapropels (Nijenhuis *et al.*, 1998).

Extraction and total lipid fraction

Ground, freeze-dried sediment samples (0.1 to 3 g) were Soxhlet extracted with dichloromethane/methanol (1:1, v/v) mixture for 24 h. The extracts were concentrated with a rotary evaporator at 30°C. Total lipid fractions (TLF) were obtained using a Pasteur capillary

pipette (150 mm), packed with silica gel and eluted with ethyl acetate to remove very polar material and silylated using N,O-bis(trimethylsilyl)trifluoroacetamide (BSTFA); (1 h; 80°C). 10-Nonadecanone was used as an internal standard. The TLF was dried under a gentle stream of nitrogen and analysed using gas chromatography (GC) and GC-mass spectrometry (GC-MS). Quantitation was performed by integration of relevant peak areas of biomarkers of interest and the internal standard. C₃₀ 1,15-diol and keto-ol, co-eluting with their isomers (C₃₀ 1,14-1,12-diols) were quantified by integration of individual peak areas in mass chromatograms using characteristic m/z values.

Calculations of accumulation rates were performed using absolute biomarker amounts ($\mu\text{g g}^{-1}$ dry weight sediment), assuming (i) a synchronous start and end of sapropel formation at the three locations, (ii) a duration of sapropel formation of approximately 7000 years (Nijenhuis and de Lange, 2000) and (iii) a constant sedimentation rate during sapropel formation (Menzel *et al.*, 2002). Accumulation rates in the homogeneous intervals were not calculated, because sedimentation rates are expected to be substantially different during times of sapropel and non-sapropel formation.

Fractionation of compound classes

An aliquot of the total extract (1.5 to 3 mg) was fractionated using a Pasteur capillary pipette (150 mm length) packed with C_{18} (activated for 2.5 h at 120°C). The apolar fraction (F1) was eluted using a mixture of hexane/dichloromethane (9:1, v/v; 4 ml). Subsequently, the ketone fraction (F2) was eluted using hexane/dichloromethane (1:1, v/v; 4 ml). Finally, the polar fraction was obtained using dichloromethane/methanol (1:1, v/v; 4 ml). Lipids in the polar fraction were derivatized using BSTFA (30 min at 60°C) with a known isotope value of -49.29 ‰ and corrected accordingly to obtain $\delta^{13}\text{C}$ values. All fractions were dried under a flow of nitrogen and analysed by GC, GC-MS and isotope-ratio monitoring (inn)-GC-MS.

Gas chromatography, GC-mass spectrometry and irm-GC-MS

GC was performed on a Hewlett-Packard 6890 series gas chromatograph equipped with a fused silica capillary column (50 m x 0.32 mm or 25 m x 0.32 mm) coated with CP-Sil 5 (film thickness 0.12 μm). Helium was used as a carrier gas. The samples were injected on-column at 70°C and the oven was subsequently programmed to 320°C at 4°C/min, where it remained isothermal for 20 min. Compounds were detected using a flame ionisation detector (FID).

GC-MS analyses were performed using a Hewlett-Packard 5890 series II gas chromatograph connected to a Fisons instruments VG platform II mass spectrometer operated at 70 eV, with a mass range m/z 50-650 and cycle time of 0.65 s (resolution 1000). The capillary column and temperature programme were as described for the GC analyses.

Isotope-ratio-monitoring gas chromatography-mass spectrometry (inn-GC-MS) was performed using a Delta-plus XL-inn-GC-MS system (cf. Schouten *et al.*, 1998), equipped with an on-column injector and fitted with a 25 m x 0.32 mm fused silica capillary column coated with CP-Sil5 (film thickness 0.12 μm). Helium was used as carrier gas and the oven was programmed from 70 to 130°C at 20°C/min., followed by an increase of 4°C/min. to

320°C (20 min.). Isotopic values were calculated by integrating the mass 44, 45 and 46 ion currents of the peaks produced by combustion of the chromatographically separated compounds and those of CO₂-spikes produced by admitting CO₂ with a known ¹³C-content at regular intervals into the mass spectrometer. Two analyses were carried out for each sample and the results were averaged to obtain a mean value. δ¹³C values have been corrected for carbon added during derivatization and have typically an error of <0.5‰.

RESULTS

Phytoplankton biomarkers

The TLF of the extracts of the homogeneous intervals (TOC up to 0.2%) below and above the sapropels are dominated by n-alkanes and n-alcohols with relatively small amounts of fatty acids, sterols and long-chain unsaturated ketones (Fig. 4.2A).

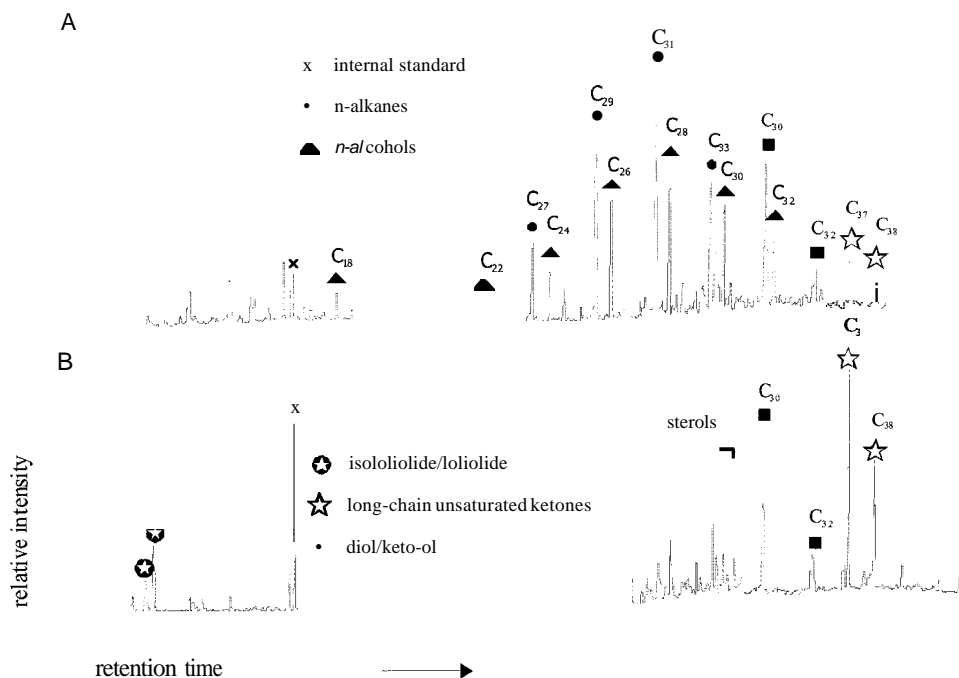


Figure 4.2 Gas chromatograms of the total lipid fractions of (A) the homogeneous interval before sapropel formation (C_{org} up to 0.12%), and (B) the sapropel (C_{org} up to 30%) of Site 969E-6H-6.

The substantially higher contribution of land plant to these TLFs is indicated by the odd-over-even predominance of the long-chain (C₂₃-C₃₃) n-alkanes and even-over-odd carbon number predominance of the dominant C₂₄-C₃₀ n-alcohols. In contrast, the TLF of the sapropels (TOC up to 30%) are dominated by biomarkers derived from phytoplankton, either directly biosynthesized lipids (e.g. long-chain alkenones, dinosterol, long-chain diols) or compounds formed from lipids or carotenoids by early diagenetic reactions (e.g. loliolide/isololiolide,

long-chain keto-ols, Fig. 4.2B). The relative contribution of terrestrial lipids to the TLF of the sapropels was insignificant and is probably caused by the overprinting marine biomarkers (Fig. 4.2B). Four biomarkers, each characteristic for a specific phytoplankton class, were used to reconstruct changes in phytoplankton composition during sapropel formation (cf. ten Haven *et al.*, 1987a).

Table 4.1 Biomarker contents and accumulation rates (AR) of the homogeneous intervals and sapropels.

Compound	Sapropel position	ODP	AR	ODP	AR	OOP	AR
		964D-10-1	(mgm ⁻² yr ⁻¹)	969E-6H-6	(mgm ⁻² yr ⁻¹)	967C-8H-4	(mgm ⁻² yr ⁻¹)
Loliolidelisololiolide (µg/g OC)	above	0		60		0	
	within (n=8)	100-730	0.03-2.0	35-315	0.03-2.5	30-840	0.02-1.7
	below	0		0		0	
Long-chain alkenones (µg/g OC)	above	305		255		120	
	within (n=8)	170-1180	0.1-4.7	90-630	0.08-2.6	160-1485	0.09-1.9
	below	80		115		320	
Dinosterol (µg/g OC)	above	0		70		0	
	within (n=8)	20-280	0.01-0.65	5-90	0.005-0.5	60-400	0.06-1
	below	45		0		38	
C ₃₀ 1,15-diol and keto-ol (µg/g OC)	above	325		105		170	
	within (n=8)	100-1020	0.07-2.3	55-310	0.05-1.93	130-1030	0.05-1.4
	below	53		57		280	

Loliolidelisololiolide is derived on a mole to mole basis from anoxic degradation of fucoxanthin (Repeta, 1989), the major carotenoid in diatoms, but also in dinoflagellates and haptophytes (Klok *et al.*, 1984; Jeffrey and Vesk, 1997). Diatom blooms are characteristic of highly productive areas, like upwelling regions where cold and nutrient-rich waters reaches the euphotic zone. Loliolide/isololiolide was absent in the homogeneous intervals below the sapropels at all three sites. The Site 967 and 964 sapropels showed the highest mean contents of ~380 µg/g DC and lower contents of 215 DC were measured a Site 969 (Table 4.1, Fig. 4.3). Above the sapropel, at Site 969 loliolide/isololiolide content of 60 DC was measured (Fig. 4.3). Accumulations rates (ARs) in the sapropel ranged from 0.02-2.5 mg.m⁻².yr⁻¹ (Table 4.1, Fig. 4.4B).

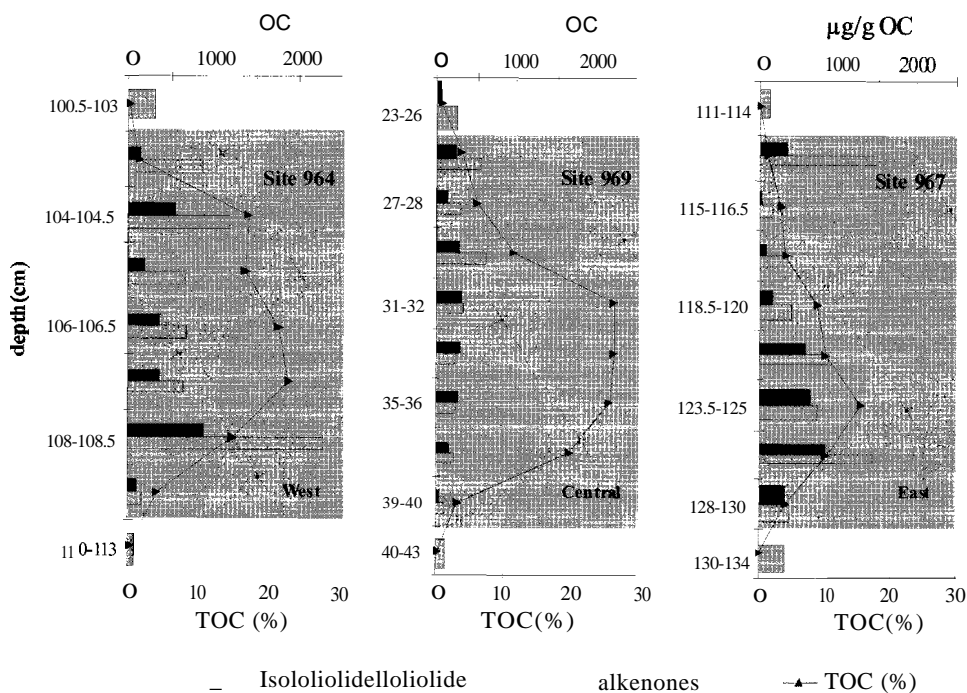


Figure 4.3 Loliolide/isololiolide and alkenone contents (nonnormalized to TOC) and TOC contents plotted against depth of the sapropels. Light grey shaded regions represent the sapropel. White regions represent the homogeneous calcareous ooze.

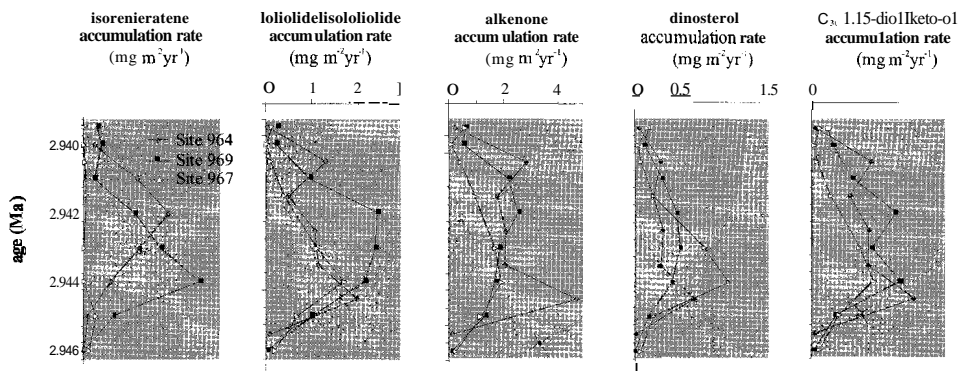
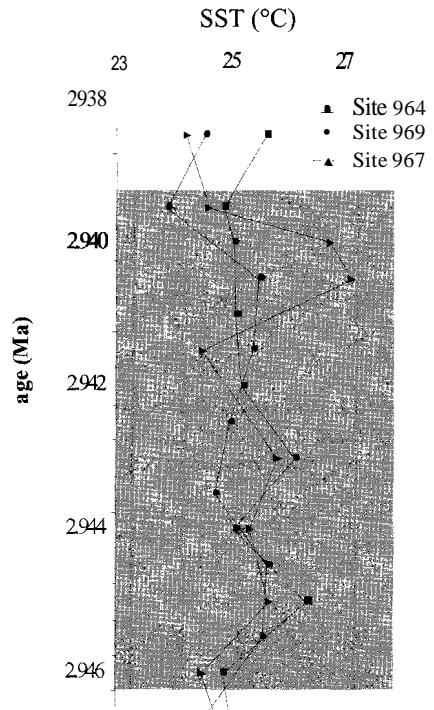


Figure 4.4 Accumulation rates of isorenieratene (A), loliolide/isololiolide (B), alkenone (C), dinosterol (D), and C₃₀ 1,15-diol/keto-ol (E) at Sites 967, 969 and 964. Light grey shaded regions represent the sapropel. White regions represent the homogeneous calcareous ooze.

Long-chain alkenones are exclusively biosynthesised by some haptophyte algae (Volkman *et al.*, 1980; Marlowe *et al.*, 1984a), which are found in the phytoplankton living in low to moderate productive areas, such as the present-day Mediterranean Sea (Dugdale and Wilkerson, 1988). Mean contents of long-chain alkenones in the homogeneous intervals,

below the sapropels, ranged from 80 to 320 $\mu\text{g/g}$ OC decreasing towards the western Eastern Mediterranean basin (Table 4.1, Fig. 4.3). In the sapropels, mean contents ranged from 320 to 930 $\mu\text{g/g}$ OC. In the homogeneous interval above the sapropel, mean contents were lower ranging from 120 to 305 $\mu\text{g/g}$ OC. The AR in the sapropels showed an east to west trend with values between 0.08 to 4.7 $\text{mg}\cdot\text{m}^{-2}\cdot\text{yr}^{-1}$ (Table 4.1, Fig. 4.4C). The distribution of C₃₇:2 and C₃₇:3 alkenones (as expressed in the $U_{37}^{k'} = \frac{[37:2]}{[37:2]+[37:3]}$), which is correlated with sea surface temperature (SST; Brassell *et al.*, 1986), was used for SST reconstruction using the temperature calibration established for the north-western Mediterranean Sea by Ternois *et al.* (1997). Inferred SSTs ranged from 24°C to 27°C (Fig. 4.5).

Figure 4.5 SST (°C) reconstruction based on the $U_{37}^{k'}$ -SST correlation reported by Ternois *et al.*, 1997 for the northwestern Mediterranean Sea. Light grey shaded regions represent the sapropels. White regions represent the homogenous calcareous ooze.



Dinosterol is produced by many dinoflagellates (Boon *et al.*, 1979), although exceptional occurrences have been observed in diatoms (Volkman *et al.*, 1993). Dinosterol mean contents in the homogeneous intervals below the sapropels ranged from 0 to 40 $\mu\text{g/g}$ OC (Table 4.1, Fig. 4.6). In the sapropels, the highest mean dinosterol contents revealed a range from 60 to 120 $\mu\text{g/g}$ OC (Fig. 4.6). ARs in the sapropels at all three sites ranged from 0.005 to 1 $\text{mg}\cdot\text{m}^{-2}\cdot\text{yr}^{-1}$ (Table 4.1, Fig. 4.4D).

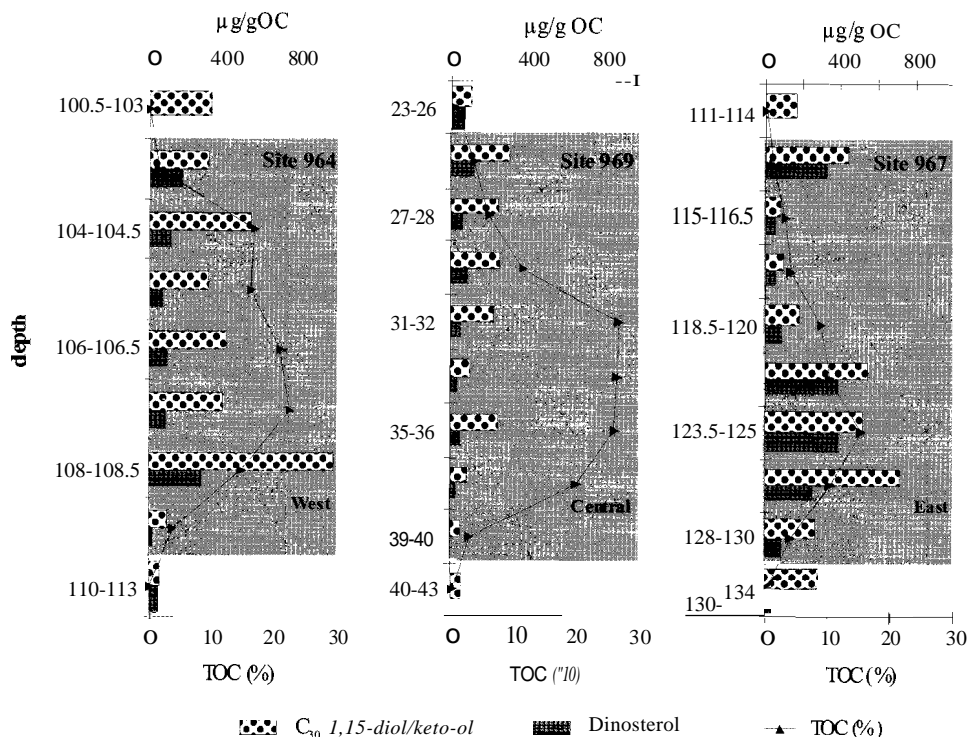


Figure 4.6 Dinosterol and C_{30} 1,15-diolketo-ol contents (normalized to TOC) and TOC contents plotted against depth of the sapropels. Light grey shaded regions represent the sapropel. White regions represent the homogenous calcareous ooze.

C_{30} 1,15-diolketo-ol were quantified to estimate the abundance of eustigmatophyte algae. C_{30} 1,15-diolketo-ol is biosynthesised by eustigmatophytes (Volkman *et al.*, 1992; Volkman *et al.*, 1999; Gelin *et al.*, 1999). C_{30} 1,15-keto-ol is probably an oxidation product (Ferreira *et al.*, 2001) of the C_{30} 1,15-diolketo-ol formed during settling of particles in the water column or in the sediment. Direct evidence for the formation through oxidation was obtained through the increase of the keto-ol relative to the diolketo-ol at the post-depositional oxidation front in the Mediterranean S1 sapropel (Ferreira *et al.*, 2001). In the homogeneous intervals, below the sapropels the mean summed diolketo-ol contents ranged from 50 to 280 $\mu\text{g/g OC}$ (Table 1, Fig. 4.6). In the sapropels mean contents ranged from 190 to 440 $\mu\text{g/g OC}$. The homogeneous intervals above the sapropels showed mean contents from 105 to 325 $\mu\text{g/g OC}$. ARs in the sapropels showed an increase from the east to the west ranging from 0.05 to 2.3 $\text{mg}\cdot\text{m}^{-2}\cdot\text{yr}^{-1}$ (Fig. 4.4E).

Compound-specific $\delta^{13}\text{C}$ measurements

The $\delta^{13}\text{C}$ values of the $C_{37:2}$ alkenones at Site 969 below the sapropel and at Site 964 below and above the sapropel were not measured, because their content was too low. $C_{37:2}$ alkenones in the sapropel showed slightly depleted $\delta^{13}\text{C}$ values towards the sapropel centre,

compared with the homogeneous intervals at all three sites (Fig. 4.7A-C). Site 967 showed mean values of -25.2‰ in the homogeneous calcareous ooze and values of -25.7‰ in the sapropel (Fig. 4.7C). Site 969 in the central part of the eastern Mediterranean Sea, showed a general depletion of ca. 1‰ in $\delta^{13}\text{C}$ compared with Sites 976 and 964 (Fig. 4.7B). Above the sapropel the $\delta^{13}\text{C}$ value was -26.8‰ , whereas the mean $\delta^{13}\text{C}$ value in the sapropel was -26.4‰ (Fig. 4.7B). The average $\delta^{13}\text{C}$ value of -25.4‰ in the sapropel at Site 964 is similar to Site 967 (Fig. 4.7A). $\delta^{13}\text{C}$ measurements of loliolide/isololiolide were only performed in the sapropel of Site 969. Like the $\delta^{13}\text{C}$ values of $\text{E}_{37:2}$ alkenones, loliolide/isololiolide showed slight depletion in $\delta^{13}\text{C}$ through the sapropel. The average $\delta^{13}\text{C}$ value was -25.7‰ (Fig. 4.7B).

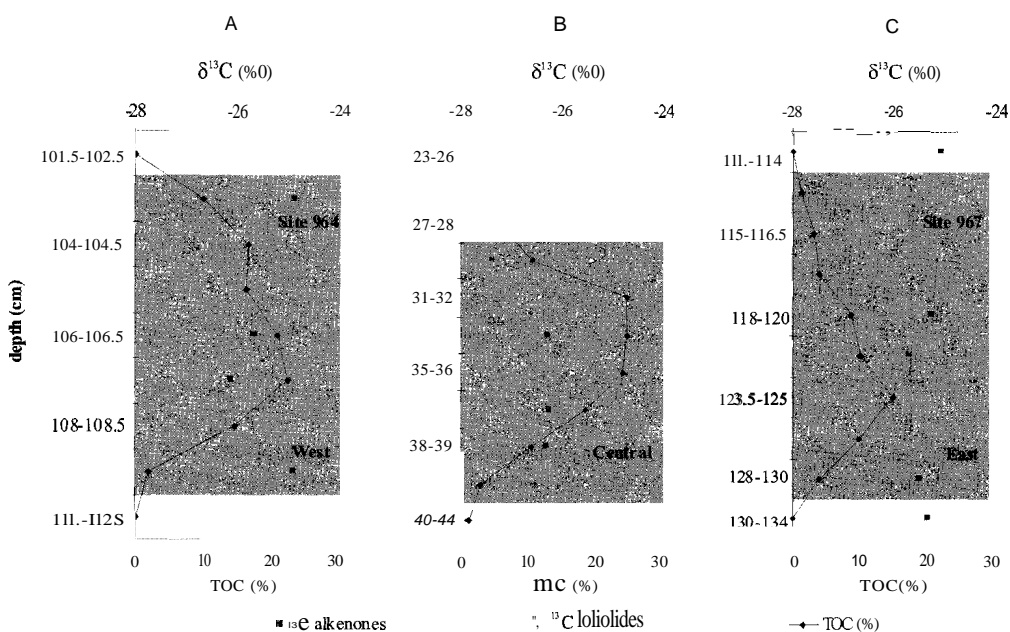


Figure 4.7 $\delta^{13}\text{C}$ measurements of alkenones at sapropel Sites 964 (A), 969 (B) and 967 (C) and loliolide/isololiolide at Site 969. Light grey shaded regions represent the sapropel. White regions represent the homogeneous calcareous ooze.

DISCUSSION

Changes in palaeoexport productivity

A primary signal of enhanced export productivity in these Pliocene sapropels has been shown by the enrichment of barium/aluminium data (Nijenhuis and de Lange, 2000), a common palaeoproxy used in the marine environment (e.g. Dehairs et al, 1987). The resulting high OM fluxes consequently caused a higher oxygen demand leading to anoxia and in turn played an important role in preservation of OM (Passier *et al.*, 1999a). Evidence of phosphate regeneration in the most recent sapropel S1 has been reported by enhanced Corg/Porg ratios by Slomp *et al.* (2002) showing the enhanced release of phosphate from organic matter in the

sediments under anoxic pore water conditions. In Pliocene sapropels at Site 969, the Corg:Porg ratios were even a factor of four higher than those of the S1 sapropel (Slomp *et al.*, 2003.), indicating that phosphate regeneration may have played an important role in sustaining elevated export productivity in the euxinic basin.

At all three sites phytoplankton biomarker contents, normalized to TOC, were substantially higher in contents in the sapropel than in the homogeneous intervals below and above the sapropel (Table 1). These differences between homogeneous intervals and sapropels are predominantly caused by different redox conditions in the sediment and water column before, during and after sapropel deposition. This was recently demonstrated by a biomarker study of Arabian Sea sediments deposited in and below the oxygen minimum zone (Sinninghe Damste *et al.*, 2002). During the formation of these sapropels the water column was euxinic up into the photic zone as evidenced by the presence of isorenieratene, a pigment derived from anoxygenic photosynthetic sulphur bacteria (Fig. 4.4A; cf. Passier *et al.*, 1999a; Menzel *et al.*, 2002). Consequently, sedimentary pore waters were anoxic during sapropel deposition, resulting in significantly less oxic degradation of organic matter and biomarkers. The largest contents of the four phytoplanktonic biomarkers within the sapropel are observed at Sites 967 and 964 (Fig. 4.3 and 4.6). At Site 969, OC-normalized biomarker contents were generally lower. This may have been caused by a lower export flux of biomarkers or a higher export flux of TOC. During deposition of the homogeneous intervals below and above the sapropel, the pore waters were probably oxic and the organic matter (including the biomarkers) was severely affected by oxic degradation processes. It has been shown that biomarkers are more susceptible to oxic degradation than TOC (Hoefs *et al.*, 2002; Sinninghe Damste *et al.*, 2002c), which probably explains the decrease in biomarker content (normalized to OC) outside the sapropel albeit that this may also partly be due to a larger contribution to TOC of terrestrial TOC. The significant difference in redox conditions during deposition has also implications for the *relative* biomarker distribution since sterols like dinosterol are degraded to a greater extent than other marine biomarkers such as alkenones and long-chain diols/keto-ols (Hoefs *et al.*, 2002; Sinninghe Damste *et al.*, 2002). During oxic depositional conditions, formation of loliolide from fucoxanthin is highly unlikely since it is an anoxic degradation product (Repeta, 1989) and carotenoids are very sensitive to oxic degradation. These considerations indicate that there are severe complications to compare biomarker contents from within the sapropel with those from the homogeneous intervals (Fig. 4.3 and 4.6). However, because sedimentary pore waters were anoxic during sapropel formation (Menzel *et al.*, 2002), biomarker contents within the sapropels can be compared directly. In fact, they were transformed to ARs to remove potential "dilution" effects of the inorganic matrix and to obtain further insights concerning the differences in export production between these three different sites studied (Fig. 4.4A-E).

Phytoplanktonic biomarkers generally showed a strong increase in ARs towards the centre of the sapropel, reflecting an increase in export production to the seafloor caused by increased productivity (Fig. 4.4B-E), and a subsequent decrease. These biomarker AR profiles generally correspond well with the TOC profile at a particular site; e.g. the maximum ARs of biomarkers at Site 967 is reached at one third of the sapropel (Fig. 4.4B-E), just as observed for the TOC profile (Fig. 4.3). In general, highest ARs were observed at Site 969, in

good agreement with the high TOC values for this site. Enhanced export productivity is noted for all four plankton taxa but the increase from the base of the sapropel to the centre is most evident for loliolide/isololiolide, the biomarker for diatoms (Fig. 4.4). Diatoms are the most important phytoplankton species in spring blooms and upwelling events, if silicate is delivered to the photic zone (Nybakken, 1993; Abrantes and Moita, 1999) and thus indicate nutrient-rich conditions. Consequently, the rapid increase in loliolide/isololiolide ARs reveals a rapid change to nutrient-rich conditions, probably caused by the increased nutrient delivery from the Nile and surrounding rivers as a consequence of the increased monsoonal activity (e.g. Rossignol-Strick, 1985). Dinosterol and C30 1,15-diollketo-ol ARs showed successive increase in phytoplankton growth, with highest ARs at the middle part of the sapropel. An increase in the ARs of alkenones in the upper part of the sapropel and succeeding decrease of loliolide/isololiolide ARs indicates most probably a tendency towards nutrient-poorer conditions.

Sapropels at sites 967 and 964 show alkenone ARs corresponding directly to their TOC profile (Figs. 4.3 and 4.4C). It is worthy of note that Site 964 showed highest ARs of alkenones implying that growth conditions favoured haptophytes, which proliferate at lower nutrient conditions (Table I, Fig. 4.4C, Fig. 4.8). Lower nutrient conditions favour smaller photosynthetic organisms, like haptophytes and very small flagellates that have a proportionately greater surface area to adsorb the nutrients, but a lower relative need (Nybakken, 1993).

Reconstruction of phytoplankton composition during sapropel deposition

Although ARs of biomarkers provided direct insights into changes in export production of the different phytoplankton species, changes in the phytoplankton composition are somewhat difficult to assess from these data. To overcome these problems, relative abundances of biomarker were used to reconstruct phytoplankton patterns during sapropel formation. Based on biomarker contents the relative distribution of the four main phytoplankton classes during sapropel formation was determined (Fig. 4.8). To some degree this is a biased view of export productivity, because biomarker contents may vary depending upon the type of algae and even within one class of algae (e.g. Brassell, 1993).

Considering the diatom population at Site 967, the contribution of diatoms is highest in the lower part of the sapropel and decreases through the sapropel. This probably reflects the nutrient supply at this site derived from the Nile River. The sapropel at Site 969 showed a successive increase in diatom populations reaching highest abundances in the middle part of the sapropel at the maximum of TOC content. This probably indicates that the high productivity of diatoms in the central part of the eastern Mediterranean basin (Fig. 4.4B) was for a substantial part responsible for the significantly increased TOC flux. At Site 964, the diatom population appears with sapropel onset and remained constant during sapropel formation.

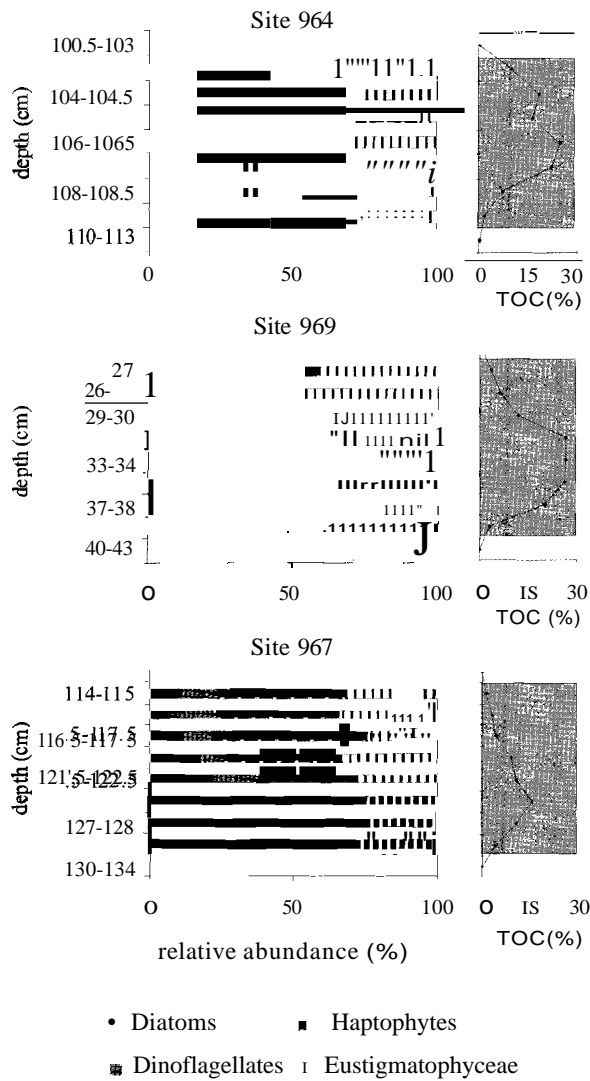


Figure 4.8 Relative distribution of four phytoplankton classes at sapropel Sites 967, 969 and 964 and their TOC profile,

Generally, the relative abundances of loliolide/isololiolide in the sapropels correspond roughly with their TOC profiles, which may indicate a consistent contribution of diatoms to TOC accumulated in these sapropels. In contrast, haptophyte and eustigmatophyte algal abundances decrease relative to the other two algal classes, except at Site 964, where relatively high amounts of haptophytes are maintained during sapropel formation, possibly resulting from less nutrient-rich conditions.

The presence of both loliolide isomers was previously reported from sediments underlying highly productive surface waters e.g. Peruvian shelf (Repeta, 1989) and from Mediterranean sapropels (ten Haven *et al.*, 1987b). Based on isorenieratene data and diatom patterns, nutrient supply probably triggered high productivity at the easternmost part of the Levantine basin, subsequently spreading to the western part of the Levantine basin. Consequently, excessive oxygen depletion resulted in euxinic conditions up into the upper water column. Continued high productivity was controlled by the release of regenerated phosphate from the sediment resulting in high C_{org} burial. In addition, the increase of the abundances in diatoms and dinoflagellates relative to the haptophytes and eustigmatophytes in the standing crop during sapropel deposition can be considered as evidence for nutrient rich and highly productive episodes. Based on reconstructed SST data, changes in the phytoplankton composition were not influenced by SST variations, which is consistent with SST data reported by Rinna *et al.* (2002) for another Pliocene, TOC-rich sapropel.

$\delta^{13}C$ results of alkenones and loliolide-palaeoproxy of enhanced biological productivity?

To further investigate the increase in productivity during sapropel formation, changes in the carbon isotopic compositions of alkenones and loliolide (only at Site 969) were studied. The isotopic signature $\delta^{13}C$ depends on factors such as light, concentration and $\delta^{13}C$ of DIC, growth rate, cell size and morphology, and species composition (Rau *et al.*, 1996; Laws *et al.*, 1995; Popp *et al.*, 1998; Rost *et al.*, 2002). Because of the absence of carbonate skeletons in the sapropel by overprinting or dissolution caused by the prevailing palaeoenvironmental conditions, the $\delta^{13}C_{CO_2(aq)}$ could not be estimated. Consequently, it was not possible to calculate the carbon isotopic fractionation effect during photosynthesis ($\epsilon_p = \delta^{13}C_{CO_2(aq)} - \delta^{13}C_{biomass}$). However, two features were observed related to the $\delta^{13}C_{C_{37:2}}$ alkenone records measured in the homogeneous ooze marls and sapropels. Firstly, measurements in the homogeneous intervals at Sites 967 and 964 showed approximately equal values. In the sapropels a slight depletion of 0.3-1‰ in $\delta^{13}C$ is observed. Secondly, Site 969 showed a general depletion in the $C_{37:2}$ alkenones of 1‰ reaching values of -27.4‰. $\delta^{13}C$ measurements of loliolide/isolololide also showed a depletion of ca. 1‰ through the sapropel, similar to the observation of the $\delta^{13}C$ of $C_{37:2}$ alkenones at all three sites. The anticipated increase in $^{13}C/^{12}C$ of the phytoplankton population resulting from an increased rate of uptake of CO_2 (relative to the CO_2 supply) during times of high productivity was not found. Assimilation of isotopically light DIC (e.g. from riverine and anoxic deep water) in foraminifera and $\delta^{13}C_{(TOC)}$ was reported during deposition of sapropel S5 at Site 967 (Struck *et al.*, 2001). Extensive recycling of respired CO_2 close to the chemocline during enhanced productivity could provide an explanation for the depleted $\delta^{13}C$ values. The isotopic fractionation (ϵ_p) depends on growth rate/ $[CO_2]_{aq}$ (Bidigare *et al.*, 1997; Riebesell *et al.*, 2000) and would thus be expected to decrease upon increased productivity. This would, however, be counteracted by increased CO_2 concentrations and isotopic depletion of DIC by substantially increased recycling of isotopically depleted, respired CO_2 formed by OM mineralisation and advection to the photic zone by occasional erosion of the chemocline during storms. Based on the lighter $\delta^{13}C$ values of $C_{37:2}$ alkenones at Site 969, recycling of respired CO_2 was probably more intensive at this site. This is consistent with the highest

isorenieratene ARs at this site compared with Sites 967 and 964, indicating a shallower chemocline enabling a more substantial delivery of respired, isotopically depleted CO₂ to the photic zone.

CONCLUSIONS

Biomarkers representing four classes of phytoplankton were used to obtain insights into the changes in export productivity during sapropel formation in the eastern Mediterranean basin. Enhanced productivity resulted in increased export production and consequently led to oxygen depletion in the pore waters and water column. High relative abundances of diatoms at the lower part of sapropel, Site 967 and the increasing tendency at Site 969 indicated that most likely nutrients were transported from the Nile and surrounding rivers into the eastern basin, which spread across to the western part of the Levantine basin. Based on the $U_{37}^{k'}$ data, productivity was not influenced by changes in sea surface temperature, but was mainly nutrient-controlled. Compound specific measurements of diatom and haptophyte biomarkers showed no significant changes during sapropel formation most probably implying enhanced recycling of CO₂ from below the chemocline, which probably buffered the growth rate effect on isotope fractionation in lipids.

ACKNOWLEDGEMENTS

We thank the Ocean Drilling Program, Bremen, for supply of samples, IPPU for funding a Ph.D. position, M. Kienhuis for assistance with the inn-GC-MS at NIOZ, T. Zalm for analytical help at the University Utrecht, Enno Schefuss and the two referees for helpful discussions.

Chapter 5

Membrane tetraether lipids of planktonic Crenarchaeota in Pliocene sapropels of the eastern Mediterranean Sea

Diana Menzel, Ellen C. Hopmans, Stefan Schouten and Jaap S. Sinninghe Damste

ABSTRACT

The distribution of glycerol dibiphytanyl glycerol tetraethers (GDGTs), biomarkers of planktonic crenarchaeota, was studied in three time-equivalent Pliocene sapropels as well as in the homogeneous intervals, below and above the sapropel. In both the homogeneous intervals and sapropels the dominance of GDGT-O and crenarchaeol among the GDGTs indicated planktonic crenarchaeota as their source similar to what was found in many other marine sediments. In the homogeneous intervals highest GDGT abundances (normalized to TO_e) were measured at the easternmost study Site 967 of the eastern Mediterranean Sea and decreased at the central and western Sites 969 and 964. Within the three studied sapropels large variations in GDGT abundance were observed. The newly established sea surface temperature (SST) proxy, the TEX₈₆ index, derived from GDGTs of planktonic crenarchaeota was used to estimate past SST. Comparison with previous obtained SST data using the alkenones from haptophyte algae revealed substantial differences. Whereas the U₃₇^K-based SSTs showed almost constant values of ca. 25°C in both the homogeneous intervals and the sapropels, the TEX₈₆-based SSTs were 26-29°C in the homogeneous intervals and decreased to 15-17°C in the sapropels. The TEX₈₆-based SST values outside the sapropel probably reflect summer SST based on a comparison with the present-day Mediterranean Sea. The surprisingly low TEX₈₆-based SST estimates for the sapropels showed similarities with those obtained for the contemporary euxinic Black Sea. The marine crenarchaeota of the modern Black Sea thrive at the deeper and colder chemocline, leading to a reduction in TEX₈₆ which in turn would result in artificially low SST estimates. A similar situation is inferred for the Pliocene eastern Mediterranean during sapropel deposition since the SST anomaly co-occurs with the build-up of a shallow chemocline.

INTRODUCTION

Life on Earth can be classified into three fundamentally different domains: Bacteria, Archaea and Eukaryota (Woese, 1987). Archaea are known to live under extreme environmental conditions, such as high temperature, high salinity, high pressure, anoxia, and low and high pH, that are hostile to most other forms of life. Archaea are divided into three kingdoms, Crenarchaeota, Euryarchaeota and Korarchaeota (Woese *et al.*, 1990; Barns *et al.*, 1996; Takai and Sako, 1999). Since the application of molecular techniques to microbial

ecology, in particular the use of 16S rRNA as a molecular marker, archaea have revealed to be widespread in different ecosystems and have been shown not to be restricted to extremophilic environments as was previously thought (Ward *et al.*, 1992). A particularly exciting result was the discovery of the widespread occurrence of planktonic archaea in marine plankton in the Pacific Ocean and coastal waters of North America (Fuhrmann *et al.*, 1992; de Long, 1992). Among marine archaea, two major groups originating from the euryarchaeal and crenarchaeal group were identified in oceans, lakes and polar waters (e.g. Hershberger *et al.*, 1996; McGregor *et al.*, 1997; Massana *et al.*, 1998). Pelagic euryarchaeota and crenarchaeota showed different patterns of abundance in the open sea. High abundances of crenarchaeota accounting for up to 40% of total DNA-containing picoplankton in meso- (150-1,000 m) and bathypelagic waters (1,000-3,500 m) (Karner *et al.*, 2001; Church *et al.*, 2003) were detected. In contrast, pelagic euryarchaeota showed higher abundances in coastal surface waters (Massana *et al.*, 1997; Murray *et al.*, 1999b; de Long *et al.*, 1999).

Membrane lipids of cultivated hyperthermophilic crenarchaeota consist of diphytanyl glycerol diethers and glycerol dibiphytanyl glycerol tetraethers (GDGTs), (de Rosa and Gambacorta, 1988). The occurrence of ether-bound acyclic and cyclic biphytanes in particulate organic matter (POM) from the water column and surface sediments (e.g. Hoefs *et al.*, 1997; King *et al.*, 1998) as detected by chemical degradation studies, hinted to the presence of planktonic crenarchaeota, and, thus confirmed the molecular ecological studies (e.g. Karner *et al.*, 2001). The development of a high performance liquid chromatography/mass spectrometry technique has enabled the characterization of intact GDGTs (Hopmans *et al.*, 2000). Using this technique, marine crenarchaeota were found to contain GDGTs with zero to four cyclopentane rings (Schouten *et al.*, 2000). A novel GDGT containing four cyclopentane rings and one cyclohexane ring was exclusively found in planktonic crenarchaeota and was called crenarchaeol (Schouten *et al.*, 2000, Sinninghe Damste *et al.*, 2002a). The biosynthesis of this GDGT, in particular the cyclohexane ring, is thought to be a membrane adaptation to allow these descendants of (hyper)thermophilic crenarchaeota to cope with the relatively low temperatures of the ocean (Sinninghe Damste *et al.*, 2002a). The dominant presence of these membrane lipids confirmed their high contribution to the marine picoplankton in modern oceans (Schouten *et al.*, 2000; Sinninghe Damste *et al.*, 2002a).

The number of cyclopentane rings in GDGTs of cultivated (hyper)thermophilic archaea increases with increasing growth temperature (Gliozzi *et al.*, 1983). A study of marine surface sediments showed that non-thermophilic crenarchaeota also adjust the number of cyclopentane rings in their GDGT membrane lipids according to temperature (Schouten *et al.*, 2002). This response was quantified in the so-called TEX₈₆ index (Schouten *et al.*, 2002), which revealed a strong linear correlation with sea surface temperature (SST) and can be used to reveal past SST (Schouten *et al.*, 2003). In this study we analysed GDGTs in three time-equivalent Pliocene sapropels to obtain insight in temporal and spatial changes in the abundances and distribution pattern of this biomarker. Additionally, the newly established palaeo proxy for SST reconstruction, the TEX₈₆, was compared with previous results (Menzel *et al.*, 2003) obtained from a more commonly used proxy for SST reconstruction in palaeoceanography, the $U_{37}^{K'}$, which derives from the long-chain unsaturated alkenones from

haptophyte algae (Brassell *et al.*, 1986). These two SST palaeo proxies give divergent results for the three studied Pliocene sapropels. Whereas the U_{37}^K -based SST showed values of ca. 25°C, the TEX₈₆ revealed a significant trend to lower temperatures down to IS-17°C. Possible causes are discussed.

MATERIAL AND METHODS

Samples

Core samples were taken during ODP Leg 160 in the eastern Mediterranean Basin (Emeis *et al.*, 1996). Site 967 (Eratosthenes Seamount) and Site 969 (Mediterranean Ridge) are located in the Levantine Basin. Site 964 is located in the Ionian Basin (Fig. 5.1a). The detailed chronology for these cores obtained by astronomical tuning enabled us to select three laterally equivalent sapropels with an age of 2.943 Ma (Lourens *et al.*, 1996). Relevant sections (967C-8H-4, 111-134 cm; 969E-6H-6, 23-43 cm; 964D-IOH-1, 100.5 -113 cm) were sub-sampled in 0.5-1.5 cm slices above, through and below the sapropel. Total organic carbon (TOC) was reported previously and showed distinct differences between these sapropels (Nijenhuis *et al.* 1998; Fig. 5.1 b).

Lipid analyses

Ground, freeze-dried sediment samples (0.1 to 3 g) were Soxhlet extracted with dichloromethane/methanol (1:1, v/v) mixture for 24 h. The extracts were concentrated with a rotary evaporator at 30°C. An aliquot of the total extract (1.5 to 3 mg) was fractionated using a Pasteur capillary pipette (150 mm length) packed with Al₂O₃ (activated for 2.5 h at 120°C). The apolar fraction (F1) was eluted using a mixture of hexane/dichloromethane (9:1, v/v; 4 ml). Subsequently, the ketone fraction (F2) was eluted using hexane/dichloromethane (1:1, v/v; 4 ml). Finally, the polar fraction was obtained using dichloromethane/methanol (1:1, v/v; 4 ml). The polar fraction was used to identify and quantify glycerol dibiphytanyl glycerol tetraethers (GDGTs) by high performance liquid chromatography/mass spectrometry analyses (HPLC/MS). Absolute GDGT amounts (µg g⁻¹ dry weight sediment) were used to calculate accumulation rates (ARs), assuming (i) a synchronous start and end of sapropel deposition at the three locations, (ii) a duration of sapropel deposition of 7000 years (Nijenhuis and de Lange, 2000) and (iii) a constant sedimentation rate during sapropel deposition (Menzel *et al.*, 2002). ARs in the homogeneous intervals were not calculated because sedimentation rates are expected to be different during times of deposition of sapropel and the homogeneous intervals.

High performance liquid chromatography/mass spectrometry (HPLC/MS)

Analyses were performed using an HP (Palo-Alto, CA, USA) 1100 series LC-MS equipped with an auto-injector and Chemstation chromatography manager software. Separation was achieved on a Prevail Cyano column (2.1 x 150 mm, 3 µm; Alltech, Deerfield, IL, USA), maintained at 30°C. Injection volumes varied from 1 to 5 µl. Tetraethers were eluted isocratically with 99% A and 1% B for 5 min, followed by a linear gradient to 1.8% B in 45 min, where A = hexane and B = propanol. Flow rate was 0.2 ml/min. After each

analysis the column was cleaned by back-flushing hexane/propanol (90:10, v/v) at 0.2 ml/min for 10 min. Detection was achieved using atmospheric pressure positive ion chemical ionization mass spectrometry (APCI-MS) of the eluent. Conditions for APCI-MS were as follows: nebulizer pressure 60 psi, vaporizer temperature 400°C, drying gas (N_2) flow 6 l/min and temperature 200°C, capillary voltage -3 kV, corona 5 μA (~ 3.2 kV). Positive ion spectra were generated by scanning m/z 950-1450 in 1.9 s. Mass spectra typically represented the peak-apex spectrum and are corrected for background.

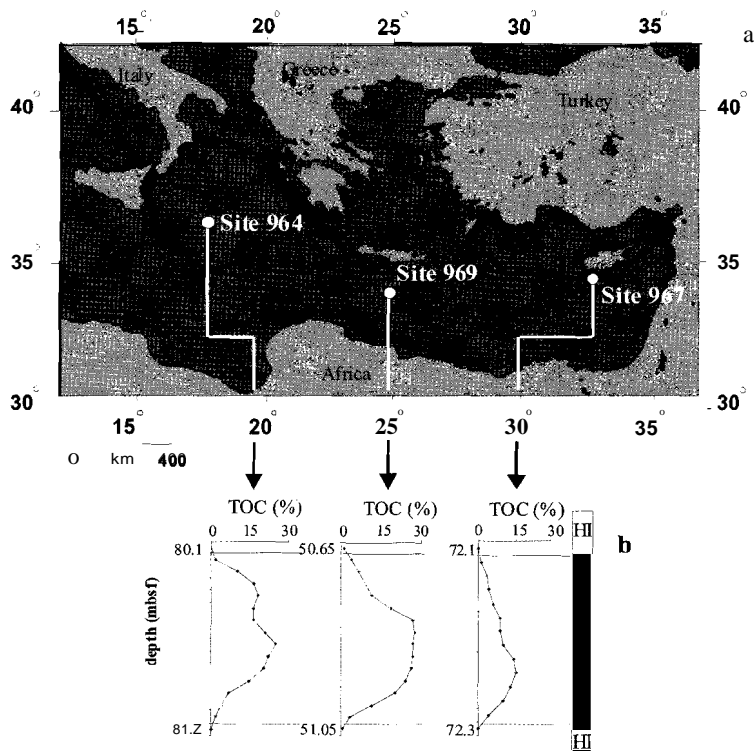


Figure 5.1 (a) Location of ODP drilling sites and (b) lithological description (HI = homogeneous calcareous ooze, S = sapropel) and TOC profiles of the investigated Pliocene sapropel (data from Nijenhuis *et al.*, 1998).

RESULTS

GDGT distribution

The HPLC/MS base peak chromatograms revealed the presence of the GDGTs I-VI in both, the sapropels and the homogeneous sediments below and above the sapropel at the three sites (Fig. 5.2). GDGT-O (I) and crenarchaeol (V) were the dominant GDGTs (Fig. 5.2). The GDGT distribution between the homogeneous interval and sapropel of Site 967 indicated internal variations in the relative distribution of the analysed GDGTs. In the homogeneous

intervals of the sapropels (Fig. 5.2a) higher relative abundances of GDGT-2, GDGT-3 and crenarchaeol (V+VI) were detected, compared with the GDGT distribution in the sapropel (Fig. 5.2b). Smaller variations in the relative distribution of GDGTs within the three time-equivalent sapropels were also observed as is expressed by variations in TEX₈₆ values (see below).

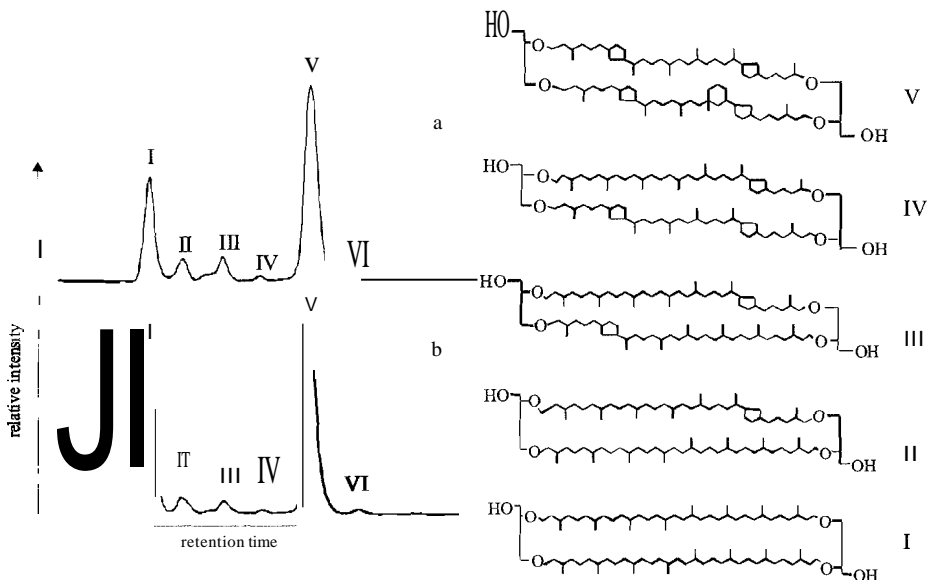


Figure 5.2 HPLC/MS base peak chromatograms of (a) the homogeneous interval of ODP Site 160-967C-8H-4, 130-134 cm and (b) the sapropel of ODP Site 160-967C-8H-4, 121.5-122.5 cm series were identified as: GDGT-O=I, GDGT-1=II, GDGT-2 = III, GDGT-3 = IV, crenarchaeol = V and an isomer of crenarchaeol =VI (cf. Hopmans et al., 2000).

Temporal and spatial distribution pattern of tetraether lipid abundance

The total GDGT content showed below sapropel deposition at Site 967 values of 1670 $\mu\text{g/g TOe}$ and reached a maximum of 2790 $\mu\text{g/g TOe}$ when the TOe content was the highest (Fig. 5.3). After the maximum was reached, the GDGT content decreased substantially in the central part of the sapropel to values of about 100 TOe and increased again in the upper part of the sapropel to 1600 TOe. Above the sapropel the GDGT is 550 $\mu\text{g/g TOe}$. Site 969 showed below the sapropel GDGT amounts of 640 TOe (Fig. 5.3). In the lower and central part of the sapropel the values remained relatively constant and then increased to maximum value of 2150 TOe. After the maximum was reached, the GDGT content decreased noticeably towards the top of the sapropel to values of about 150 TOe. Above the sapropel the GDGT content decreased to values of 40 TOe. Site 964 revealed below the sapropel GDGT values of 160 $\mu\text{g/g TOe}$ (Fig. 5.3). At the base of sapropel the GDGT content increased to values of 1200 $\mu\text{g/g TOe}$, but then decreased considerably to values of about 100 $\mu\text{g/g TOe}$ in the central part of the sapropel. Maximum concentrations of GDGT occur in the upper part of the sapropel with 1900 TOe. Above the sapropel the GDGT content was negligible.

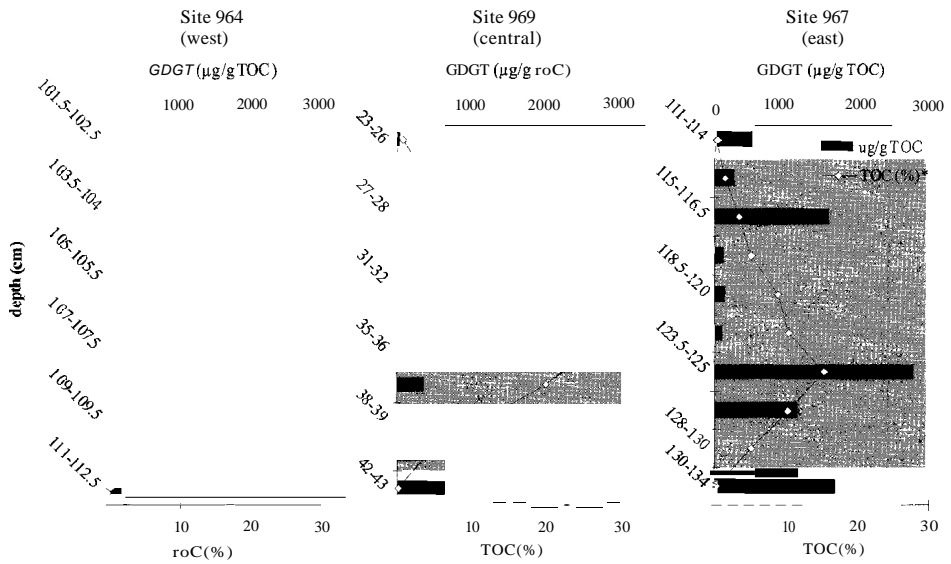


Figure 5.3 Summed GDGT concentrations (normalized to TOC) and TOC content (*data from Nijenhuis *et al.* 1998) plotted against depth for the three sapropels at ODP Sites 967, 969 and 964, Light grey shaded regions represent the sapropel. White regions represent the homogeneous calcareous ooze.

In the lower part of sapropel at Site 967, GDGT accumulation rates (ARs) (see experimental for details) reached a maximum value of $12.3 \mu\text{g m}^{-2} \text{yr}^{-1}$ and reduced to values ranging between 0.2 and $0.04 \mu\text{g m}^{-2} \text{yr}^{-1}$ at the central part of the sapropel were these low values remained up to the upper part of the sapropel (Fig. 504). At Site 969, GDGT ARs increased steadily reaching a maximum value at the central part of the sapropel with values of $17.2 \mu\text{g m}^{-2} \text{yr}^{-1}$ (Fig. 504). After the maximum was reached, GDGT ARs decreased considerably to values of $0.7 \mu\text{g m}^{-2} \text{yr}^{-1}$ at the upper part of the sapropel. Site 964 showed the lowest GDGT ARs with a slight increase in the lower part of the sapropel of $0.8 \mu\text{g m}^{-2} \text{yr}^{-1}$. Through the entire central part of the sapropel low ARs of about $0.3 \mu\text{g m}^{-2} \text{yr}^{-1}$ were shown, whereas in the upper part of the sapropel a maximum value of $4.6 \mu\text{g m}^{-2} \text{yr}^{-1}$ was reached (Fig. 504). After the GDGT AR has reached the maximum it decreased dramatically as was observed at the other two sites.

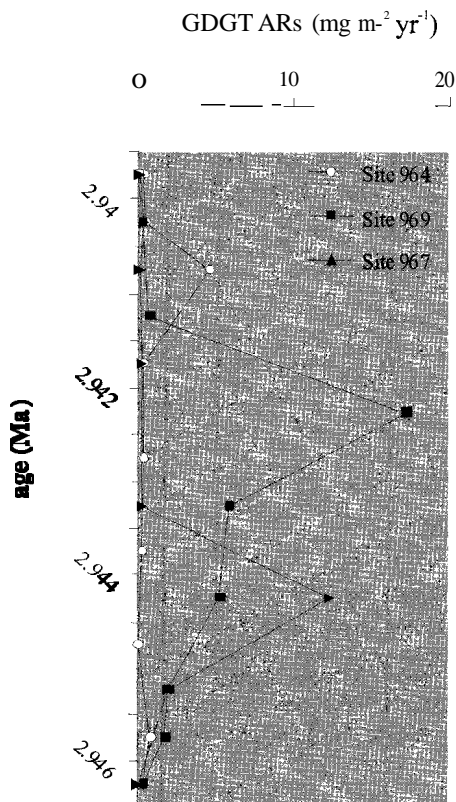


Figure 5.4 Summed GDGT accumulation rates in the three sapropels of the three ODP Sites 967,969 and 964.

Sea surface temperature estimation based on using the TEX_{S6}

The TEX_{S6} index (TetraEther index of GDGTs consisting of 86 carbon atoms) is defined as:

$$TEX_{86} = \frac{[III]+[IV]+[VI]}{[II]+[III]+[IV]+[VI]}$$

and can be used to reveal past SST (Schouten *et al.*, 2002). The distribution of GDGTs correlates with SST, i.e. with higher SST the number of cyclopentane rings of the tetraether membrane lipids increases, i.e. GDGT-2, GDGT-3 and crenarchaeol increase in abundance relative to tetraether lipids GDGT-O and GDGT-I (Fig. 5.2). The TEX_{S6} showed distinct temperature changes between the homogeneous intervals and Pliocene sapropels at all three studied ODP sites (Fig. 5.5). In the homogeneous intervals below the sapropel, the TEX_{S6} revealed highest SST at Site 969 of 29°C and slightly lower SST's at Site 967 and 964 of 27°C and 25°C, respectively. In all sapropels, the TEX_{S6}-based SST showed a substantial decrease. The largest drop (15°C) is observed at Site 967 in the lower part of the sapropel (Fig. 5.5). In the upper part of the sapropel the SST slowly increased to values of 22°C. In the homogeneous interval, above the sapropel the SST reached 26°C. At Site 969, the SST

dropped within the sapropel to values around 17°C in the central part of the sapropel and increased also slowly towards the top of the sapropel to values of 21°C. In the homogeneous interval above the sapropel the SST remained at 21°C (Fig. 5.5). In the sapropel at Site 964 the SST at the base of the sapropel was the highest with 33°C and then decreased towards the top of the sapropel to values of 18°C. In the homogeneous interval above this sapropel, some GDGT isomers were below the detection limit and no TEX₈₆ values could be obtained (Fig. 5.5).

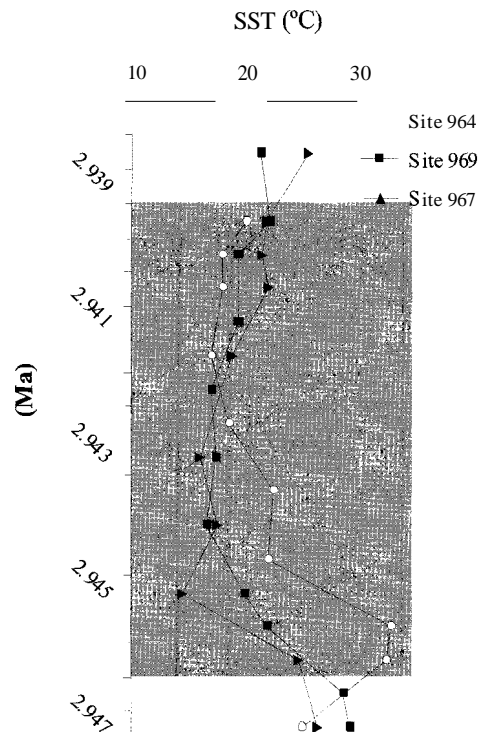


Figure 5.5 SST (°C) reconstruction based on the TEX₈₆ proxy (after Schouten *et al.*, 2002) of the three time-equivalent Pliocene sapropels of the eastern Mediterranean Sea. Light grey shaded regions represent the sapropel. White regions represent the homogeneous calcareous ooze.

DISCUSSION

Origin of GDGT lipids

GDGT-O (I) is a general archaeal core membrane lipid (e.g. Koga *et al.*, 1998) and occurs not only in planktonic crenarchaeota but also in methanogens (Koga *et al.*, 1993). Crenarchaeol (V) has been assigned as a specific core membrane lipid of planktonic crenarchaeota (Schouten *et al.*, 2000; Sinninghe Damste *et al.*, 2002a). The dominance of GDGT-O and crenarchaeol in both the homogeneous intervals and the sapropels (Fig. 5.2) is characteristic for the GDGTs of planktonic crenarchaeota (Sinninghe Damste *et al.*, 2002b; de Long *et al.*, 1998). Such GDGT membrane lipid distributions were also observed in many other marine sediments (Schouten *et al.*, 2002) and marine POM from the North Sea

(Wuchter *et al.*, 2003) and the Arabian Sea (Sinninghe Damste *et al.*, 2002b). GDGTs in the water column of the Black Sea also showed a predominance of GDGT-O and crenarchaeol in the upper 400 m (Wakeham *et al.*, 2003). By contrast, GDGTs derived from anaerobic, methane-oxidizing archaea, which reside in the deeper anoxic zone (> 1000 m water depth) have a distinct distribution of carbon isotopically depleted GDGTs. A dominance of GDGT-O and crenarchaeol in GDGT distributions was found in sinking particles collected with sediment traps in the Black Sea. The GDGTs derived from methane-oxidizing archaea were not detected in sediment traps or underlying surface sediments, showing that the sedimentary GDGTs are predominately derived from surface waters. This is apparently caused by efficient transport mechanism (e.g. grazing and production of fecal pellets) of GDGTs in surface waters (Wakeham *et al.*, 2003).

Coolen *et al.* (2002) proposed that metabolically active marine chemoorganotrophic crenarchaeota are present in late Pleistocene sapropels of the eastern Mediterranean Basin. These authors suggested that, in comparison with the homogeneous intervals, sapropels exhibit elevated microbial cell numbers with crenarchaeota constituting a fraction of ca. 16%. Increased enzyme activities of anaerobic microbial degradation using carbon substrates originating from the sapropel organic matter were measured and ascribed, in part, to metabolically active crenarchaeota (Coolen *et al.*, 2002). This indicates that the GDGTs found in our sapropels could derive from physiologically active crenarchaeota in the sapropels and do not represent chemical fossils derived from planktonic crenarchaeota. However, the GDGT abundances of a sapropel showed large fluctuation on a cm scale (Fig. 5.3), which is inconsistent with chemoorganotrophic crenarchaeota using sapropel organic matter as carbon source as the source of these GDGTs. The ^{13}C contents of biphytanyl moieties of crenarchaeol from both present-day and ancient marine environments (Hoefs *et al.*, 1997; Kuypers *et al.*, 2001) and their ^{14}C content (Pearson *et al.*, 2001) indicated that marine crenarchaeota probably fix bicarbonate. ^{13}C label experiments confirmed a light-independent bicarbonate uptake (Wuchter *et al.*, 2003), indicating chemoautotrophy and not chemoorganotrophy (cf. Coolen *et al.*, 2002) by marine crenarchaeota. In addition to the large variations in the absolute abundances of GDGTs, also large variations in the GDGT distributions within the sapropel are observed. As these represent physiological adaptation of their membrane to temperature (see detailed discussion below), this provides an additional argument for their origin from planktonic crenarchaeota and not from chemoorganotrophic crenarchaeota within the sapropel, which would encounter identical sedimentary temperature conditions.

SST reconstructions using $U_{37}^{K'}$ and TEX_{86}

$U_{37}^{K'}$ -based SST derived from the haptophyte algae revealed almost similar SST values of 24-26°C obtained in the three time-equivalent Pliocene sapropels and their corresponding homogeneous intervals (Fig. 5.6) (cf. Menzel *et al.*, 2003). In contrast, the TEX_{86} -based SST estimates showed substantial differences between the homogeneous intervals and the sapropels as well as between these sapropels (Fig. 5.6). The reason for this large difference must lie in the fact that both SST proxies originate from two different organisms occupying different habitats in the eastern Mediterranean Basin.

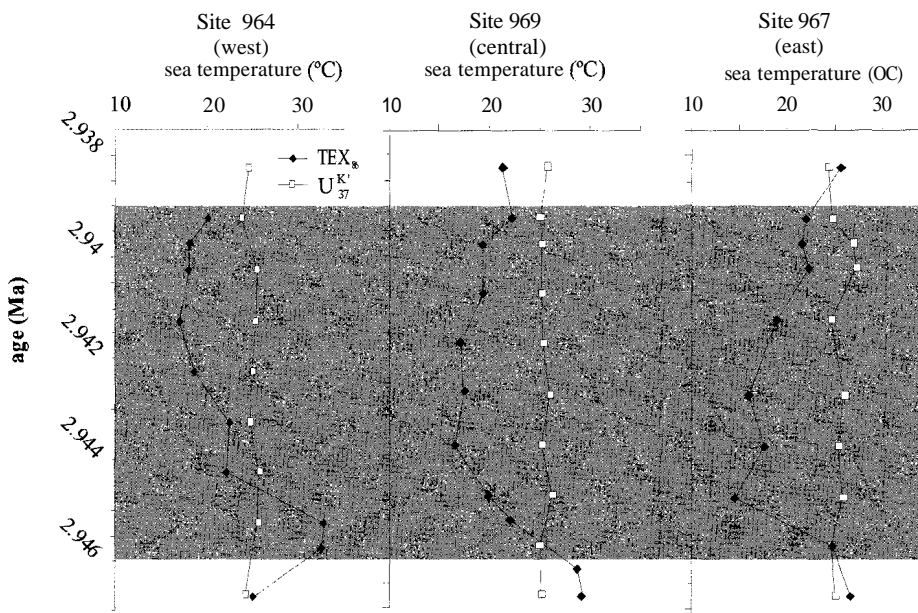


Figure 5.6 Reconstruction of the SST ($^{\circ}\text{C}$) during Pliocene sapropel deposition using two different SST proxies $U_{37}^{K'}$ and TEX_{86} in the sapropels at ODP Sites 967, 969 and 964.

In the contemporary oligotrophic eastern Mediterranean Sea the annual phytoplankton bloom occurs in winter as soon as deep water mixing occurs, providing nutrients to the photic zone, and ceases when phosphate is depleted (Krom *et al.*, 2003). After the winter bloom, water column stratification occurs in March-April, which results in the formation of a deep chlorophyll maximum that is characteristic for the remainder of the year (Krom *et al.*, 2003). Haptophytes live in the upper 200 m and are the most common eukaryotes followed by diatoms and dinoflagellates (Kimor *et al.*, 1987). An $U_{37}^{K'}$ -based SST of ca. 19°C was estimated from suspended matter collected in sediment traps (Ternois *et al.*, 1997) and surface sediments of the Mediterranean Basin (Emeis *et al.*, 2000), reflecting the SST in winter when haptophyte production is most pronounced. Planktonic crenarchaeota typically have their main growth phase during the annual cycle outside the main period of phytoplankton blooms. A negative correlation was obtained between the abundance of chlorophyll *a* and particulate organic carbon and the abundance of crenarchaeota for Antarctic coastal waters and Southern Ocean (polar regions) (Murray *et al.*, 1998; Murray *et al.*, 1999b) and the Santa Barbara Channel (Murray *et al.*, 1999a). Schouten *et al.* (2002) also inferred different growing seasons for haptophytes and marine crenarchaeota in the eastern South Atlantic. Indeed, TEX_{86} values in surface sediments of the eastern Mediterranean Sea indicate an SST of ca. 26°C (Sinninghe Damste *et al.*, unpublished data), which reflects the SST during summer in the Mediterranean Sea. Thus, the $U_{37}^{K'}$ - and TEX_{86} -based SSTs in the homogeneous intervals (thought to reflect periods in the Pliocene comparable with the modern oligotrophic eastern Mediterranean Sea)

are likely reflecting the winter and summer SST, respectively. These SST estimates are realistic values considering the warmer climate conditions during the Pliocene, compared with the present-day conditions (e.g. Poore and Sloan, 1996).

During sapropel deposition, the precession minimum caused warmer and especially more humid climate conditions with a stronger seasonal climate contrast (e.g. Rossignol-Strick *et al.*, 1982; Rossignol-Strick, 1985; Prell and Kutzbach, 1987; Hilgen, 1991). Due to warmer summer and colder winter periods, lower U_{37}^K -based and higher TEX₈₆-based SSTs could be expected, if the timing of the bloom season did not change. The $U_{37}^{K'}$ values in the sapropel, compared with those in the homogeneous intervals, indicated a maximum increase in SST of 1°C. U_{37}^K -based SST's obtained for other Pliocene sapropels (3.058 Ma, Lourens *et al.*, 1996) showed a slight decrease of 1°C in SST (Rinna *et al.*, 2002). U_{37}^K values of late Pleistocene to Holocene sapropels, relative to those of the homogeneous intervals also only revealed a small change in SST of a few degrees (Emeis *et al.*, 1998). In strong contrast with the $U_{37}^{K'}$ -based SST estimates in the Pliocene sapropels, the TEX₈₆-based SST revealed an unexpected cooling, i.e. a drop of 10-12°C in SST (Fig. 5.6), which appears in contrast with the reported climatic change. This must indicate that either the ecological niche of the planktonic crenarchaeota or the timing of their growth season must have been fundamentally different at the time of sapropel deposition.

During Pliocene sapropel deposition a substantial increase in primary productivity, compared to the situation before and after sapropel deposition (represented by the homogeneous intervals), is indicated by the enhanced Ba flux (Nijenhuis and de Lange, 2000) and was caused by increased nutrient delivery to the basin (Passier *et al.*, 1999a). The increased primary productivity is also revealed by increasing accumulation rates of specific biomarkers for the major groups of phytoplankton (diatoms, haptophytes, dinoflagellates, eustigmatophytes) towards the centre of the sapropel (Menzel *et al.*, 2003). The enhanced organic matter flux to the sea floor led to oxygen depletion, sulphate reduction and ultimately to the presence of sulphide in the photic zone of the water column. The presence of such a shallow chemocline was indicated by the presence of isorenieratene derivatives (Passier *et al.*, 1999a) and intact isorenieratene (Menzel *et al.*, 2002), the characteristic pigment of anaerobic, photolithotrophic green sulfur bacteria, which require both sulphide and light. Such conditions are currently found in the Black Sea (Repeta *et al.*, 1989), the world's largest euxinic basin. Therefore, the Black Sea is good model to compare environmental situations related to sapropel deposition in the Mediterranean Sea. Marine primary productivity in the Black Sea (210 gC m⁻²yr⁻¹, Karl and Knauer, 1991) is substantially higher than in the oligotrophic eastern Mediterranean Sea (26 gC m⁻²yr⁻¹, Bethoux, 1989), and similar to that estimated for the eastern Mediterranean Sea during Pliocene sapropel deposition (ca. 150 gC m⁻²yr⁻¹), based on Ba profiles (Passier *et al.*, 1999a). The Black Sea shows in general two major phytoplankton blooms, a diatom and silicoflagellate bloom in spring and a haptophyte bloom in autumn (Honjo *et al.*, 1987).

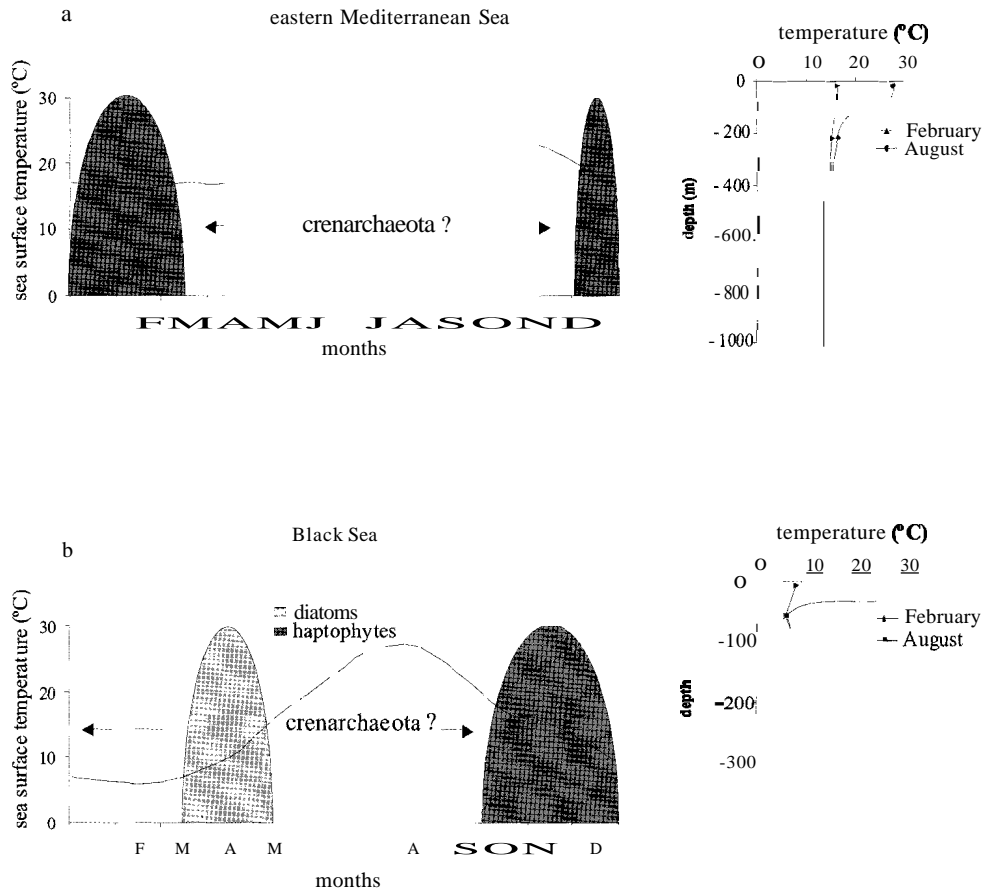


Figure 5.7 Illustration of monthly (average) sea surface temperature (SST, °C), water temperature depth profile and the seasonal cycle of the major phytoplankton bloom in (a) the eastern Mediterranean Sea and (b) the Black Sea based on data from (www.nemoc.navy.mil/images/climo/med).

The $U_{37}^{K'}$ -based SST of 13°C obtained from the Black Sea surface sediments (Freeman and Wakeham, 1992) is reflecting autumn SST's. A TEX_{86} -based SST of SoC was determined for settling particles collected with a sediment trap and 11°C for surface sediment (0-1 em) (Schouten *et al.*, 2002). This TEX_{86} value gives an even lower SST than observed with the $U_{37}^{K'}$ -based SST. Both values are low considering the means of the annual range in SST for the Black Sea (Fig. 5.7). The low TEX_{86} -based SST, compared with the $U_{37}^{K'}$ -based SST, shows similarities of SST data obtained from the studied Pliocene sapropels (Fig. 5.8). It should be noticed that the SSTs reported from the Black Sea show in general colder SSTs, compared with the Mediterranean Sea, because of its location at higher latitude.

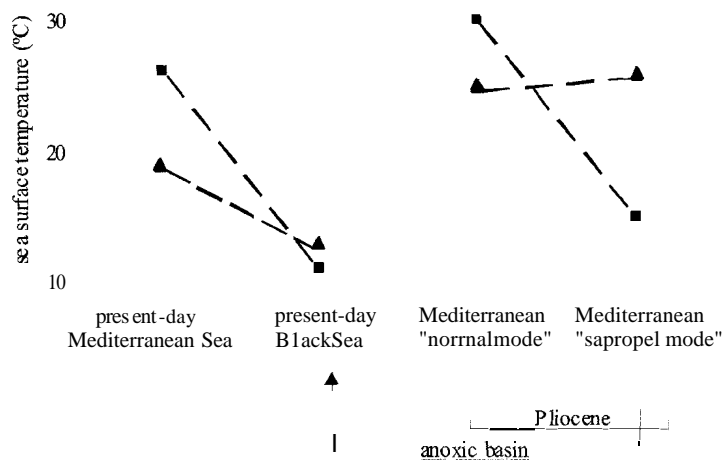


Figure 5.8 Sea surface temperature reconstruction using the $U_{37}^{K'}$ (▲) and TEX_{86} (■) between the Mediterranean Sea at present-day, during homogeneous intervals and sapropel deposition as well as the present Black Sea.

Water column studies of the Black Sea could provide insight in the observed TEX_{86} -based SST "anomaly". In the Black Sea water column, a sharp peak in GDGT concentrations at the chemocline (ca. 100 m) was revealed for both summer (July 1988) (Wakeham *et al.*, 2003) and winter (December 2001) without a substantial difference in absolute abundance between the summer and winter situation (Sinninghe Damste *et al.*, unpublished data), suggesting that there is no large contrast in the seasonal abundance of the crenarchaeota. If the GDGT distribution would reflect the average annual SST, temperatures of ca. 17°C would be expected. However, average TEX_{86} -based SSTs of 9°C in July 1988 (Schouten *et al.*, 2002) and 6°C in December 2001 (Sinninghe Damste *et al.*, unpublished data) for water column POM from 0-400 m were measured. This is in accordance with the relatively low TEX_{86} -based estimates for sediment traps and the surface sediment. The relatively low TEX_{86} -based SST estimates may be related to the specific distribution of crenarchaeota in the Black Sea (i.e. peaking at the chemocline) in combination with the strong thermal stratification in summer (Fig. 5.7). This stratification results in low temperatures (ca. 8°C) at the chemocline throughout the annual cycle. It is likely that this population of crenarchaeota also contributes to the GDGT flux to the sediments since, in contrast to the much deeper dwelling population of methane-oxidizing crenarchaeota, these archaea can still be grazed upon. This could explain the anomalously low TEX_{86} -based SST estimates in the Black Sea.

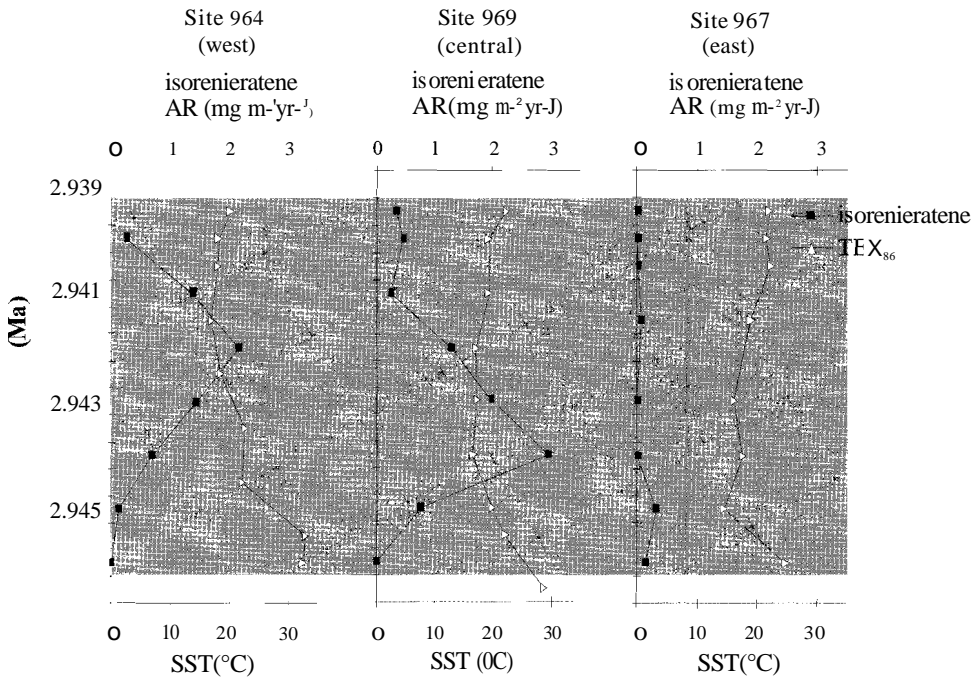


Figure 5.9 Comparison of isorenieratene accumulation rates and TEX_{s6} -based SST estimates in the sapropel at Sites 967, 969 and 964.

It is likely that the observed TEX_{s6} -based SST "anomaly" in the Pliocene sapropels results from the same mechanism as in the Black Sea. Indeed, the large drop in TEX_{s6} -based SST is in all sapropels associated with the shoaling of the chemocline (Fig. 5.9). It seems that the availability of nutrients drives the planktonic crenarchaeota to a different ecological niche, in contrast with the oligotrophic Mediterranean Sea, where the TEX_{s6} -based SST derives from the upper 200 m during the summer (Fig. 5.7). However, at present, the ecophysiological factors determining the abundance of planktonic crenarchaeota are still unknown to fully understand this relationship.

CONCLUSIONS

The dominance of GDGT-0 and crenarchaeol among the GDGTs, large variations in absolute abundances of GDGTs and their GDGT distribution (expressed as TEX_{s6} -index) within the three Pliocene sapropels and their corresponding homogeneous intervals indicated the presence of fossil GDGTs derived from planktonic crenarchaeota. Differences in $U_{37}^{K'}$ - and TEX_{s6} -based SST estimates obtained in both, the homogeneous intervals and sapropels are due to the fact that both SST proxies originate from two different organisms occupying different habitats in the eastern Mediterranean Basin. Whereas the $U_{37}^{K'}$ -based SST estimates showed hardly any differences between the homogeneous intervals and the sapropels, the

TEX_{s6}-based SST estimates revealed a cooling of 10-12°C during sapropel deposition. TEX_{s6}-based SST estimates obtained in the homogeneous intervals showed similarities with the modern oligotrophic Mediterranean Sea, while the TEX_{s6}-based SST estimates in the sapropels showed similarities with the contemporary euxinic Black Sea. It is assumed that this TEX_{s6}-based SST trend is caused by a shallowing chemocline during sapropel deposition, which has driven planktonic crenarchaeota to a different ecological niche compared with the situation during the deposition of homogeneous intervals. Ecophysiological studies on planktonic crenarchaeota are required to further unravel this TEX_{s6}-based SST "anomaly".

ACKNOWLEDGEMENTS

We would like to thank Iort Ossebaar for analytical help and IPPU for funding a Ph.D. position.

Chapter 6

Higher plant vegetation changes during Pliocene sapropel formation

Diana Menzel, Stefan Schouten, Pim. F. van Bergen and Jaap S. Sinninghe Damste

Published in *Organic Geochemistry* (2004, in press)

ABSTRACT

The $\delta^{13}\text{C}$ values of higher plant wax C_{27-33} n-alkanes were determined in three, time-equivalent Pliocene (2.943 Ma) sapropels and homogeneous calcareous ooze from three different sites forming an east-west transect in the eastern Mediterranean Basin to study the composition of the vegetation on the continents surrounding the Mediterranean Sea. A two-end member mixing model transformed the measured $\delta^{13}\text{C}$ values into the contribution of C_4 plants to the terrestrial vegetation. These calculations indicated a high C_4 plant contribution (i.e. 40-50%) in the periods just before and just after sapropel formation. During sapropel deposition the C_4 plant contribution increased by up to 20% at all sites. This is interpreted to record the increased overall plant coverage of the Mediterranean borderlands resulting from the change of formerly barren desert areas into C_4 grass-dominated savannah's as a response to the wetter climate during sapropel deposition. Enhanced accumulation rates (ARs) of long-chain n-alkanes (C_{27-33}) and n-alkan-1-ols (C_{26-30}) towards the middle of the sapropel in concert with a decrease in the *TilAl* ratio confirm an increased delivery of terrigenous organic matter at all sites. These biomarkers were probably predominantly fluviially transported to the Mediterranean Sea, not only by the Nile but by fossil wadi river systems on the northern African continent.

INTRODUCTION

Pliocene Mediterranean sapropels are characterized by extremely high total organic carbon (TOC) contents (over 30%, Emeis *et al.*, 1996), much higher than those of Quaternary sapropels. The actual mechanism responsible for the deposition of these extremely TOC-enriched sediments is still widely debated. Enhanced productivity and/or improved preservation (e.g. Canfield, 1994; Bouloubassi *et al.*, 1999; Calvert and Pedersen, 2001) or a combination of both (e.g. Passier *et al.*, 1999a) are all considered. Recently we have shown that oxygen depletion of the water column was so extreme that "Black Sea" conditions (overlapping photic and euxinic zones) prevailed in the eastern Mediterranean Sea during Pliocene sapropel formation (Menzel *et al.*, 2002). These conditions were optimal for the

preservation of marine organic matter (OM) but were probably induced by an increase in the marine primary productivity. This increased productivity resulted from the increased influx of nutrients from the continents induced by the climatic change leading to more humid conditions in the Mediterranean area.

Terrestrial OM is generally thought to represent <5% of the OM in the sapropels and to play a trivial role in the formation of sapropels. In contrast, in the homogeneous intervals just below and above the sapropels, the TOC content is much lower (<0.1%) and the terrestrial OM contribution is expected to be much higher due to its greater resistance to oxidative degradation relative to marine OM (Hoefs *et al.*, 2002). However, the values in the homogeneous intervals are higher than those of the sapropels (Fig. 6.1c; Nijenhuis and de Lange, 2000). This is in contrast to what would be expected if the homogeneous calcareous ooze contained a higher terrestrial OM fraction since Quaternary terrestrial OM is commonly isotopically depleted relative to marine OM (Tyson, 1995). This apparent contradiction may be explained if the terrestrial OM was not only comprised of C₃ plant material ($\delta^{13}\text{C} \approx -27\text{‰}$), but also contained a substantial C₄ plant component ($\delta^{13}\text{C} \approx -12\text{‰}$). A distinct east-west trend of increasingly more negative $\delta^{13}\text{C}_{\text{TOC}}$ values in both the homogeneous and sapropel intervals was also noted for the same set of sapropels (Fig. 6.1c; Nijenhuis and de Lange, 2000). This may be explained if the C₄ plant material was delivered to the eastern Mediterranean Basin predominantly by the Nile river.

At present, the tropical and subtropical climate zones of northern and central Africa covering mainly the Sahara, Sahel and Savannah zones are characterized by predominantly a C₄ plant vegetation (White, 1983). During the Pliocene the African continent was exposed to generally warmer and wetter climate/vegetation zones than at present (Haywood *et al.*, 2000). However, around 3 Ma ago, northern African environments appear to have shifted towards a drier and somewhat cooler state (deMenocal, 1995). At this time interval, pollen and other evidence suggest more widespread grassland in eastern Africa and the extension of deserts in northern Africa (Leroy and Dupont, 1994). C₄ biomass was generally of minor importance in the Miocene, but expanded substantially in the Pliocene and Pleistocene (Ceding, 1992). Subtropical African climate varied primarily at precessional periodicities (19-23 kyr), responding to precipitation changes controlled by monsoon intensity (deMenocal, 1995). Sapropel formation is directly correlated with precession minima (Northern Hemisphere insolation maxima), resulting in the increase in monsoonal activity (Rossignol-Strick, 1983).

Based on $\delta^{13}\text{C}_{\text{TOC}}$ values measured in the homogeneous intervals, we anticipated a substantial contribution of C₄ plants to the terrestrial OM before, during and after Pliocene sapropel formation. In addition, we would expect climate-induced changes in plant vegetation during formation of these sapropels favouring C₃ plant over C₄ plant vegetation with increasing humid climate conditions. To verify this hypothesis, samples from three time-equivalent Pliocene sapropels and adjacent homogeneous calcareous ooze obtained from three different sites forming an east-west transect in the eastern Mediterranean Basin were studied. Long-chain odd-carbon-numbered C₂₇ to C₃₃ n-alkanes, constituents of terrestrial higher plant epicuticular waxes (Eglinton and Hamilton, 1967), were used for compound-specific carbon isotope analyses to evaluate C₄/C₃ plant vegetation changes during sapropel formation. Additionally, accumulation rates of terrestrial n-alkanes and n-alkan-1-ols were

determined to obtain insight into the temporal and spatial contribution of terrestrial OM during sapropel deposition.

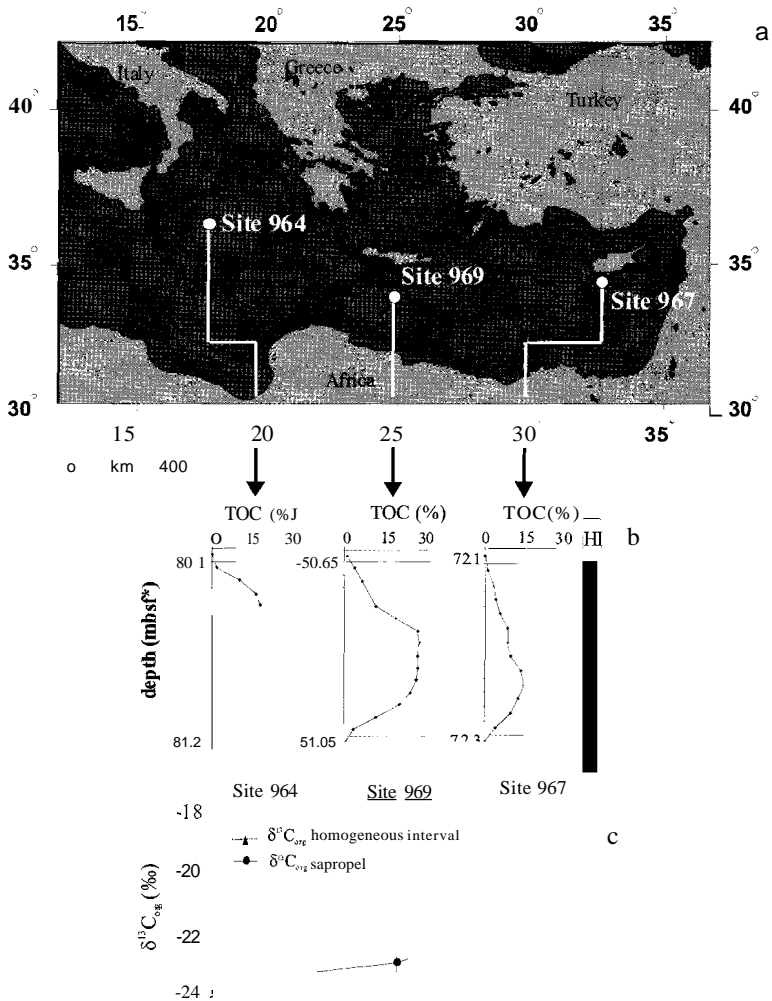


Figure 6.1 (a) Location of ODP drilling sites, (b) lithological description (HI = homogeneous interval, S = sapropel) and TOC profiles of the investigated Pliocene sapropel (data from Nijenhuis et al., 1998, * metres below seafloor) and (c) $\delta^{13}C_{TOC}$ (‰) of the homogeneous intervals and the sapropels of the eastern Mediterranean Sea (data are from Nijenhuis and de Lange (2000)). Error bars represent the standard deviation.

MATERIAL AND METHODS

Samples

Core samples were taken during ODP Leg 160 in the eastern Mediterranean Basin (Emeis *et al.*, 1996). Site 967 (Eratosthenes Seamount) and Site 969 (Mediterranean Ridge) are located in the Levantine Basin. Site 964 is located in the Ionian Basin (Fig. 6.1a). The detailed chronology for these cores obtained by astronomical tuning enabled us to select three laterally equivalent sapropels with an age of 2.943 Ma (Lourens *et al.*, 1996). Relevant sections (967C-8H-4, 111-134 cm; 969E-6H-6, 23-43 cm; 964D-IOH-1, 100.5 -113 cm) were sub-sampled in 0.5-1.5 cm slices above, through and below the sapropel. Total organic carbon (TOC) was reported previously and showed distinct differences between these sapropels (Nijenhuis *et al.*, 1998; Fig. 6.1b).

Extraction and fractionation of biomarkers

Ground, freeze-dried sediment samples (0.1 to 3 g) were Soxhlet extracted with a mixture of dichloromethane/methanol (1:1, v/v) for 24 h. The extracts were concentrated with a rotary evaporator at 30°C. An aliquot of the total extract (1.5 to 3 mg) was fractionated using a Pasteur capillary pipette (150 mm length) packed with C_{18} (activated for 2.5 h at 120°C). The apolar fraction was eluted using a mixture of hexane/dichloromethane (9:1, v/v; 4 mL). Subsequently, the saturated hydrocarbon fraction was obtained using a Pasteur capillary pipette (150 mm length) packed for 1/3 with AgNO₃-impregnated silica and for 2/3 with C_{18} (activated for 2.5 h at 120°C). This fraction was eluted with hexane. All fractions were dried under a flow of nitrogen and analysed by gas chromatography (GC), GC-mass spectrometry (MS) and isotope-ratio monitoring (irm)-GC-MS. Quantification was performed by integration of the relevant peak areas of interest and the internal standard (squalane). *n*-Alkan-1-ols were identified from the total lipid fraction (see Menzel *et al.*, 2003 for details), which was derivatised using N,O-bis(trimethylsilyl)trifluoroacetamide (30 min at 60°C).

Instrumental analysis

GC was performed on a Hewlett-Packard 6890 series gas chromatograph equipped with a fused silica capillary column (50 m x 0.32 mm or 25 m x 0.32 mm) coated with CP-Sil 5 (film thickness 0.12 μm). Helium was used as the carrier gas. The samples were injected on-column at 70°C and the oven was subsequently programmed to 130°C at 20°C/min, followed by an increase of 4°C/min to 320°C, where it remained isothermal for 10 min. Compounds were detected using a flame ionisation detector (FID).

GC-MS analyses were performed using a Hewlett-Packard 5890 series II gas chromatograph connected to a Fisons instruments VG platform II mass spectrometer operated at 70 eV, with a mass range m/z 50-650 and cycle time of 0.65 s (resolution 1000). The capillary column and temperature programme were as described for the GC analyses.

Isotope-ratio-monitoring gas chromatography-mass spectrometry (irm-GC-MS) was performed using a Finnigan Delta-plus XL-irm-GC-MS system, equipped with an on-column injector and fitted with a 25 m x 0.32 mm fused silica capillary column coated with CP-Sil5 (film thickness 0.12 μm). Helium was used as carrier gas and the oven was programmed as

described for the GC analyses. Isotopic values were calculated by integrating the m/z 44, 45 and 46 ion currents of the peaks produced by combustion of the chromatographically separated compounds and those of CO_2 -spikes produced by admitting CO_2 with a known ^{13}C content at regular intervals into the mass spectrometer. They are reported in permil versus the VPDB standard. Duplicate analyses were carried out for each sample and the results were averaged to obtain a mean value. $\delta^{13}\text{C}$ values typically have an error of <0.5 ‰.

Quantitation

Quantitation was performed by integration of the peak areas of interest and that of the internal standard (squalane for n-alkanes, nonadecan-10-one for n-alcohols). C_{26} , C_{28} and C_{30} n-alkan-1-ols, which were sometimes co-eluting with other lipids, were quantified by integration of individual peak areas in mass chromatograms using characteristic m/z values (i.e. $M+15$). Typical quantitation errors are $<10\%$. Calculations of accumulation rates (ARs) were performed using absolute biomarker amounts ($\mu\text{g g}^{-1}$ dry weight sediment), assuming (i) a synchronous start and end of sapropel formation at the three locations, (ii) a duration of sapropel formation of 7000 years (Nijenhuis and de Lange, 2000) and (iii) a constant sedimentation rate during sapropel formation (Menzel *et al.*, 2002). ARs in the homogeneous intervals were not calculated because sedimentation rates are expected to be different during times of deposition of sapropel and the homogeneous intervals.

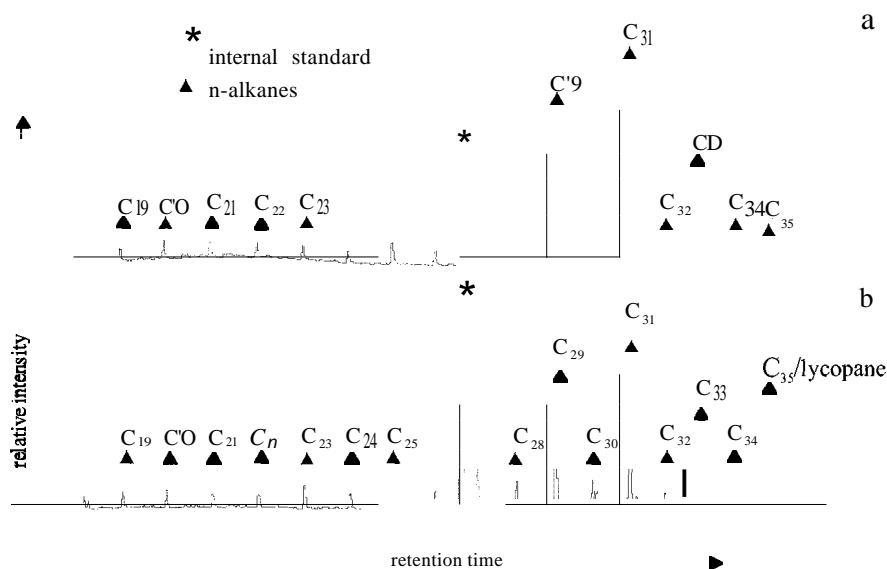


Figure 6.2 Partial gas chromatograms of typical saturated hydrocarbon fractions of solvent extracts of (a) a homogeneous interval of Site 967, 111-114 cm and (b) a sapropel of Site 967, 115 - 116.5 cm.

RESULTS

n-Alkane and n-alkan-1-ol accumulation rates

Biomarkers in the saturated hydrocarbon fractions of the organic solvent extracts of the sediments were dominated by a homologous series of n-alkanes ranging from C₁₇ to C₃₅ in both the homogeneous intervals and the sapropels (Fig. 6.2). The C₃₅ n-alkane co-elutes with lycopane, which is especially abundant in the sapropels due to the anoxic bottom waters during sapropel deposition (Fig. 6.2b; *cf* Sinninghe Oamste *et al.*, 2003). The n-alkanes in the n-C₂₄ to n-C₃₅ range possess a strong odd-over-even carbon number predominance values of 5-8), indicative of a predominant higher plant origin of the n-alkanes (Eglinton and Hamilton, 1963). In the homogeneous interval below the sapropel the organic carbon-normalized abundances of C₂₇₋₃₃ n-alkanes were 1040 TOC at OOP Site 967, 280 TOC at OOP Site 969 and 450 TOC at OOP Site 964 (Fig. 6.3a). In the sapropel C₂₇₋₃₃ n-alkanes contents were lower with mean values of 72 TOC at OOP Site 967, 70 TOC at OOP Site 969 and 215 TOC at OOP Site 964 (Fig. 6.3a). In the homogeneous interval above the sapropels the C₂₇₋₃₃ n-alkane contents were higher than in the sapropel with values of 225 TOC at OOP Site 967, 110 TOC at OOP Site 969 and 370 TOC at OOP Site 964 (Fig. 6.3a).

The C₂₆₋₃₀ n-alkan-ols with a strong even-over-odd carbon number predominance are likely also derived from terrestrial higher plants (Logan *et al.*, 1995). Their concentration profiles were similar to those of the n-alkanes. In the homogeneous interval below the sapropel the n-alkan-ol contents were 290 TOC at OOP Site 967, 330 TOC at OOP Site 969 and 90 TOC at OOP Site 964 (Fig. 6.3b). Within the sapropel n-alkanols are less abundant: 86 TOC at OOP Site 967, 50 TOC at OOP Site 969 and 80 µg/g TOC at OOP Site 964. In the homogeneous interval above the sapropel, n-alkan-1-ol abundances increased to 260 TOC at OOP Site 967, and 60 TOC at OOP Site 969; the highest abundance occurred at OOP Site 964 with 1500 TOC.

Assuming a constant sedimentation rate within the sapropel and duration of sapropel formation of 7000 years, accumulation rates (ARs) for these terrestrial biomarkers were calculated (see Menzel *et al.*, 2003 for a detailed discussion) and compared between the three sites. Oue to the likely substantially increased sedimentation rates in the homogeneous interval and poor preservation of OM no ARs were calculated for these intervals. C₂₇₋₃₃ n-alkane (Fig. 6.4a) and C₂₆₋₃₀ n-alkan-1-ol ARs (Fig 6.4b) at all three sites generally showed an increase from the base of the sapropel towards the middle section and sunsequently a drop towards the top with exceptions from this general trend for some individual samples. The highest ARs for the n-alkanes were found in the middle section of sapropel OOP Site 969 with values of about 600 µg.m⁻².yr⁻¹. The ARs for n-alkanes for the other two sites were substantially lower. The n-alkan-1-ol ARs at the three sites showed less variation; the maximum AR was noted for OOP Site 969 with 550 µg.m⁻².yr⁻¹.

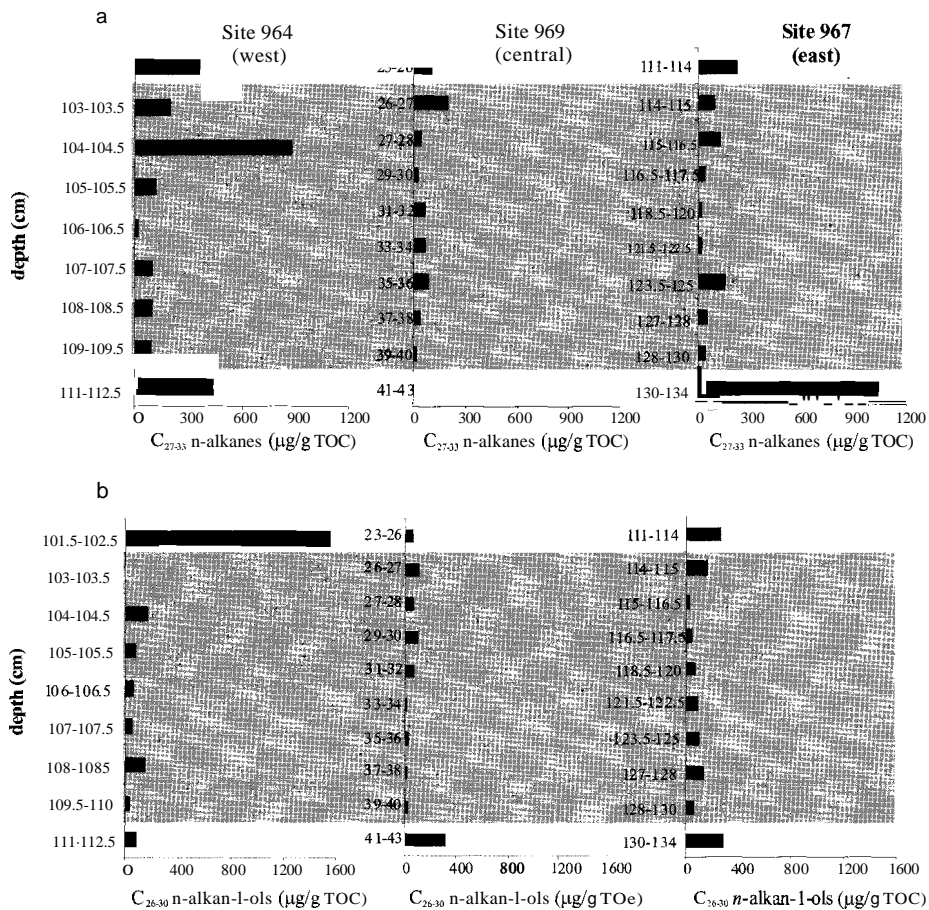


Figure 6.3 Bar plots showing the absolute abundance of (a) C_{27-33} n-alkanes and (b) C_{26-30} n-alkan-1-ols in the homogeneous intervals and sapropels at Site 967, 969 and 964. Light grey shaded regions represent the sapropel. White regions represent the homogeneous calcareous ooze.

Compound-specific isotopic analyses of long-chain n-alkanes (C_{27-33})

The $\delta^{13}\text{C}$ values of the C_{27-33} n-alkanes varied between -24‰ and -31.5‰ (Fig. 6.5). Generally, the C_{27} and C_{33} n-alkanes are more enriched in ^{13}C relative to the C_{29} and C_{33} n-alkanes, $n-C_{33}$ is more enriched relative to $n-C_{27}$ in the sapropel than the homogeneous interval. The weighted average $\delta^{13}\text{C}$ values of the C_{27-33} n-alkanes (Table 6.1) in the homogeneous intervals were more negative than those in the sapropels. ODP Site 967 showed $\delta^{13}\text{C}_{27-33}$ n-alkane mean values of -28.8‰ , ODP Sites 969 and 964 values of -30.3‰ and -29.6‰ , respectively. In the sapropels II-alkane values at ODP Site 967 were -27.4‰ and more negative at ODP Site 969 (-28.8‰) and at ODP Site 964 (-28.3‰) (Table 6.1).

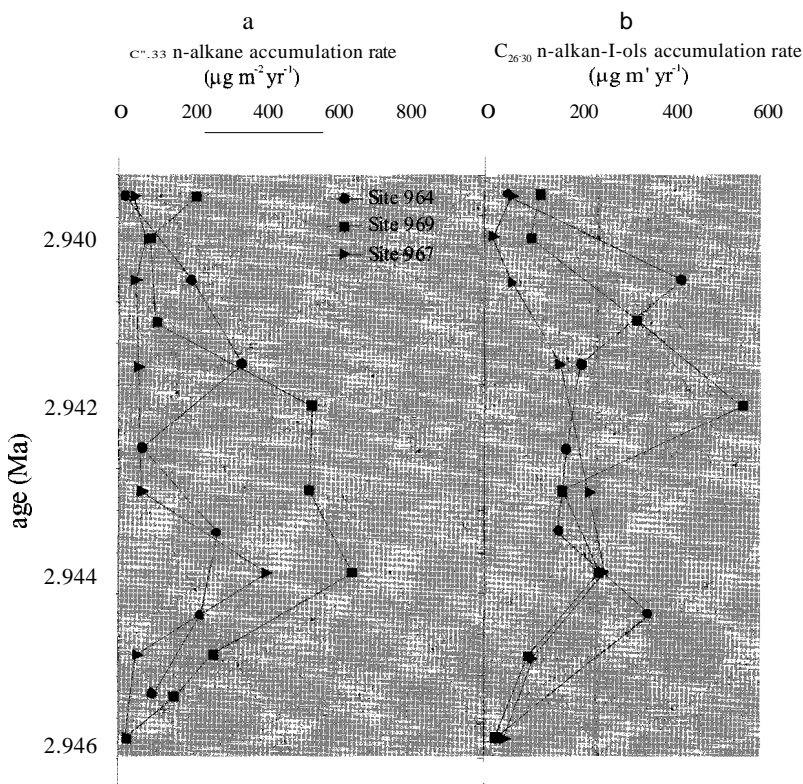


Figure 6.4 Accumulation rates of (a) C_{27-33} n-alkanes and (b) C_{26-30} n-alkan-1-ols in the sapropel sections at Sites 967, 969 and 964.

DISCUSSION

Origin of n-alkanes

The strong odd-over-even carbon number predominance of the long-chain n-alkanes (Fig. 6.2) provides evidence that they derive from waxes of terrestrial higher plant vegetation. The $\delta^{13}C$ values of the individual n-alkanes (C_{27-33}) ranged between -24‰ and -31.5‰ . This wide range revealed that they originate from a mixture of C_3 plants ($\delta^{13}C$ leaf wax lipids C_3 plants = -36‰ ; Rieley *et al.*, 1991; Collister *et al.*, 1994) and C_4 plants ($\delta^{13}C$ leaf wax lipids C_4 plants = -21.5‰ ; Rieley *et al.*, 1991; Collister *et al.*, 1994) both during times of sapropel formation and deposition of the homogeneous intervals in the Pliocene (Fig. 6.5). An additional indication for the substantial contribution of C_4 plant waxes is the characteristic trend of increasing $\delta^{13}C$ values of the n-alkanes with increasing chain length (Fig. 6.5). Generally, C_3 plant leaf wax lipids become more depleted in ^{13}C with increasing number of carbon number, whereas the values of C_4 plant individual leaf wax components are constant with increasing carbon number or even increase slightly (Rieley *et al.*, 1991; Collister *et al.*, 1994; Kuypers *et al.*, 1999). The fact that $n-C_{33}$ is substantially enriched in ^{13}C

relative to $n\text{-C}_{31}$, thus, also indicates a contribution from C_4 plant wax lipids. This relative enrichment is stronger in the sapropels than in the homogeneous sediments, suggesting a larger C_4 plant wax contribution in the sapropels, consistent with the more enriched ^{13}C content of all odd n -alkanes (Fig. 6.5).

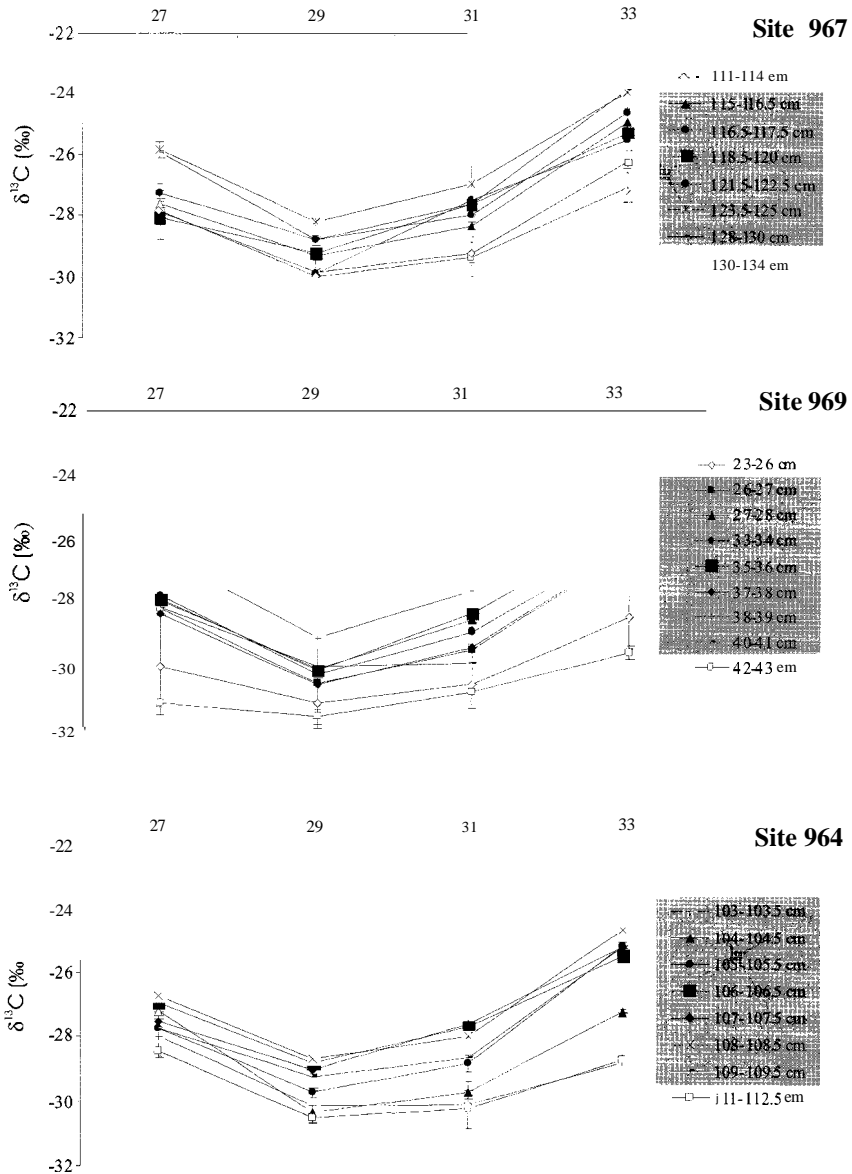


Figure 6.5 $\delta^{13}\text{C}$ values versus carbon chain length of n -alkanes. Error bars represent the standard deviation. Symbols in the light grey shaded boxes represent measurements made of the sapropel samples. Symbols in the white regions represent the homogeneous calcareous ooze.

Table 6.1 Weighted average $\delta^{13}\text{C}$ values (‰) of the C_{27-33} n-alkanes and their transformation to C_4 plant contribution (%)^a.

	Site 964	Site 969	Site 967
$\delta^{13}\text{C}_{27-33}$ (‰) homogeneous (n=2)	-29.6	-30.3 (0.4)	-28.8 (0.2)
$\delta^{13}\text{C}_{27-33}$ (‰) sapropel (n=7)	-28.3 (0.8)	-28.8 (0.6)	-27.4 (0.6)
C_4 plant vegetation (%) homogeneous (n=2)	44	39 (3)	49 (1)
C_4 plant vegetation (%) sapropel (n=7)	54 (6)	50 (4)	59 (4)

^a values are averages; values in parentheses represent the standard deviation

The C_4 plant contribution of the leaf-wax n-alkanes was estimated with a two end-member mixing model, assuming the C_4 leaf-wax lipids = -21.5 ‰ and $\delta^{13}\text{C}_3$ leaf-wax lipids = -36.0 ‰ (Collister *et al.*, 1994). These calculations showed that in the homogeneous intervals the average percentage of C_4 plant vegetation ranged between 40 and 50%, with the highest contribution at ODP Site 967, located closest to the river Nile (Fig. 6.6; Table 6.1). In the sapropels the C_4 plant contribution to the wax lipids increased by up to 20% to reach values between 50-70% for all three sites, with the highest contribution again at ODP Site 967 (Fig. 6.6, Table 6.1).

These data reveal a substantial contribution of C_4 plants to the terrestrial vegetation on the continent surrounding the Mediterranean in the Pliocene and, surprisingly, a higher contribution at times of sapropel deposition. The Pliocene (ca. 3 Ma) palaeoclimate in the European and Mediterranean region was warmer, wetter and less seasonal than at present, particularly at the middle to high latitudes (Haywood *et al.*, 2000). U_{37}^K values from alkenones in the same sapropels provide estimates for sea surface temperature of 24-27°C (Menzel *et al.*, 2003). Since it is generally believed that alkenones in the Mediterranean Sea are produced during the winter season (Ternois *et al.*, 1996), these estimates likely reflect winter temperatures, indicating that the annual air temperature during periods of insolation maximum (i.e. sapropel formation) were rather high.

Plants possessing C_3 and C_4 photosynthesis respond differently to ambient conditions of light, temperature, $p\text{CO}_2$, $p\text{a}_z$ and humidity (e.g. Collatz *et al.*, 1992). C_4 photosynthesis is insensitive to temperature whereas increasing temperature alters the kinetics of Rubisco (the primary CO_2 -fixing enzyme of plants utilising the Calvin-cycle) and thus photorespiration and CO_2 fixation in C_3 plants (Collatz *et al.*, 1998). Growth studies on C_3/C_4 grasses have shown that higher temperatures increase the frequency of C_4 photosynthesis within the grass taxa, whereas precipitation was not a critical parameter (Ehleringer *et al.*, 1997). On the other hand, Huang *et al.* (2001) have shown that the summer rainfall can be an important factor for the dominance of C_4 plants in certain environments. Schefuß *et al.* (2003) showed that the decreased air humidity, controlled by decreased sea surface temperature, was a decisive factor in the expansion of C_4 grass vegetation in southern Africa during the Mid-Pleistocene transition.

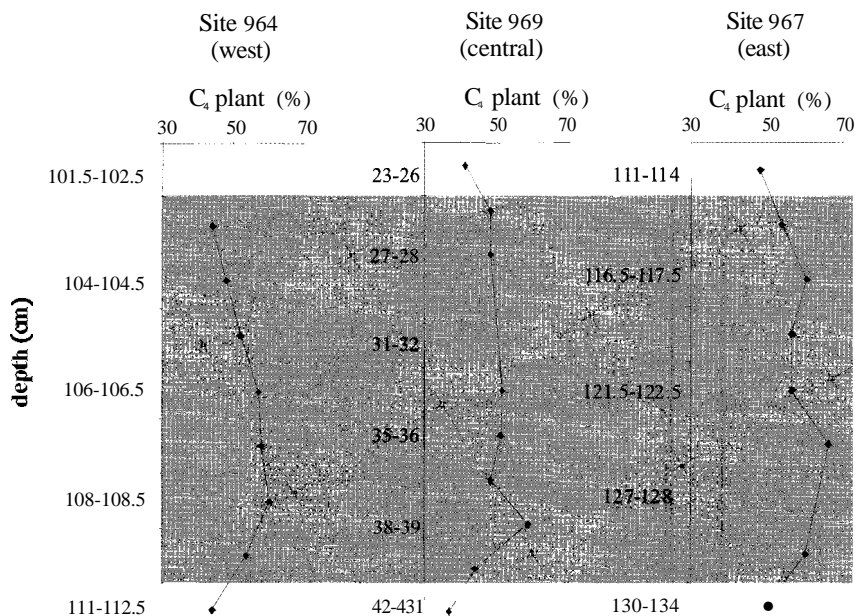


Figure 6.6 Calculated C_4 plant contribution (%) based on the weighted average $\delta^{13}C$ values of the C_{27-33} n-alkanes. Light grey shaded regions represent the sapropel. White regions represent the homogeneous calcareous ooze.

The increase (up to 20%) in C_4 plants relative to C_3 plants during time of sapropel formation may thus have been caused by the increase in air temperature. On the other hand the increased rainfall during times of sapropel formation may have substantially increased the overall plant coverage of the Mediterranean Sea borderlands by transforming formerly barren deserts of the North African continent into savannah's dominated by C_4 grasses. Such a process could also explain the increased contribution of C_4 plants relative to C_3 plants in the plant-wax n-alkanes. This interpretation is supported by the diminished delivery of Sahara dust evident from the lowered Ti/Al ratios of the sapropels (Wehausen and Brumsack, 1999; Nijenhuis and de Lange, 2000) and the increasing ARs of plant lipids towards the centre of the sapropel (see below).

Mode of transport of terrestrial plant n-alkanes

Both aeolian and fluvial transport brings terrestrial plant n-alkanes and n-alkan-1-ols to marine settings. Leaf wax n-alkanes, the major lipid constituent of the epicuticular wax layer of terrestrial plants (Eglinton and Hamilton, 1963), can easily be removed from the leaf surface by rain or wind, especially by sandblasting dust storms. They are common organic components of aerosols (Poynter et al., 1989, Schefuß et al., 2003). n-Alkan-1-ols are not as abundant in aerosols and are, therefore, mainly fluvially transported to marine settings.

The absolute abundances of C_{27-33} n-alkanes and C_{26-30} n-alkanols normalised to TOC were higher in the homogeneous interval than in the sapropels (Fig. 6.3). This difference is

probably the effect of the changing redox conditions during deposition. The sapropel was deposited in euxinic waters (Menzel *et al.*, 2002), resulting in a minimal oxygen exposure time of OM during settling through the water column and burial in surface sediments and yielding optimal preservation of biomarker lipids and OM (*ef* Hoefs *et al.*, 2002; Sinninghe Damste *et al.*, 2002c). The homogeneous intervals below and above the sapropel were, however, deposited in oxic bottom waters resulting in substantially longer oxygen exposure times. Under these conditions terrestrial n-alkanes are selectively preserved (Hoefs *et al.*, 2002; Sinninghe Damste *et al.*, 2002c), which explains the elevated TOC-normalized concentrations outside the sapropel layer. Long-chain n-alkan-1-ols are slightly more labile towards oxygen exposure than n-alkanes (Hoefs *et al.*, 2002) but the same mechanism applies. Within the sapropels labile marine OM is preserved due to the excellent conditions for preservation and the terrestrial biomarkers are "diluted", resulting in lower concentrations.

Within the sapropels the ARs of the C₂₇₋₃₃ n-alkanes and C₂₆₋₃₀ n-alkanols increased from the base of the sapropel towards the middle section and then decreased towards the top (Fig. 6.4). This is opposite to the trend in the Ti/Al ratios in the same sapropel with the lowest Ti/Al ratio is in the middle of the sapropel, suggesting a decreasing aeolian dust delivery during sapropel formation (Wehausen and Brumsack, 1999; Nijenhuis and de Lange, 2000). This difference seems to indicate that the terrigenous lipids were predominantly of fluvial rather than aeolian origin. Low K/Al and Mg/Al ratios in the sapropels confirm that fluvial input during sapropel formation indeed increased (Wehausen and Brumsack, 1999, Nijenhuis and de Lange, 2000). Interestingly, both n-alkane and n-alkan-1-ol ARs at ODP Site 967, located closest to the mouth of the Nile river are not higher than those at ODP Sites 969 and 964. This observation may indicate that not only the Nile river had increased fresh water discharge during sapropel formation, but also the discharge of the fossil river (wadi) of the North African margin increased as has been proposed for the Quaternary 85 sapropel (Rohling *et al.*, 2002). The increased flux of land-plant derived lipids towards the middle section of the sapropel is consistent with the suggested increased overall plant coverage of the Mediterranean borderlands.

Implications for $\delta^{13}\text{C}_{\text{TOC}}$ values

Assuming that the long-chain n-alkanes were mostly fluvially transported into the eastern Mediterranean Basin during Pliocene sapropel formation, $\delta^{13}\text{C}$ values of C₂₇₋₃₃ n-alkanes can be used, with care, as a proxy for the isotopic composition of bulk terrestrial OM, which predominantly originated from fluvially transported terrigenous OM. The $\delta^{13}\text{C}$ values of C₂₇₋₃₃ n-alkanes in the homogeneous intervals suggest a contribution of 40-50% of C₄ plants to the terrestrial OM (Fig. 6.6), implying that bulk terrestrial OM may also be composed of a substantial part of C₄ plants. Assuming $\delta^{13}\text{C}$ bulk C₃ = -27 ‰ and bulk C₄ plants \approx -12 ‰ (Tyson, 1995), we can estimate that terrestrial OM derived for ca. 50% from C₄ plants will have a $\delta^{13}\text{C}$ value of ca. -19.5 ‰. This is exactly the $\delta^{13}\text{C}_{\text{TOC}}$ value measured at ODP Site 967 in the homogeneous intervals (Fig. 6.1c). In these sediments with a TOC content smaller than 0.1%, it is likely that a substantial part of the TOC is derived from more refractory terrestrial OM and the substantial contribution of C₄ plants explains the

counter intuitive shift towards more enriched $\delta^{13}\text{C}$ values from sapropel to the homogeneous interval. The distinct east-west trend of increasingly more negative $\delta^{13}\text{C}$ values in the homogeneous intervals (Fig. 6.1c) suggests that C_4 plant material was transported predominantly by the Nile river, consistent with the higher calculated C_4 plant contribution for the terrestrial wax lipids at ODP Site 967 (Fig. 6.6). In the sapropel, $\delta^{13}\text{C}_{\text{ROC}}$ values are predominantly determined by more ^{13}C -depleted marine OM relative to terrestrial OM. The east-west trend for these values (Fig. 6.1c) is to some extent also seen in the $\delta^{13}\text{C}$ of alkenones (Menzel *et al.*, 2003) but may, in part, also be caused by the higher contribution of C_4 plant material to the relatively small terrestrial OM contribution to ODP Site 967.

CONCLUSIONS

$\delta^{13}\text{C}$ values of C_{27-33} n-alkanes reveal a contribution of a mixture of C_3 and C_4 land plant OM to the eastern Mediterranean Basin before, during and after sapropel deposition in the Pliocene. The $\delta^{13}\text{C}$ values of C_{27-33} n-alkanes in the homogeneous intervals revealed an eastward increase in the C_4 plant contribution, perhaps explaining the increased enriched $\delta^{13}\text{C}_{\text{ROC}}$ values towards the east by apparently discharges of the Nile river. Based on a two-end member mixing model, the contribution of C_4 plants to the wax lipids increased by up to 20% in the sapropels at all sites. This somewhat unexpected shift from C_3 to C_4 plant vegetation may be explained by the increased air temperature during the Northern hemisphere insolation maximum associated with sapropel deposition. Alternatively, and perhaps more likely, the increased rainfall at times of sapropel deposition resulted in an increase of overall plant coverage of the Mediterranean borderlands resulting from conversion of formerly barren desert areas into C_4 plant dominated-savannah's. This scenario is supported by the decreased Ti/Al ratio's recorded in sapropels pointing to a decreased delivery of Sahara dust and the increased terrigenous OM delivery (based on n-alkane and n-alkanol ARs) during sapropel deposition. This delivery was caused by an increased fluvial transport resulting from the wetter conditions and was most probably delivered not only by the Nile river system but also by fossil river systems of the North African coast (e.g. Libyan Basin) into the Mediterranean Sea.

ACKNOWLEDGEMENTS

We thank ODP for samples, IPPU for funding, M. Kienhuis for assistance with the irm-GC-MS at NIOZ and Dr. E. Schefuß for helpful discussions. Dr. P.A. Meyers and Dr. I. Rullkötter provided helpful reviews.

Chapter 7

The molecular composition of kerogen in Pliocene Mediterranean sapropels and associated homogeneous calcareous ooze

Diana Menzel, Pim F. van Bergen, Harry Veld, Henk Brinkhuis and Jaap S. Sinninghe Damste

Submitted to *Organic Geochemistry*

ABSTRACT

The organic matter of three time-equivalent Pliocene sapropels was characterized as Type II kerogen being dominated by amorphous organic matter, originating mainly from marine organisms. This was witnessed by the relatively high abundances of algaenan- and chlorophyll-derived pyrolysis products in the Curie-point pyrolysates of the kerogens of the sapropels. However, a small amount of terrigenous organic matter was also observed in the form of pollen and spores that most probably yielded the oxygenated aromatic pyrolysis products known to derive from sporopollenin. Lignin pyrolysis products, such as methoxyphenol and catechol (1,2-benzenediol), which are commonly used as unequivocal evidence for contribution of terrestrial higher plants, were absent in the kerogen pyrolysates of the sapropels. No major spatial and temporal differences in the kerogen composition of the three time-equivalent sapropels were observed. Palynological studies revealed that the homogeneous intervals, below and above the sapropels, consisted of pollen, spores and amorphous organic matter. This is confirmed by Curie-point pyrolysis - *GC/MS* results showing a relatively high abundance of algaenan-derived compounds and the presence of oxygenated aromatic pyrolysis products. The differences observed between the kerogen pyrolysates of the sapropels and their homogeneous intervals are suggested to be governed primarily by enhanced preservation conditions, resulting in increased preservation of labile marine organic matter in the sapropels.

INTRODUCTION

The sedimentary record of the eastern Mediterranean Basin is characterized by the occurrence of so-called sapropels, organic-rich sediments containing >2% total organic carbon (TOC) (Kidd *et al.*, 1978). Presently, sediments deposited in the eastern Mediterranean Sea have TOC contents of 0.3% at maximum (Calvert, 1983; Calvert and Pedersen, 1992). The switch between the deposition of sapropels and homogenous TOC-lean oozes must reflect periodical changes in depositional setting (Olausson, 1961; Kidd *et al.*, 1978; Cita and Grignani, 1982). These changes are thought to be caused by the changing

climate conditions at the pace of the astronomical precession cycle (Rossignol-Strick *et al.*, 1982; Rossignol-Strick, 1985; Hilgen, 1991; Lourens *et al.*, 1996). A wetter climate results in an increased delivery of nutrients to the basin and consequently increased marine productivity and consequently to enhanced preservation. Ultimately, this leads to the deposition of sediments with a high organic matter (OM) contents (2-30% TOC, Emeis *et al.*, 1996). Pliocene sapropels are characterized by very high TOC contents (> 26%, e.g. Emeis *et al.*, 1996; Nijenhuis and de Lange, 2000) and can be considered as extremes and are thus worth to be studied in this respect. In addition to the analysis of biomarkers (e.g. Bosch *et al.*, 1998; Rinna *et al.*, 2002; Menzel *et al.*, 2002, 2003), the characterization of macromolecular OM and the identification of its precursors can be important for the reconstruction and understanding of the mechanisms resulting in sapropel deposition.

In thermally immature sediments, including Mediterranean sapropels, the largest fraction (>90%) of sedimentary organic matter (OM) consists of OM insoluble in common organic solvents, so-called kerogen (Durand, 1980). Over the last 30 years, a number of kerogen formation pathways have been proposed, including the neogenesis model (Tissot and Welte, 1984), the selective preservation pathways (e.g. Tegelaar *et al.*, 1989) and the *in-situ* polymerization pathway (Collinson *et al.*, 1998; Stankiewicz *et al.*, 1998, 2000). The neogenesis model is based on depolymerisation-recondensation reaction that results in the preservation of amorphous organic matter (AOM), the composition of which strongly depends on the source organisms and more importantly on the diagenetic processes involved in its formation (Tissot and Welte, 1984). In the selective preservation model a substantial fraction of OM is derived from mixtures of selectively preserved, sometimes altered, resistant biomacromolecules (Tegelaar *et al.*, 1989a). These resistant macromolecular biomolecules become concentrated during mineralisation of the more abundant but more easily hydrolysable biopolymers such as proteins and carbohydrates. An alternative source for the occurrence of high-molecular-weight sedimentary OM in this model results from the incorporation of inorganic sulphur species into low-molecular-weight lipids and carbohydrates (Sinninghe Damste *et al.*, 1998). In particular, depositional environments favouring the activity of sulphate-reducing bacteria and with a limited supply of available iron induce the formation of these highly resistant sulphur-containing substances (Sinninghe Damste *et al.*, 1988, 1989; Sinninghe Damste and de Leeuw, 1990). Stankiewicz *et al.*, (2000) have proposed an alternative model of kerogen formation: conversion of free aliphatic molecules into a resistant aliphatic macromolecule via *in-situ* polymerisation.

Many types of resistant aliphatic biopolymers have been identified in organisms. These macromolecules have been encountered in cell walls of chlorophyceae and eustigmatophytes (as algaenans, de Leeuw and Largeau, 1993; Gelin *et al.*, 1997; Blokker *et al.*, 1998), in higher plant cuticles (as cutans, Nip *et al.*, 1986a,b; Tegelaar *et al.*, 1989b), in periderm tissues (as suberans, Tegelaar *et al.*, 1995; Collinson *et al.*, 1994), in inner seed coats of freshwater plants (as tegmens, van Bergen *et al.*, 1994) and in spores and pollen grains of higher land plants (as the major part of sporopollenins, van Bergen *et al.*, 1993, 2004). Aromatic biopolymers, such as lignins with their phenolic structure, occur in higher land plants (Sarkanen and Ludwig, 1971), phlorotannins in brown macroalgae (e.g. Grosse-Darnhues and Glombitza, 1984) and, partly, in sporopollenins (Schenk *et al.*, 1981; van

Bergen *et al.*, 1993, 2004). These biopolymers can be traced back in the geological record, e.g. in coals (e.g. McKinney and Hatcher, 1996) and freshwater sediments (Goth *et al.*, 1988). In marine sediments, algal aliphatic biopolymers, i.e. algaenans, are the most abundant macromolecules derived from the primary producers living in the euphotic zone. This has been confirmed by geochemical analysis of particulate organic matter (POM) in sediment traps in the Mediterranean Sea (Peulve *et al.*, 1996).

In this study, macromolecular OM of three time-equivalent Pliocene sapropels, as well as sediments above and below the sapropel, were studied using Rock-Eval pyrolysis, palynology and Curie-point pyrolysis-gas chromatography/mass spectrometry (Py-GC/MS). Using Rock-Eval pyrolysis the hydrogen index (HI) and oxygen index (OI) can be determined. These parameters are related to the origin and thermal maturity of the total OM (Tissot and Welte, 1984). Palynological analysis is applied to identify microscopically recognizable macromolecular OM (e.g. spores, pollen, algae material) to determine its origin. Curie-point pyrolysis of macromolecular OM in combination with GCIMS is able to characterize the composition of macromolecular OM at the molecular level by providing a semi-quantitative distribution of various molecular types in the kerogen macromolecule (Larter and Horsfield, 1993). With the combination of these different methods the composition of the macromolecular structure of the kerogen can be thoroughly studied. The present study aims to determine the source materials for the kerogen fraction in time-equivalent sections from three sites in the eastern Mediterranean reflecting the time before, during and after sapropel deposition.

MATERIAL AND METHODS

Samples

Cores at different locations in the eastern Mediterranean Basin were taken during ODP Leg 160 (Emeis *et al.*, 1996). Site 967 (Eratosthenes Seamount), and Site 969 (Mediterranean Ridge) are located in the Levantine Basin. Site 964 is located in the Ionian Basin (Fig. 7.1a). The detailed chronology of these cores, obtained by astronomical tuning (see Lourens *et al.*, 1996 for details), enabled us to select three laterally equivalent sapropels (967C-8H-4, 111-134 cm, 969E-6H-6, 23-43 cm, 964D-10H-1, 105-113 cm) with an age of 2.943 Ma. These sapropels have TOC contents up to 30% (Fig. 7.1b; Nijenhuis *et al.*, 1998). The sapropels were sub-sampled in 0.5 - 1.5 cm slices. The homogeneous intervals above and below the sapropels (Nijenhuis and de Lange, 2000) are composed of light-coloured, organic-poor, nannofossil and foraminiferal marl ooze (Calvert, 1983) and were sampled in slices of several cm. Ground, freeze-dried sediment samples (0.1 to 3 g) were Soxhlet extracted with dichloromethane/methanol (1:1, v/v) for 24 h to remove the solvent soluble fraction from the sediments.

Rock-Eval pyrolysis

Rock-Eval pyrolysis was performed on freeze-dried, powdered whole sediments using a Rock-Eval VI instrument following procedures described by Lafargue *et al.* (1998).

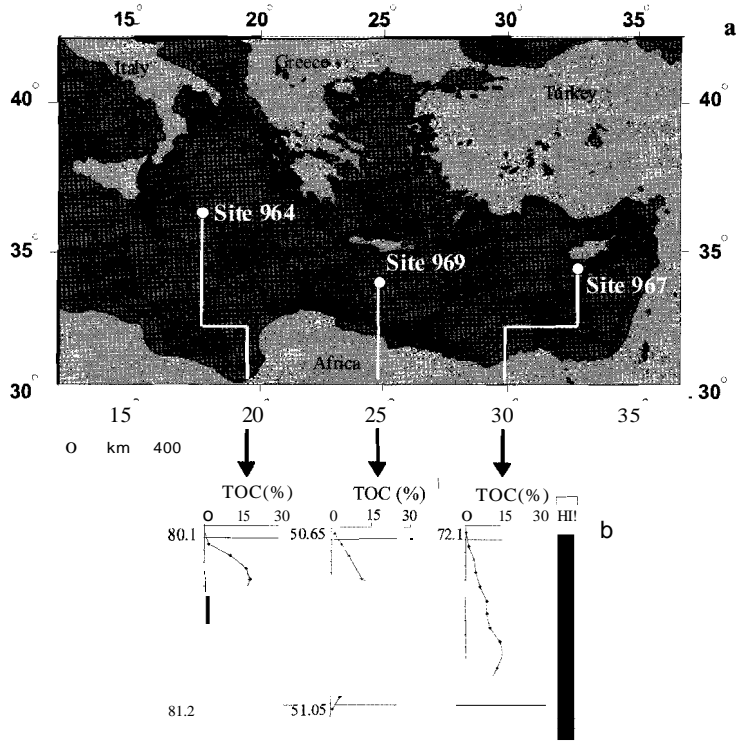


Figure 7.1 (a) Location of ODP drilling sites, (b) lithological description (HI = homogeneous calcareous ooze, S = sapropel) and TOe profiles of the investigated Pliocene sapropel (data from Nijenhuis *et al.*, 1998)

Palynological sample preparation

Extracted sediments (ca. 1 g of the sapropels, ca. 3 g of the sediments of the homogenous interval) were treated with 30% hydrochloric acid (HCl) to remove carbonates. After the initial treatment H₂O was added to the suspension. The sample in HCl/H₂O was left at room temperature overnight. Subsequently, the liquid was decanted, H₂O was added and the sample was centrifuged (7 min, 2000 rpm). The liquid was decanted and 38% hydrofluoric acid (HF) was added to dissolve silicates. The samples were agitated for 2 h, H₂O was added and the mixture left overnight. The HCl/HF treatment was repeated once again. The liquid was then decanted, 30% HCl was added to dissolve the silica-gel. The gel dissolved immediately after adding HCl, and the liquid was separated from the residue by way of decanting after settling overnight. The samples were washed until a pH of 4-5 was reached. The size of the palynomorphs ranges from 5 µm to > 200 µm. A 250 µm mesh sieve was used to remove oversized organic material. Sieving with a 10 µm mesh allowed the collection of the fraction containing pollen, spores and dinoflagellates. After sieving, a small part of the residue was mounted on a slide, embedded with glycerine jelly, covered, sealed with paraffin wax and studied using a microscope.

Isolation of kerogen from calcareous oozes for Py-GCIMS analysis

Extracted sediments (typically ca. 3 g) were treated following the protocol "palynological sample preparation" (see above) up to and including the washing procedure to pH of 4-5. Thereafter, samples were extracted using a vortex sample tube shaker with methanol (3x) and subsequently with methanol/dichloromethane (1:1, v/v) (3x). After each addition of solvent the liquid was removed by centrifugation (15 min, 2000 rpm). Finally, the samples were freeze-dried and ground. The yield of kerogen obtained from the homogeneous intervals of ODP Site 967 above the sapropel, and below and above the sapropel from ODP Site 964, was extremely low and the kerogen fraction could, therefore, not be studied using Curie-point pyrolysis-GCIMS.

Curie-point pyrolysis-gas chromatography/mass spectrometry

The freeze-dried, extracted sapropels and isolated kerogens from the calcareous oozes were pressed onto a flattened ferromagnetic wire with a Curie temperature of 610°C. The interface temperature of the pyrolysis unit was set at 200°C. Flash pyrolysis was conducted by inductive heating of the sample-coated wires to the Curie temperature at which it was held for 10 s. Py-GCIMS analyses were performed using a FOM-5LX Curie-Point pyrolyser connected to a Hewlett-Packard 5890 series II gas chromatograph (GC) and a Fisons instruments VG platform II mass spectrometer (MS). The GC was equipped with a CP-sil 5CB-MS silica column (50 m x 0.32 mm, film thickness 0.4 µm). The GC oven temperature was programmed from 40°C (5 min) to 310°C (isothermal for 10 min) at a rate of 5°C.min⁻¹. Helium was used as carrier gas. The MS was operated at 70 eV, scanning the range *m/z* 50-650 with a cycling time of 0.65 s.

Identification and quantification of flash pyrolysis products

Compound identification was based on comparison of mass spectral and retention time data with literature data (Sinninghe Damste *et al.*, 1988, 1992b; Hartgers *et al.*, 1992; van Bergen *et al.*, 1994). Relative amounts of the individual compounds in the pyrolysates were determined by integration of individual peak areas from summed mass chromatograms using relevant *m/z* values. These *m/z* values represent only part of the total ion count of the mass spectrum. Therefore, the measured peak areas were multiplied by a correction factor to compensate for this (Table 7.1). Correction factors, which were not available from literature, were determined using authentic standards as described by Hartgers *et al.*, 1992.

Table 7.1 Characteristic m/z values and correction factors used to calculate the relative abundances and internal distribution in the pyrolysates.

Compound class	Characteristic mass fragments (m/z)	Corr. factor
n-alkanes	55+57	2.9*
n-alkenes	55+57	4.9*
unsaturated isoprenoids	55+57	4.9
saturated isoprenoids	55+57	2.9
Methylketones	58	3.6#
Alkylbenzenes	78+91+92+105+106+119+120+133+134	1.6*
Alkylthiophenes	84+97+98+111+112+125+126+139+140	2.5*
Alkylphenols	94+107+108+121+122	2.2*
Alkylpyrroles	80+81+94+95+108+109+122+123+136+137	1.5
oxygenated aromatics	78+91+92+105+106+119+120+133+134	2.6
alkylindenes	115+116+129+130+143+144	1.8*
Indoles	117+132	7.0
phytadienes/phytenes	55+57+68+70+82+95+97+123	2.4
prist-1-ene/prist-2-ene	55+57	4.9
3-ethyl-4-methyl-1H-pyrrole-2,5-dione	53+67+96+110+124+139	2.9
6,10,14-trimethyl-2-pentadecanone	58	7.5
C ₂₀ isoprenoid thiophenes	98+111+125	2.6

* from Hartgers *et al.*, 1992, 1994b# from Hoefs *et al.*, 1996

RESULTS

Rock-Eval pyrolysis

Sapropels are characterized by hydrogen index (HI) values between 200 and 460 mg HC/g TOe and oxygen index (OI) values between 80 and 205 mg C₀₂/g TOC, indicating a mixture of Type II and III kerogen in the pseudo-van Krevelen diagram (Fig. 7.2a). The HI and OI of the homogeneous intervals are not reliable because TOC contents were <0.5% (Whelan and Thompson-Rizer, 1993). A plot of the TOe contents versus the HI values shows that generally the sapropels with a higher TOC content also have a higher HI (Fig. 7.2b). This is true for all three sites.

Palynological characterization of the kerogen

The kerogen of the homogeneous intervals are characterized by (not "fluffy") AOM and palynomorphs. The major palynomorphs are bisaccate pollen, other pollen, spores and different dinocysts.

The sapropels kerogen are dominated by "fluffy" AOM. The major palynomorphs are bisaccate pollen, other pollen and few spores. Also a few dinocysts of *Polyspaeridium zoharyi* were found.

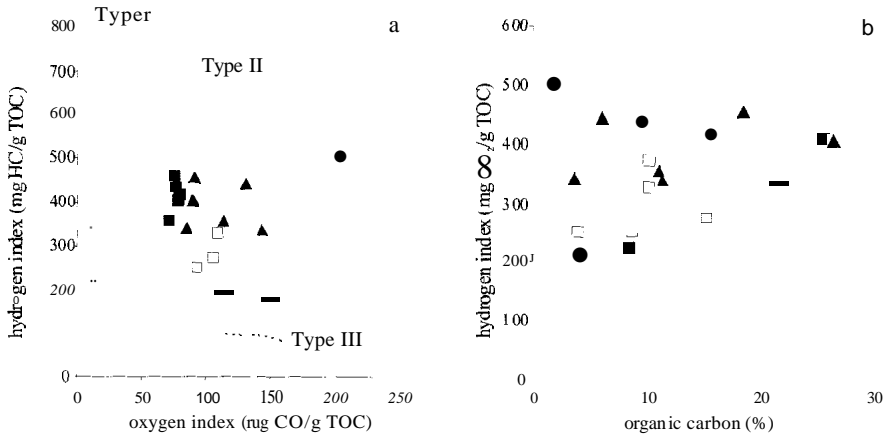


Figure 7.2 (a) Rock-Eval pyrolysis data of bulk sediments plotted in a pseudo van Krevelen diagram for sedimentary organic matter. Thermal alteration pathways of organic matter Types I, II and III are indicated by dashed lines and (b) cross-plot of TOC content and Rock-Eval hydrogen index values of the sapropels. The different symbols indicate the different sites: 967 (●), 969 (▲) and 964 (◻).

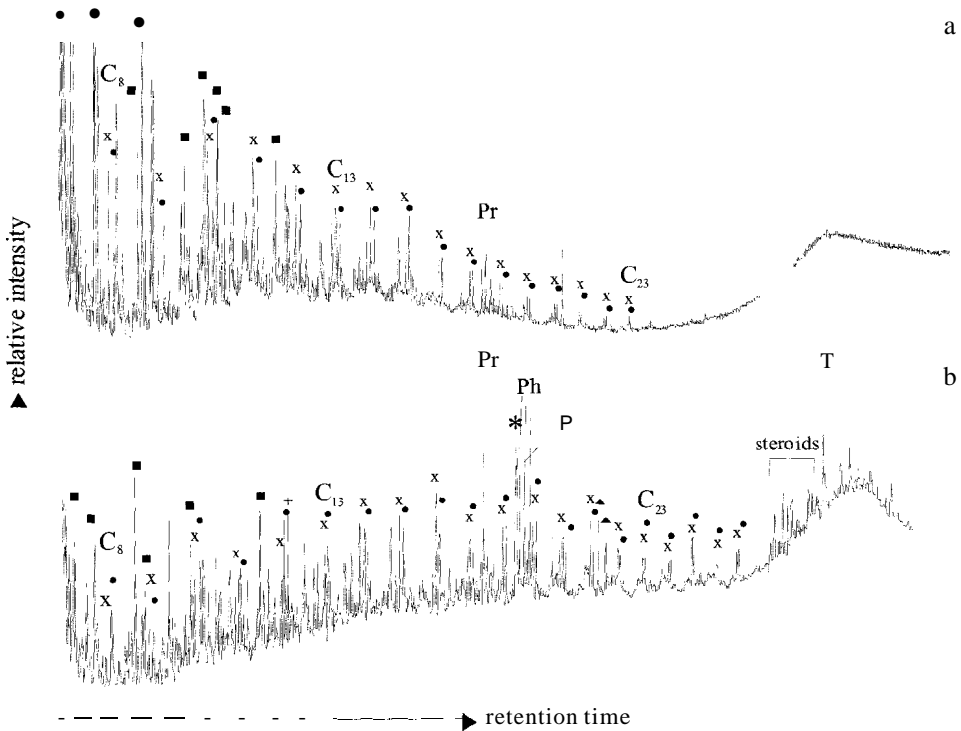


Figure 7.3 Total ion current (TIC) traces of the flash pyrolysates of the kerogens from Site 967, (a) homogeneous interval (967C-8H-4, 130-134 em) and (b) sapropel (967C-8H-4, 127-128 em). Key: ● = n-alkanes, x = n-alk-1-enes, • = alkylbenzenes, + = 3-ethyl-4-methyl-1H-pyrrole-2,5-dione, Pr = prist-1-ene, * = 6,10,14-trimethyl-2-pentadecanone, Ph = phytadienes, P = phytene. ▲ = C₂₀ isoprenoid thiophene. T = a-tocopherol.

Pyrolysis GC-MS

General composition of the kerogen pyrolysates

Sub-samples of the sapropels and homogeneous intervals from the three different ODP sites with total organic carbon (TOC) contents ranging between 0.2 and 27% were studied using flash pyrolysis-GC/MS. The molecular composition of the kerogen pyrolysates of the homogeneous intervals and sapropels differs substantially as is illustrated by the total ion current (TIC) traces in Fig. 7.3. The relative abundance of the various compound classes encountered in the pyrolysates of the homogeneous intervals and sapropels are compiled for the three ODP sites in Fig. 7.4. These data represent the average for the sapropels and the homogeneous intervals. As an indication for the variability within the sapropel the standard deviation is also indicated in Fig. 7.4.

The pyrolysates of the kerogens of the homogeneous intervals of the Sites 967 and 969 deposited below and above the sapropel are dominated by alkylbenzenes, n-alkanes/n-alk-1-enes and alkylthiophenes (Fig. 7.4). Acyclic isoprenoids (including prist-1-ene/prist-2-ene), methylketones (including 6,10,14-trimethyl-2-pentadecanone), oxygenated aromatics and alkylphenols show relatively minor contributions and alkylpyrroles are absent (Fig. 7.4). The pyrolysates of the sapropel kerogens from the three studied ODP sites show an increase in the relative abundance of the compound classes of n-alkanes/n-alk-1-enes, acyclic isoprenoids, methylketones, oxygenated aromatics, alkylphenols and alkylpyrroles when compared with those of the homogeneous intervals (Fig. 7.4). A relative decrease by approximately a factor of 2 is observed in the alkylbenzenes and alkylthiophenes. The relatively high abundances of prist-1-ene/prist-2-ene, phytene, phytadiene and 6,10,14-trimethyl-2-pentadecanone (i-C₁₈ MK) in the pyrolysates of the sapropel kerogens are notable (Fig. 7.3b). The relative abundance of the individual compound classes within the sapropel show only minor changes. The pyrolysates of the kerogens of the three different ODP sites show similar compositions (Fig. 7.4). Other pyrolysis products, such as 3-ethyl-4-methyl-1H-pyrrole-2,5-dione, C₂₀ isoprenoid thiophene, α-tocopherol, cholest-3,5-diene, tris-norhopane, hop-17(21)-ene and 17P,21P(H)-homohopane were only detected in kerogen pyrolysates of the sapropels (Fig. 7.3b) but were not considered in the calculation of the relative abundance of compound classes.

Detailed observations for the distribution pattern of the various major compound classes is given below and will be illustrated using pyrolysis data obtained with sediments from Site 967. These data are representative for the observations at all three sites.

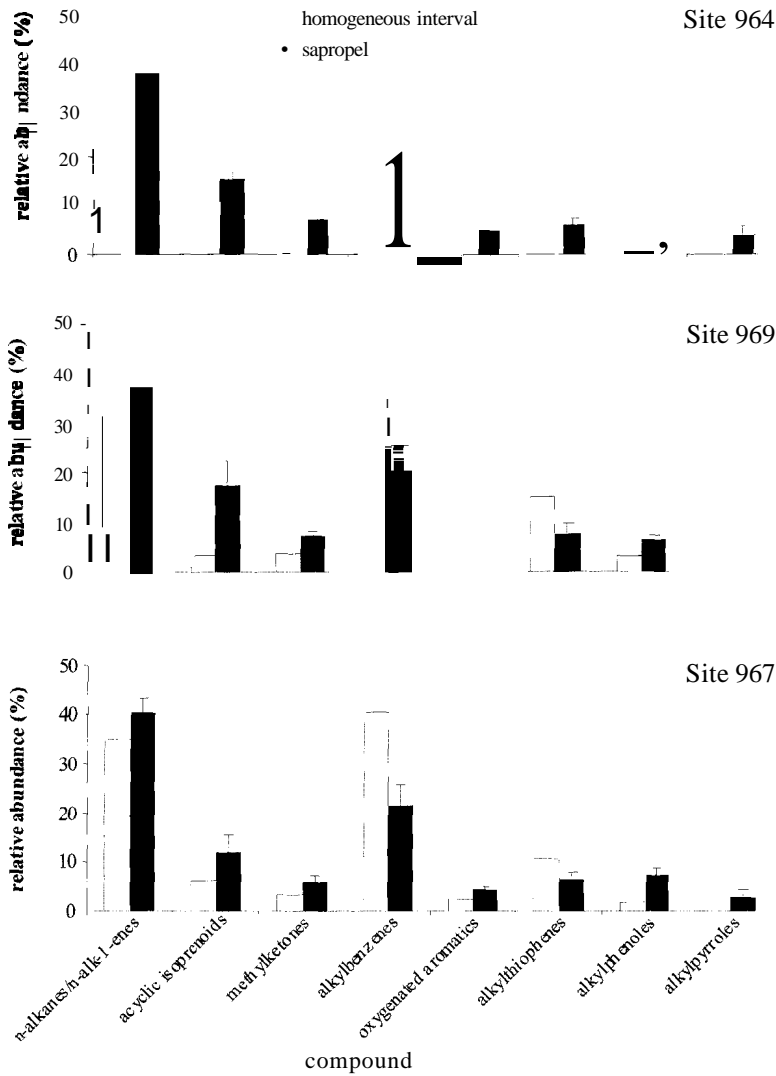


Figure 7.4 Bar plots showing relative abundances of the various compound classes in the kerogen pyrolysate of the homogeneous intervals and sapropels of Site 964, Site 969 and Site 967. Kerogen pyrolysate data of sapropels represent the average of all samples and error bars reflect standard deviations ($n = 7$).

Aliphatic pyrolysis products

n-Alkanes/n-alk-1-enes. The kerogen pyrolysates of the homogeneous intervals show relatively higher abundances of n-alkanes compared with the n-alk-1-enes (Fig. 7.5a). The distribution pattern of the n-alkanes in the homogeneous interval shows a dominance of short-chain members, ranging from C_6 to C_{26} and maximising between C_6 to C_{15} with a relative dominance of C_8 , C_{10} and C_{12} n-alkanes. This is clearly reflected in the average chain

length (ACL) of 13.5 and 13.9 in the kerogen pyrolysates of Sites 967 and 969, respectively (Table 7.2). The carbon number distribution of the *n*-alkanes in the pyrolysates of the sapropel kerogens shifts towards increasing carbon chain length, resulting in higher ACLs of 14.3 in Site 967, 15.5 in Site 969 and 15.9 in Site 964 (Table 7.2). The relatively high abundances of the C_{15} and C_{18} *n*-alkanes in the kerogen pyrolysates of the three sapropels are worth noting.

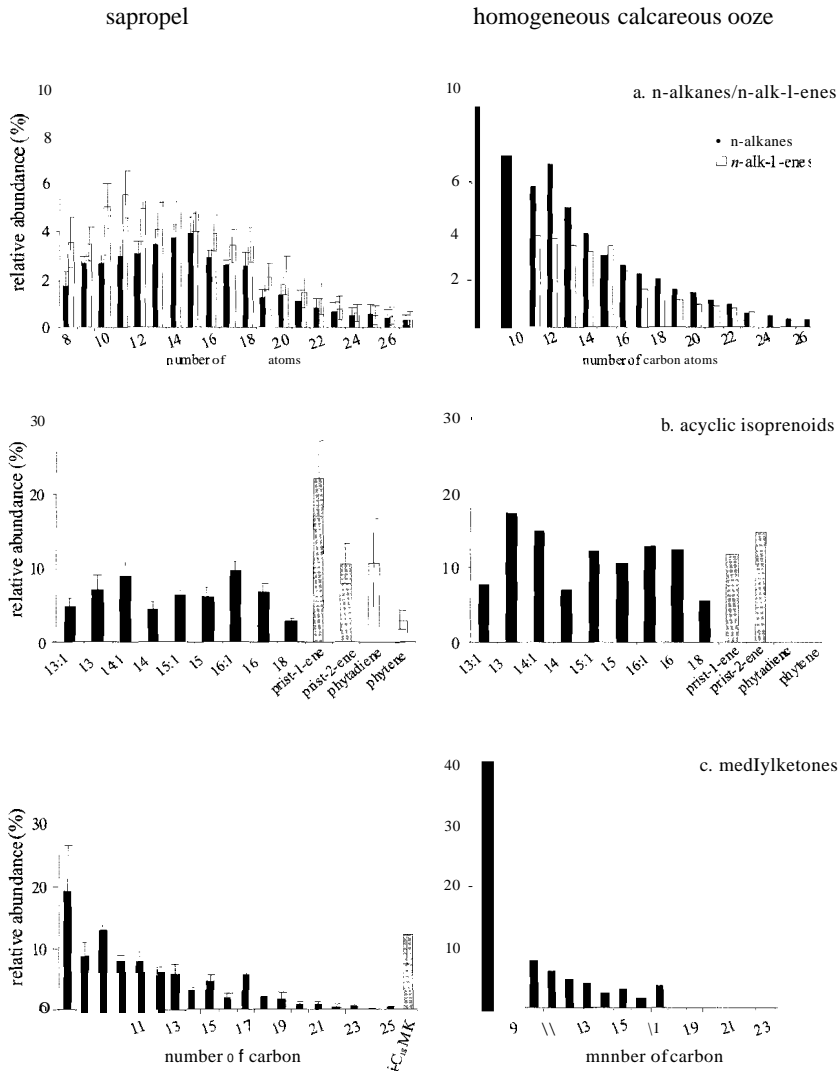


Figure 7.5 (a-c) Internal distribution patterns of different aliphatic compound classes between the homogeneous, calcareous ooze and sapropel of Site 967. Kerogen pyrolysate data of the sapropels represents means and error bars are standard deviations ($n = 7$) (i -C₁₈ MK = 6,10,14-trimethyl-2-pentadecanone).

The distribution pattern of n-alk-I-enes in the homogeneous interval is similar to that of the n-alkanes ranging from C₈ to C₂₃ with a relative dominance of C₉ and CIS n-alk-I-enes (Fig. 7.5a). The ACLs are generally lower than those for the n-alkanes, with values of 12.5 and 12.6 in the homogeneous intervals of Sites 967 and 969, respectively (Table 7.2). In the kerogen pyrolysates of the sapropels n-alk-I-enes show a dominance of short carbon chain members, maximizing between C₁₀ to CIS (Fig. 7.5a). The ACLs are 13.7 at Site 967, 15.4 at Site 969 and 15.7 at Site 964 (Table 7.2).

Table 7.2 Average chain length (ACL) of various compound classes in the flash pyrolysate of the homogeneous intervals and the sapropels of ODP Sites 967, 969 and 964. $ACL = \sum(iX_i) / \sum X_i$, where X is abundance and i ranges from 8 to 27.

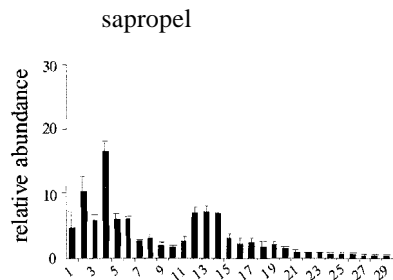
Kerogen pyrolysate	Compound class	ODP	ODP	ODP
		964	969	967
homogeneous intervals	n-alkanes	n.d.	13.9	13.5
	n-alk-I-enes	n.d.	12.6	12.5
	methylketones	n.d.	8.8	9.3
Sapropels	n-alkanes	15.9	15.5	14.3
	n-alk-I-enes	15.7	15.4	13.7
	methylketones	12.3	12.3	11.0

Acyclic isoprenoids. Prist-I-ene/prist-2-ene are present in the kerogen pyrolysate of both the homogeneous interval and sapropel, but show relatively higher abundances in the sapropel with a concomitant increase in the prist-I-ene/prist-2-ene ratio (Fig. 7.5b). Phytadiene and phytene are only present in the pyrolysates of the sapropel kerogens (Fig. 7.5b). The C₁₃, C₁₃:I, C₁₄, C₁₄:1, CIS, C₁₅:1, C₁₆, and CIS isoprenoid alkanes/alkenes are especially abundant in the pyrolysates of the sapropel kerogens and show a relative increase of the C₁₃ and C₁₆:1 members in the kerogen pyrolysates of the homogeneous interval (Fig. 7.5b).

Methylketones. Methylketones are present in the kerogen pyrolysates of both the homogeneous intervals and sapropel (Fig. 7.5c). The odd-over-even carbon number predominance is more pronounced in the kerogen pyrolysate of the sapropels: in all kerogen pyrolysates a predominance of C₁₃, CIS and C₁₇ is observed. The ACLs show the lowest values in the homogeneous interval with values of 8.8 at Site 969 and 9.3 at Site 967 (Table 2). In the pyrolysate of the sapropels the ACL increases from 11.0 at Site 967 to 12.3 at Sites 969 and 964 (Table 2). i-CIS MK is relatively abundant in the sapropel kerogen pyrolysates, but absent in the kerogen pyrolysates of the homogeneous interval (Fig. 7.5c).

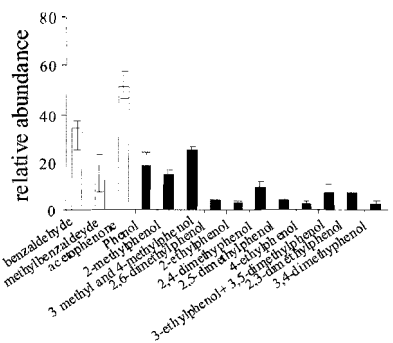
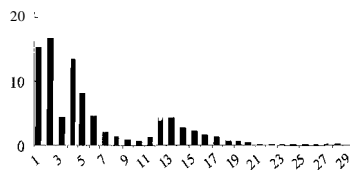
Aromatic pyrolysis products

Alkylbenzenes. A wide variety of alkylbenzenes is identified in the pyrolysates. In the kerogen pyrolysates of the homogeneous intervals, benzene, toluene and styrene are most abundant (Fig. 7.6a). In the sapropels, a relative increase in the abundance of 1,3+1,4 dimethylbenzene and 1,2,3,4-tetramethylbenzene (TMB) is observed (Fig. 7.6a).

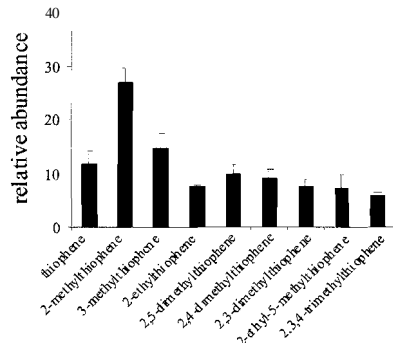
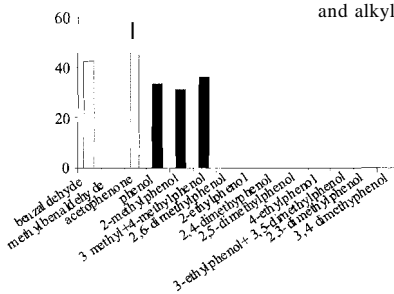


homogeneous calcareous ooze

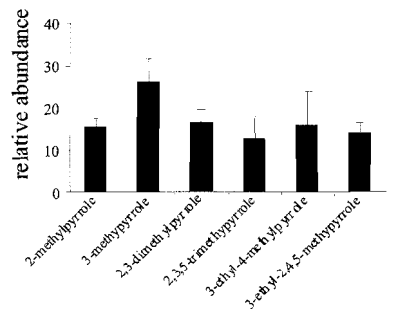
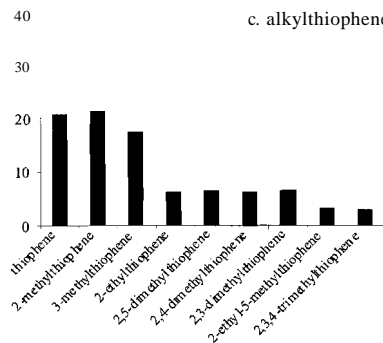
a. alkylbellenes



b. aromatics and alkylphenols



c. alkylthiophenes



d. alkylpyroles

not present

Figure 7.6 (a-d, page 90) Comparison of the internal distribution pattern of different aromatic compound classes between the homogeneous, calcareous ooze and sapropel of Site 967. Kerogen pyrolysate data of the sapropels are means and error bars are standard deviations ($n = 7$). (a) Key to alkybenzenes: 1 - benzene, 2 - toluene, 3 - ethylbenzene, 4 - 1,3+1,4-dimethylbenzene, 5 - styrene, 6 - 1,2 - dimethylbenzene, 7 - n-propylbenzene, 8 - 1-methyl-3-ethylbenzene, 9 - 1-methyl-4-ethylbenzene, 10 - 1,3,5-trimethylbenzene, 11 - 1-methyl-2-ethylbenzene, 12 - 1,2,4-trimethylbenzene, 13 - 1,2,3-trimethylbenzene, 14 - 1,2,3,4-tetramethylbenzene, 15 - n-butylbenzene, 16 - n-pentylbenzene, 17 - n-hexylbenzene, 18 - n-heptylbenzene, 19 - n-octylbenzene, 20 - n-nonylbenzene, 21 - n-decylbenzene, 22 - n-undecylbenzene, 23 - n-dodecylbenzene, 24 - n-tridecylbenzene, 25 - n-tetradecylbenzene, 26 - n-pentadecylbenzene, 27 - n-hexadecylbenzene, 28 - n-heptadecylbenzene, 29 - n-octadecylbenzene.

Oxygenated aromatics and alkylphenols. Among the oxygenated aromatics, only benzaldehyde and acetophenone are common in the kerogen pyrolysates of the homogeneous intervals. In the pyrolysates of the sapropel kerogens methylbenzaldehyde is also present, albeit in relatively low abundance (Fig. 7.6b). Phenol, 2-methylphenol and the co-eluting 3- and 4-methylphenol were identified in the pyrolysates of the kerogens of the homogeneous intervals. In the sapropel kerogen pyrolysates, these alkylphenols are still dominant, but C₂ alkylated phenols were also detected (Fig. 7.6b).

Alkylthiophenes. In the kerogen pyrolysates of the sapropels and homogeneous intervals nine alkylthiophenes were identified. Thiophene and C₁ alkylated thiophenes are dominant in the pyrolysates of the kerogen of the homogeneous intervals (Fig. 7.6c). In the pyrolysates of the sapropel kerogens, thiophene showed a relative decrease whereas C₂ and C₃ alkylthiophenes increased, in relative abundance.

Alkylpyrroles. They appear exclusively in the sapropels with 3-methylpyrrole and 3-ethyl-4-methylpyrrole relatively abundant (Fig. 7.6d). Distributional variations of this compound class in the pyrolysates of the sapropel kerogens are small.

DISCUSSION

OM sources: Rock-Eval pyrolysis and palynological observations

Based on the results obtained from Rock-Eval pyrolysis, the OM present in the three time-equivalent sapropels is a mixture of Type II and Type III kerogen (Fig. 7.2a; Espitalie *et al.*, 1977; Tissot and Espitalie, 1975). HI and O₁ values similar to those measured here have been reported for other Pliocene/Pleistocene sapropels of the eastern Mediterranean Sea (Bouloubassi *et al.*, 1999). Type II kerogen is characterized mainly by aliphatic, but also aromatic OM, originating predominantly from marine organisms. Type III kerogen is characterized mainly by aromatic material derived from terrestrial plants (Tissot *et al.*, 1974). Alternatively, this type of kerogen may also derive from oxic degradation of marine OM (Kenig *et al.*, 1994). Reworking of hydrogen-rich marine OM during settling in the water column and burial in the sediment, typically results in an increase in O₁ and decrease of HI (Pratt, 1984), specifically with long residence time at the oxic water-sediment interface. Hollander *et al.* (1990) observed, in a modern lacustrine setting, that OM deposited in an anoxic water column had higher atomic H/C ratios and lower atomic O/C ratios than OM deposited in an oxic water column.

The high OIs and the only moderately high HIs (200-500 mg HC/g TOC) compared with other TOC-rich sediments (Espitalie *et al.*, 1977; Kenig *et al.*, 1994) is somewhat surprising for these sapropels with TOC contents up to 30%. Previous studies of these Pliocene sapropels revealed anoxic conditions up into the photic zone during sapropel deposition (Menzel *et al.*, 2002), implying optimal conditions for preservation of relatively labile marine OM. A reason for the high OIs and relatively low HIs of the sapropels may be that sediments, rather than isolated kerogen were analysed by Rock-Eval pyrolysis. A number of workers have reported that certain minerals, particularly the clay minerals smectite and illite, cause catalytic effects with whole rock pyrolysis and give artificially low HIs, when compared with isolated kerogen (e.g. Orr, 1983; Katz, 1983; Peters, 1986). This observation is particularly evident for sediments off the Louisiana Coast in the Gulf of Mexico, known to contain high amounts of smectite (Whelan and Thompson-Rizer, 1993). It is known that the Pliocene sapropels contain substantial amounts of smectite as a result of the wet climate conditions during their deposition (Foucault and Melieres, 2000). Therefore, the presence of smectite is likely responsible for the high OIs and only moderately high HIs of the sapropels.

Palynological studies of the sapropels indicate the dominance of AOM of marine origin (Tyson, 1995). The minor contribution of pollen and spores embedded in the AOM is evidence for only a small contribution to the OM derived from terrestrial higher plant material. This indicates that the Rock-Eval pyrolysis data indicating Type VIII kerogen is likely not related to the admixture of Type III kerogen from the continent with kerogen of a marine origin but more likely due to the effects of oxic degradation or, more likely, the artificial low HI values due to the presence of smectite. The positive relationship of Rock-Eval HIs and the TOC content in the sapropels at all three sites (Fig. 7.2b) appears to imply a progressive enrichment and preservation of hydrogen-rich aliphatic components with higher accumulation of OM. This has been observed before for many other sediments (e.g. Herbin *et al.*, 1986; Hue *et al.*, 1992; Kenig *et al.*, 1994; Bouloubassi *et al.*, 1999).

Palynological observations in the homogeneous intervals showed pollen, spores, dinocysts and AOM, which is different to the kerogen composition obtained of the sapropels. Based on these palynological observations, the kerogen of the homogeneous intervals should be described as a mixture of resistant marine and terrestrial OM, which has persisted aerobic decomposition.

OM sources: molecular evidence

The molecular composition of the flash pyrolysates is in agreement with a predominant marine source for the OM in the sapropels. The composition is similar to that of pyrolysates of other marine kerogens (e.g. Hoefs *et al.*, 1995, 1996) and settling of macromolecular OM in the marine water column (Peulve *et al.*, 1996).

Algaenan-derived compounds

n-Alkanes/n-alk-1-enes and methylketones are relatively abundant compound classes in the kerogen pyrolysates of the sapropels, and to a lesser extent, also in those of the homogeneous intervals (Fig. 7.4). Temporal and spatial distributional variations of these compound classes in the kerogen pyrolysate of the sapropels were only minor. These

abundant pyrolysis products have been described earlier as being derived from non-hydrolyzable aliphatic macromolecules, possibly algaenan, biosynthesized by marine algae (e.g. Derenne *et al.*, 1989, 1992; Behar *et al.*, 1995; Gelin *et al.*, 1996). Thermal rearrangement reactions of the ether bridges during pyrolysis account for the formation of the methylketones (Gelin *et al.*, 1993). To date, algaenans have only been found as outer cell wall constituents in eustigmatophytes and some marine chlorophytes (Gelin *et al.*, 1999). None of the diatoms and prymnesiophytes studied to date and only one dinoflagellate were shown to contain algaenan (Gelin *et al.*, 1999). Therefore, the origin of algaenans seems limited to only two classes, eustigmatophytes and chlorophyte microalgae of phytoplankton among the wide range of primary producers. The presence of eustigmatophytes in the water column is confirmed by the high abundances in the sapropels of its characteristic lipid biomarker, the C₃₀ 1,15-alkyldiol (Menzel *et al.*, 2003).

The origin of the series of C₁₃-C₁₈ isoprenoid alkanes/alkenes is less clear; they have been proposed to derive from non-hydrolyzable aliphatic macromolecules with isoprenoid carbon skeletons that form an ether-linked macromolecule biosynthesized by an as yet unknown marine algae (Derenne *et al.*, 1989, 1990; *et al.*, 1998). The presence of 6,10,14-trimethyl-2-pentadecanone in kerogen pyrolysates of the Madeira Abyssal Plain (MAP) turbidites was also proposed to originate from isoprenoid algaenans (Hoefs *et al.*, 1996). Alternative sources are discussed below.

Chlorophyll- and tocopherol-derived compounds

Phytadiene and phytene are distinct products in the kerogen pyrolysates of the sapropels (Fig. 7.5b). Phytadiene and phytene are derived from the phytol side chain of chlorophyll (van de Meent *et al.*, 1980a,b; Ishiwatari *et al.*, 1991). Czo isoprenoid thiophenes and phytene presumably originate from pyrolysis of sulphur-bound phytol (Sinninghe Damste *et al.*, 1987; Schouten *et al.*, 1993). Alkylpyrroles, present only in the pyrolysates of the sapropel kerogens, are likely derived from chlorophyll and/or other tetrapyrrole pigments (Sinninghe Damste *et al.*, 1992b).

Both pristene isomers (prist-1-ene and prist-2-ene) have been demonstrated to derive primarily from kerogen-bound tocopheryl moieties through an intramolecular rearrangement reaction, rather than from chlorophyll-a (Goosens *et al.*, 1984). This is supported by the presence of intact α -tocopherol in the kerogen pyrolysate of the sapropels (Fig. 7.3b; cf. van Bergen *et al.*, 1994). Tocopherol is relatively abundant in chloroplasts of most autotrophic organisms.

The presence of chlorophyll and tocopherol pyrolysis products in the kerogen pyrolysates of the sapropels but not in those of the homogeneous intervals just below and above the sapropel implies optimal preservation conditions for these relatively labile lipids. Both compound classes are likely of marine origin. They can be produced in the terrestrial realm but their labile nature prevents their transport (with concomitant exposure to oxygen) over long distances.

Higher-plant-derived compounds

Py-GCIMS analysis of the kerogen pyrolysates revealed the presence of oxygenated aromatics, i.e. benzaldehyde, methylbenzaldehyde and acetophenone (Fig. 7.6b) for both the sapropels and the homogeneous intervals. These pyrolysis products, can be derived from sporopollenin expected to be selectively preserved (i.e. the structural constituents in the outer wall of pollen and spores from vascular plants) (van Bergen *et al.*, 1993,2004), confirmed by the presence of pollen and spores in the sapropels and the homogeneous intervals. There is no evidence for the presence of pyrolysis products of cutans and suberans, biopolymers also derived from terrestrial higher land plants, since in that case a range of n-alkanes/n-alk-1-enes up to C₃₅ would be expected (Nip *et al.*, 1986a,b; Tegelaar *et al.*, 1989b). Analysis of the biomarker lipids in these samples confirm the presence of some terrigenous OM in both the homogeneous intervals and in the sapropels as witnessed by the presence of long-chain n-alkanes and n-alcohols (Menzel *et al.*, in press).

The presence of the aromatic biopolymer lignin can also be indicative for a contribution of terrigenous OM. If so, the kerogen pyrolysates should contain methoxyphenols and, in case of more degraded lignin, catechols and ultimately phenols (Hatcher and Clifford, 1997; van Bergen *et al.*, 2000). Diagenetic transformation of methoxyphenol moieties into phenol moieties typically takes tens of million of years (Ewbank *et al.*, 1996; Edwards *et al.*, 1997; Abbott *et al.*, 1998). Neither methoxyphenols nor catechols were present in the kerogen pyrolysates of the sapropels or homogeneous intervals (Fig. 7.6b). This indicates, at most, only a minute contribution of lignin. Some alkylphenols are present in the kerogen pyrolysates of the sapropels but these are most likely derived from marine organisms (cf. van Heemst *et al.*, 1999), as previously proposed from the distribution pattern of phenols obtained in the kerogen pyrolysate of OM collected in sediments traps in the Mediterranean Sea (Peulve *et al.*, 1996).

Origin of other pyrolysis products

Alkylthiophenes can be formed during the early stage of diagenesis by the incorporation of reduced inorganic sulphur, originating from bacterial sulphate reduction, interacting with organic material (presumably carbohydrates) (van Kaam-Peters *et al.*, 1998; Kok *et al.*, 2000). It has been proposed that the degree of OM sulphurization is primarily controlled by the supply of reactive iron (Sinninghe Damste and de Leeuw, 1990). Sulphate reduction rates were high during sapropel formation based on the euxinic conditions in Mediterranean waters (Passier and de Lange, 1998; Passier *et al.*, 1999b), which explains the presence of alkylthiophenes in the kerogen pyrolysates of the sapropel.

Alkylbenzenes in kerogen pyrolysates can have many precursors in the kerogen (Hartgers *et al.*, 1994a). One group of potential precursors is formed by the aromatic carotenoids biosynthesized by photosynthetic green sulphur bacteria, which, upon pyrolysis, yield high amounts of 1,2,3,4-tetramethylbenzene (TMB), (Hartgers *et al.*, 1994b). Menzel *et al.* (2002) showed the presence of intact isorenieratene, an aromatic carotenoid, in these but it was absent in the homogenous intervals. In accordance with this, the kerogen pyrolysates of the sapropels indeed contained relatively higher amounts of TMB than those of the homogeneous intervals (Fig. 7.6a). TMB was, however, not absent in the kerogen

pyrolysates of the homogeneous intervals. This can be explained by the findings of Hoefs *et al.* (1995), who showed that there are other precursors than kerogen-bound aromatic carotenoids for TMB in flash pyrolysates of marine kerogens.

Implication for sapropel formation

Palynological studies showed differences in the kerogen composition between the homogeneous interval and sapropels. The oxic degradation of OM during the formation of homogeneous intervals may have altered the palynomorph assemblage because some taxa are more susceptible to aerobic decay than others (Cheddadi *et al.*, 1991; Cheddadi and Rossignol-Strick, 1995; Versteegh and Zonneveld, 2002). Pollen and spores are highly resistant against oxygen because of the presence of sporopollenin (Zetzsche and 1931). This explains the dominant presence of palynomorphs relative to the AOM in the homogeneous intervals. The opposite result was found in the sapropels where AOM was the predominant macromolecular OM. These palynological results are consistent with the Py-GC/MS data.

Comparison of the composition the kerogen pyrolysates of the homogeneous intervals and the sapropels showed similarities with changes in kerogen composition of the Madeira Abyssal Plain (MAP) turbidites (Hoefs *et al.*, 1996). The sedimentary record of the MAP contains a large number of OM-rich turbidites, which were formed by re-deposition of sediments deposited at the northwestern African Shelf. Due to mixing during transport these turbidites contain uniformly distributed OM in the up to 50 cm thick turbidites. The upper part of the turbidite is subjected to oxic conditions due to the diffusion of oxygen, allowing a study of the effects of post-depositional oxidation on OM composition (Hoefs *et al.*, 1996). A number of differences observed between the compositions of the kerogen pyrolysates of the oxidized and non-oxidized MAP turbidites, agree with those observed in this study for the kerogen pyrolysates of the homogeneous intervals and sapropels, respectively.

Compound classes, such as isoprenoid alkanes/alkenes and alkylphenols revealed relatively low abundances in the homogeneous intervals and relatively high abundances in the kerogen pyrolysates of the sapropels, which was also observed in the kerogen pyrolysates of the oxidized and non-oxidized MAP turbidites, respectively. In addition, (i) a shift to a lower n-alkane/n-alk-1-ene ratio, (ii) an increased ACL measured ACL for n-alkanes/n-alk-1-enes and methylketones (Table 2), and (iii) relatively higher abundance of pristenes in the kerogen pyrolysates of the sapropel compared with that of the homogeneous interval are observed (Fig. 7.5a). The degree of alkylation (not specified in detail here) of the alkylphenols, alkylthiophenes, alkylbenzenes and alkylpyrroles in the kerogen pyrolysates of the sapropels, was also higher compared than in those kerogen pyrolysates of the homogeneous intervals (Fig. 7.6a-d). Chlorophyll pigments are generally labile natural products. Earlier studies on chlorophyll have shown that pigments are much more stable under anoxic than oxic conditions (Sun *et al.*, 1991; Sun and Wakeham, 1994). This agrees with the presence of chlorophyll-derived compounds, such as phytene and alkylpyrroles, reflecting anoxic preservation conditions during sapropel deposition (Fig. 7.5b, 6d). Phytadienes were absent in the homogeneous interval, which is consistent with their absence in kerogen pyrolysates of

particulate OM collected in sediment traps deployed in the Mediterranean Sea (Peulve *et al.*, 1996).

The interpretation that the OM of the homogeneous intervals was exposed much longer to oxygen during deposition than the OM of the sapropels is in good agreement with other data. The presence of isorenieratene in the sapropels indicates that sapropels were deposited under euxinic conditions (Menzel *et al.*, 2002), in contrast with the homogeneous intervals. In surface sediments of the eastern Mediterranean this preferential degradation of labile marine OM also occurs (van Santpoort *et al.*, 2002). Surprisingly, however, values in surface sediments clearly revealed more enriched values with increasing depth (van Santvoort *et al.*, 2002). This $\delta^{13}\text{C}_{\text{org}}$ trend indicates that in the eastern Mediterranean Sea marine OM is more depleted in ^{13}C than terrestrial OM, which usually contains less ^{13}C than marine OM (Tyson, 1995).

More negative values were also observed in the upper Pleistocene-Quaternary sapropels S1 to S9 and the three studied Pliocene sapropels compared to their corresponding homogeneous intervals (Bouloubassi *et al.*, 1999; Nijenhuis *et al.*, 2000). These apparently more positive values of terrestrial OM, which is enriched in the homogeneous intervals, could be explained if terrestrial OM is derived from a mixture of C_3 and C_4 plants, which have values of ca. -27 and -12 ‰, respectively (Tyson, 1995). Indeed, studies of higher plant wax C_{27-33} n-alkanes revealed, a substantial C_4 plant contribution (i.e. 40-50 %) in the homogeneous intervals (Menzel *et al.*, in press). This could explain the more enriched $\delta^{13}\text{C}_{\text{org}}$ values (ca. -20 ‰) in the homogeneous intervals (mixture of marine/terrestrial OM), compared to the sapropels (ca. -22 ‰) (predominantly marine OM) (Nijenhuis *et al.*, 2002), where the terrestrial signal is overprinted. Although, the terrestrial OM has revealed an enrichment in $\delta^{13}\text{C}$ in the sapropels, the contribution of terrestrial OM is poor, compared with the marine OM. The more positive $\delta^{13}\text{C}_{\text{org}}$ values in the homogeneous intervals compared with the sapropels is caused by the high contribution of C_4 plants to the OM. The substantial terrestrial input of C_4 plant material was probably derived from the North African continent and transported via the river Nile and fossil wadi systems (cf. Rohling *et al.*, 2002) into the eastern Mediterranean Sea.

CONCLUSIONS

Differences in kerogen composition between the homogeneous intervals and sapropels were obtained by palynological and Curie-point pyrolysis results. The kerogen pyrolysates of homogeneous intervals consisted of a mixture of resistant marine and terrestrial macromolecular OM, which have persisted aerobic decomposition during their deposition. The kerogen pyrolysates of the sapropels originated predominately of marine and only minor terrestrial macromolecular OM, which were deposited under anoxic preservation conditions. Therefore, these differences in kerogen composition between the sapropels and their homogeneous intervals were caused by different preservation condition, rather than changes in autochthonous versus allochthonous sources. It is assumed that the unusual shift of $\delta^{13}\text{C}_{\text{org}}$ values, being more depleted in $\delta^{13}\text{C}$ in the sapropels, in contrast to the

homogeneous intervals is resulting from the higher C₄ plant relative to C₃ plant contribution of the terrestrial OM in the homogeneous intervals, which has caused the more enriched $\delta^{13}\text{C}_{\text{org}}$ values. However, the more enriched values of the terrestrial OM measured in the sapropels is overprinted by the predominately marine OM.

ACKNOWLEDGEMENTS

We thank Kathrin Reimer, Natasja Welters, Jan van Tongeren, Merlijn Sprangers and Ton Zalm for analytical help and Dr. Andy Dale for helpful discussions and IPPU for funding a Ph.D. position.

References

- Adamson, D.A., Gasse, F., Street, F.A., Williams, M.A.J., 1980. Late Quaternary history of the Nile. *Nature*, 288, 50-55.
- Abates, F. Moita, M.T., 1999. Water column and recent sediment data on diatoms and coccolithophores, off Portugal, confirm sediment record of upwelling events. *Oceanologica Acta*, 22, 319-336.
- Abbott, G.D., Ewbank, G., Edwards, D., Wang, G.Y., 1998. Molecular characterization of some enigmatic Lower Devonian fossils. *Geochimica et Cosmochimica Acta*, 62, 1407-1418.
- Aksu, A.E., Yasar, D., Mudie, P.J., Gillespie, H. 1995. Late glacial-Holocene palaeoclimatic and palaeoceanographic evolution of the Aegean Sea - micropaleontological and stable isotopic evidence. *Marine Micropaleontology*, 25, 1-28.
- Allen, H.D., 2001. Climate. In: *Mediterranean Ecogeography, Ecogeography series*, 25-44.
- Andrews, A.G., Liaaen-Jensen, S., 1972. Bacterial Carotenoids XXXVII. Carotenoids of Thiorhoaceae 9. Structural elucidation of five minor carotenoids from *Thiotheca gelatinosa*. *Acta Chemica Scandinavica*, 26, 2194-2204.
- Arthur, M.A., Dean, W.E., Neff, E.D., Hay, B.J., King, J. and Jones, G., 1994a. Varve calibrated records of carbonate and organic carbon accumulation over the last 2000 years in the Black Sea. *Global Biogeochemical Cycles*, 8,195-217.
- Arthur, M.A. and Sageman, B.B., 1994b. Marine black shales: Depositional mechanisms and environments of ancient deposits. *Annual. Review of Earth Planet Science*, 22,499-551.
- Arthur, M.A. and Dean, W.E., 1998. Organic matter production and preservation and evolution of anoxia in the Holocene Black Sea *Palaeoceanography*, 13,395-411
- Bams, S.M., Delwiche, C.F., Palmer, J.D., Pace, N.R.,1996. Perspectives on archaeal diversity, thermophily and monophily from environmental rRNA sequences. *Proceedings of the National Academy of Sciences of the United States of America*, 93, 9188-9193.
- Behar, F., Derenne, S., Largeau, C., 1995. Closed pyrolysis of the isoprenoid algaenan of *Botryococcus braunii*, L race: Geochemical implications for derived kerogens. *Geochimica et Cosmochimica Acta*, 59,2983-2997.
- Bein, A., Almogilabin, A., Sass, E., 1990. Sulfur sinks and organic-carbon relationships in Cretaceous organic-rich carbonates- implications for evaluation of oxygen-poor depositional-environments. *American Journal of Science*, 290, 882-911.
- Bergstein, T., Henis, Y., Cavari, B.Z., 1979. Investigations on the photosynthetic bacterium *Chlorobium phaeobacterioides* causing seasonal blooms in Lake Kinneret. *Canadian Journal of Microbiology*, 25,999-1007.
- Bethoux, J.P., 1989. Oxygen-Consumption, New Production, Vertical Advection and Environmental Evolution in the Mediterranean-Sea. *Deep-Sea Research Part I-Oceanographic Research Papers*, 36, 769-781.
- Bidigare, R.R., Fliigge, A., Freeman, K.H., Hanson, K.L., Hayes, J.M., Hollander, D., Jasper, J.P., King, L.L., Laws, E.A., Milder, J., Millero, F.J., Pancost, R., Popp, B.N., Steinberg, P.A. and Wakeham, S.G., 1997. Consistent fractionation in $\delta^{13}\text{C}$ in nature and in the laboratory: Growth rate effects in some haptophyte algae. *Global Biochemical Cycles*, 11,279-292.
- Biebl, H., Pfennig, N., 1978. Growth yields of green sulphur bacteria in mixed culture with sulphur and sulphate reducing bacteria. *Archives of Microbiology*, 117,9-16.
- Bishop, J.K.B., 1989. The bante-opal-organic carbon association in oceanic particulate matter. *Nature*, 332,341-343.
- Blankenship, R.E., Madigan, M.T., Bauer, C.E., (1995) Anoxygenic Photosynthetic Bacteria. (Eds.) *Dordrecht: Kluwer*.

- Blokker, P., Schouten, S., van der Ende, H., de Leeuw, J.W., Hatcher, P.G., Sinninghe Damste, I.S., 1998. Chemical structure of algaenans for the fresh water microalgae *Tetraedron minimum*, *Scenedesmus communis* and *Pediastrum bOlyanum*. *Organic Geochemistry*, 29, 1453-1468.
- Boon, J.I, Rijpstra, W.I.c., de Lange, F., de Leeuw, J.W., Yoshioka, M. and Shimizu, Y., 1979. The Black Sea sterol: molecular fossil for dinoflagellates blooms. *Nature*. 277, 125-127.
- Bosch, H.-J., Sinninghe Damste, J.S., de Leeuw, J.W., 1998. Molecular palaeontology of eastern Mediterranean sapropels: evidence for photic zone euxinia. In: *Proceedings of the Ocean Drilling Program, Scientific Results, 160* (Eds.: Robertson, A.H.F., Emeis, K.-C., Richter and Camerlenghi, A.), *Ocean Drilling Program, College Station, TX*, 285-295.
- Bouloubassi, I., Rullkötter, J., Meyers, P.A., 1999. Origin and transformation of organic matter in Pliocene- Pleistocene Mediterranean sapropels: organic geochemical evidence reviewed. *Marine Geology*, 153, 177-197.
- Boyle, E.A., Lea, D.W., 1989. Cd and Ba in planktonic foraminifera from the eastern Mediterranean: evidence for river outflow and enriched nutrients during sapropel formation. *Transactions American Geophysical Union*, 70, 1134.
- Brassell, S.C., Eglinton, G., Marlowe, L.T., Pfaumann, D., Samthein, M., 1986. Molecular stratigraphy: a new tool for climatic assessment. *Nature*, 320, 129-133.
- Brassell, S.C., 1993. Applications of biomarkers for delineating marine paleoclimatic fluctuations during the Pleistocene. In: Engel, M.H. and Macko, S.A. (Eds.), *Organic Geochemistry, Principles and Applications*. Plenum Press, New York and London, pp. 699-733.
- Britton, G., 1995. UV/Visible Spectroscopy, 1B: *Spectroscopy*, 13-62.
- Brock, T.D., 2000. Biology of microorganisms. 9th Edition (Eds.. M.T. Madigan, J.M. Martinko, J. Parker), London, pp. 455-461.
- Brown, S.R, McIntosh, H.I., Smol, J.P., 1984. Recent paleolimnology of a meromictic lake: fossil pigments of photosynthetic bacteria. *Verhandlungen del' Internationalen Vereinigung fur Limnologie*, 22,1357-1360.
- Burnsack, H.J., 1986. The inorganic geochemistry of Cretaceous black shales (DSDP Leg 41) in comparison to modern upwelling sediments from the Gulf of California. In: Summerhayes, C.P., Shackleton, N.J. (Eds.), *North Atlantic Palaeoceanography*. Geological Society Special Publications, 21, 447-462.
- Bryantsev, V.A., Ya Fashchuk, D., Ayzatullin, T.A., Bagotskity, S. and Leonov, A.V., 1988. Variation in the upper boundary of the hydrogen sulphide zone in the Black Sea: Analysis of field observations and modelling results. *Oceanology*, 28, 180-185.
- Calvert, S.E., 1983. Geochemistry of Pleistocene sapropels and associated sediments from the eastern Mediterranean. *Oceanologica Acta*, 6,255-267.
- Calvert, S.E., Pedersen, T.F., 1992. Organic carbon accumulation and preservation in marine sediments: how important is anoxia. In: J.K. Whelan and J.W. Farrington (Eds.), *Productivity, Accumulation and Preservation of Organic Matter in Recent and ancient Sediments*. Columbia University Press, New York, N.Y., pp. 231-263.
- Calvert, S.E., Nielsen, B. and Fontugne, M.R, 1992. Evidence from nitrogen isotope ratios for enhanced productivity during formation of eastern Mediterranean sapropels. *Nature*, 359, 223-225.
- Calvert, S.E., Thode, H.G., Yeung, D. and Karlin, R.E., 1996. A stable isotope study of pyrite formation in the late Pleistocene and Holocene sediments of the Black Sea. *Geochim. Cosmochim. Acta*, 60,1261-1270.
- Calvert, S.E., Pedersen, T.F., 2001. On the late Pleistocene-Holocene sapropel record of climatic and oceanographic variability in the eastern Mediterranean. *Paleoceanography*, 16, 78-94.
- Canfield, D.E., 1994. Factors influencing organic-carbon preservation in marine sediments. *Chemical Geology*, 114,315-329.

- Caumette, P., 1986. Phototrophic sulphur bacteria and sulphate-reducing bacteria causing red waters in a shallow brackish coastal lagoon (Prevost Lagoon, France). *FEMS Microbiology Ecology*, 38, 113-124.
- Cerling, T.E., 1992. Development of grasslands and savannas in east Africa during the Neogene. *Palaogeography, Palaeoclimatology, Palaeoecology*, 97, 241-247.
- Cheddadi, R., Rossignol-Strick, M., Fontugne, M., 1991. Eastern Mediterranean palaeoclimates from 26 to 5 ka B.P. documented by pollen and isotopic analysis of a core in the anoxic Bannock Basin. *Marine Geology*, 100, 53-66.
- Cheddadi, R., Rossignol-Strick, M., 1995. Improved preservation of organic matter and pollen in eastern Mediterranean sapropels. *Paleoceanography*, 10, 301-309.
- Church, M.J., de Long, E.F., Ducklow, H.W., Kamer, M.B., Preston, C.M., Karl, D.M., 2003. Abundance and distribution of planktonic Archaea and Bacteria in the waters west of the Antarctic Peninsula. *Limnology and Oceanography*, 48, 1893-1902.
- Cita, M.B., Vergnaud-Grazzini, C., Robert, C., Charnley, R., Ciaranfi, N., D'Onofrio, S., 1977. Paleoclimatic record of a long deep sea core from the eastern Mediterranean. *Quaternary Research*, 8, 205-235.
- Cita, M.B., Broglia, C., Malinverno, A., Spezzibottiani, G., Tomadin, L., Violanti, D., 1982. Late Quaternary pelagic sedimentation on the southern Calabrian Ridge and western Mediterranean Ridge, eastern Mediterranean. *Marine Micropaleontology*, 7, 135-162.
- Cita, M.B., Grignani, D., 1982. Nature and origin of late Neogene Mediterranean sapropels. In: S.O. Schlanger and M.B. Cita (Eds.), *Nature and Origin of Cretaceous Carbon-rich Facies*, Academic Press, New York, pp. 165-196.
- Collatz, G.J., Berry, I.A., Clark, I.S., 1998. Effects of climate and atmospheric CO₂ partial pressure on the global distribution of C₄ grasses: present, past and future. *Oecologia*, 114, pp. 441-454.
- Collatz, G.J., Ribas-Carbo, M., Berry, I.A., 1992. Coupled photosynthesis-stomatal conductance model for leaves of C₄ plants. *Australian Journal of Plant Physiology*, 19, 519-538.
- Collinson, M.E., van Bergen, P.F., Scott, A.C., de Leeuw, J.W., 1994. In coal and coal-bearing strata as oil-prone source rocks? In: A.C. Scott and A.I. Fleet (Eds.) *Geological Society of London, Special Publication*, 77, pp. 31-70.
- Collinson, M.E., Mosle, B., Finch, P., 1998. The preservation of plant cuticle in the fossil record: a chemical and microscopical investigation. *Ancient Biomolecules*, 2, 251-265.
- Collister, I.W., Rieley, G., Stem, B., Eglinton, G., Fry, B., 1994. Compound-specific δ¹³C analyses of leaf lipids from plants with differing carbon dioxide metabolism. *Organic Geochemistry*, 21, pp. 619-627.
- Coolen, M.J.L., Cypionka, R., Sass, A.M., Sass, R., Overmann, I., 2002. Ongoing modification of Mediterranean Pleistocene sapropels mediated by prokaryotes. *Science*, 296, 2407-2410.
- Cowie, L.C., Calvert, S.E., Pedersen, T.F., Schulz, R. and von Rad, D., 1999. Organic content and preservational controls in surficial shelf and slope sediments from the Arabian Sea (Pakistan margin). *Marine Geology*, 162, 23-38.
- Dehairs, F., Lambert, C.E., Chesselet, R. and Risler, N., 1987. The biological production in the marine suspended barite and barium cycle in the western Mediterranean Sea. *Biogeochemistry*, 4, 119-139.
- de Lange, G.I., Middelburg, J.J., and Pruyssers, P.A., 1989. Discussion: Middle and Late Quaternary depositional sequences and cycles in the eastern Mediterranean. *Sedimentology*, 36, 151-156.
- de Leeuw, I.W., Largeau, C., 1993. A review of macromolecular organic compounds that comprise living organisms and their role in kerogen, coal and petroleum formation. In: M.H. Engel and S.A. Macko (Eds.) *Organic Geochemistry*. Plenum press, New York, pp. 23-72.
- de Leeuw, I.W., Frewin, N.L., van Bergen, P.F., Sinninghe Damste, J.S., Collinson, M.E., 1995. Organic carbon as palaeoenvironmental indicator in the marine realm. In: D.W. Bosence and

-
- P.A Allison (Eds.), Marine Palaeoenvironmental Analysis from Fossils, Geological Society Special Publication, 83, pp. 43-71.
- de Long, E.F., 1992. Archaea in coastal marine environments. *Proceedings of the National Academy of Sciences of the United States of America*, 89, 5685-5689.
- de Long, E.F., King, I., Massana, R., Cittone, H., Murray, A., Schleper, C., Wakeham, S.G., 1998. Dibiphytanyl ether lipids in nonthermophilic crenarchaeotes. *Applied and Environmental Microbiology*, 64, 1133-1138.
- de Long, E.F., Taylor, L.T., Marsh, T.L., Preston, C.M., 1999. Visualization and enumeration of marine planktonic archaea and bacteria by using polyribonucleotide probes and fluorescent in situ hybridization. *Applied and Environmental Microbiology*, 65, 5554-5563.
- de Rosa, M., Gambacorta, A., 1988. The lipids of archaeobacteria. *Progress in Lipid Research*, 27, 153-175.
- de Wit, R., van Gemerden, H., 1987. Chemolithotrophic growth of the phototrophic sulphur bacterium *Thiocapsa roseopersicina*. *FEMS Microbiology Ecology*, 45, 117-126.
- Demaison, E.T., Moore, G.T., 1980. Anoxic environments and oil source bed genesis. *The American Association of Petroleum Geologists Bulletin*, 64, 1179-1209.
- deMenocal, P.R., 1995. Plio-Pleistocene African climate. *Science*, 270, 53-59.
- Derenne, S., Largeau, C., Casadevall, E., Berkaloff, C., 1989. Occurrence of a resistant biopolymer in the L race of *Botryococcus braunii*. *Phytochemistry*, 28, 1137-1142.
- Derenne, S., Largeau, C., Casadevall, E., Sellier, N., 1990. Direct relationship between the resistant biopolymer and the tetraterpene hydrocarbon in the lycopadiene race of *Botryococcus braunii*. *Phytochemistry*, 29, 2187-2192.
- Derenne, S., Berre, F.L., Largeau, C., Hatcher, P.G., Connan, J., Raynaud, J.F., 1992. Formation of ultralaminae in marine kerogens via selective preservation of thin resistant outer walls of microalgae. *Organic Geochemistry*, 19, 345-350.
- Dugdale, R.C. and Wilkerson, F.P., 1988. Nutrient sources and primary production in the Eastern Mediterranean. *Oceanologica Acta*, 9, 179-184.
- Durand, R.E., 1980. Kerogen-insoluble organic matter from sedimentary rocks. Edition Technip, Paris.
- Dymond, J., Suess, E. and Lyle, M., 1992. Barium in deep-sea sediment: A geochemical proxy for palaeoproductivity. *Palaeoceanography*, 7, 163-181.
- Edwards, D., Ewbank, G., Abbott, G.D., 1997. Flash pyrolysis of the outer cortical tissues in Lower Devonian *Psilophyton dawsonii*. *Botanical Journal of the Linnean Society*, 124, 345-360.
- Eglinton, G., Calvin, M., 1967. Chemical fossils. *Scientific American*, 261, 32-43.
- Eglinton, G., Hamilton, R.J., 1967. Leaf epicuticular waxes. *Science*, 156, 1322-1335.
- Eglinton, G., Hamilton, R.J., 1963. The distribution of n-alkanes. In: T. Swain (Ed.), *Chemical Plant Taxonomy*, Academic, London, pp. 187-217.
- Eglinton, G., Scott, P.M., Besky, T., Burlingame, A.L., Calvin, M., 1964. Hydrocarbons of biological origin from a one-billion-year-old sediment. *Science*, 145, 263-264.
- Ehleringer, J.R., Cerling, T.E., Helliker, R.R., 1997. C₄ photosynthesis, atmospheric CO₂, and climate. *Oecologia*, 112, 285-299.
- Emeis, K.C., Camerlenghi, A., McKenzie, I.A., Rio, D., Sprovieri, R., 1991. The occurrence and significance of Pleistocene and Upper Pliocene sapropels in the Tyrrhenian Sea. *Marine Geology*, 100, 155-182.
- Emeis, K.C., Robertson, A.H.F., Richter, C. et al., 1996. *Proceedings of the Ocean Drilling Program, Initial Reports, 160, Ocean Drilling Program, College Station, TX*
- Emeis, K.C., Schulz, H.M., Struck, U., Sakamoto, T., Doose, H., Erlenkeuser, H., Howell, M.W., Kroon, D., Paterne, M., 1998. Stable isotope and alkenone temperature records of sapropels from the sites 964 and 967: constraining the physical environment of sapropel formation in

- the eastern Mediterranean Sea. *Proceedings of Ocean Drilling Program, Scientific Results, 160* (Eds. Robertson, A.N.F., Emeis, K.-C., Richter, C. and Camerlenghi, A.), 309-331.
- Emeis, K.C., Struck, D., Schulz, H.M., Rosenberg, R., Bernasconi, S., Erlenkeuser, H., Sakamoto, T., Martinez-Ruiz, F., 2000. Temperature and salinity variations of Mediterranean Sea surface waters over the last 16,000 years from records of planktonic stable oxygen isotopes and alkenone unsaturation ratios. *Palaeogeography, Palaeoclimatology, Palaeoecology*, 158,259-280.
- Eppley, R.W. and Peterson, B.I., 1979. Particulate organic matter flux and planktonic new production in the deep ocean. *Nature*, 282, 677-680.
- Eraso, J.M., Kaplan, S., 2001. Photoautotrophy. *Nature Encyclopedia of Life Sciences*, 1-7.
- Espitalie, I., Laporte, J.L., Madec, M., Marquis, F., Lepat, P., Paulet, J., Boutefeu, A., 1977. Methode rapide de caracterisation des roches meres, de leur potentiel petrolier et de leur degre d evolution. *Revue De L Institut Francais Du Petrole*, 32, 23-42.
- Ewbank, G., Edwards, D., Abbott, G.D., 1996. Chemical characterization of Lower Devonian vascular plants. *Organic Geochemistry*, 25,461-473.
- Falkner, K.K., Klinkhammer, G.P., Bowers, T.S., Todd, I.F., Lewis, B.L., Landing, W.M. and Edmond, J.M., 1993. The behavior of barium in anoxic marine waters. *Geochimica et Cosmochimica Acta*, 57, 537-554.
- Ferreira, A.M., Miranda, A., Caetano, M., Baas, M., Vale, C. and Sinninghe Damste, J.S., 2001. Formation of mid-chain alkane keto-ols by post-depositional oxidation of mid-chain diols in Mediterranean sapropels. *Organic Geochemistry*, 32, 271-276.
- Fontugne, M.R., Arnold, M., Labeyrie, L., Paterne, M., Calvert, S.E. and Duplessy, J.C., 1994. Palaeoenvironment, sapropel chronology and Nile river discharge during the last 20,000 years as indicated by deep-sea sediment records in the eastern Mediterranean. In: Bar-Yosef, O., Kra, R.S. (Eds.), *Late Quaternary Chronology and Palaeoclimates of the eastern Mediterranean. Radiocarbon*, 36, 75-88.
- Foucault, A., Melieres, F., 2000. Palaeoclimatic cyclicity in central Mediterranean Pliocene sediments: the mineralogical signal. *Palaeogeography Palaeoclimatology Palaeoecology*, 158,311-323.
- Francois, R., Honjo, S., Manganini, S.J. and Ravizza, G.E., 1995. Biogenic barium fluxes to the deep sea: Implications for palaeoproductivity reconstruction. *Global Biochemical Cycles*, 9, 289-303.
- Freeman, K.H., Wakeham, S.G., 1992. Variations in the distribution and isotopic compositions of alkenones in Black Sea particles and sediments. *Organic Geochemistry*, 19,277-285.
- Fuhrmann, J.A., McCallum, K., Davis, A.A., 1992. Novel major archaeobacterial group from marine plankton. *Nature*, 356, 148-149.
- Gelin, F., Gatellier, J., Sinninghe Damste, J.S., Metzger, P., Derenne, S., Largeau, C., de Leeuw, J.W., 1993. Mechanisms of flash pyrolysis of ether lipids isolated from the green microalga *Botryococcus braunii* Race-A. *Journal of Analytical and Applied Pyrolysis*, 27, 155-168.
- Gelin, F., Boogers, I., Noordeloos, A.A.M., Sinninghe Damste, J.S., Hatcher, P.G., de Leeuw, J.W., 1996. Novel, resistant microalgal polyethers: an important sink of organic carbon in the marine environment. *Geochimica et Cosmochimica Acta*, 60, 1275-1280.
- Gelin, F., Boogers, I., Noordeloos, A.A.M., Sinninghe Damste, J.S., Riegman, R., de Leeuw, J.W., 1997. Resistant biomacromolecules in marine microalgae of the classes eustigmatophyceae and chlorophyceae: geochemical implications. *Organic Geochemistry*, 26,659-675.
- Gelin, F., Volkman, J.K., Largeau, C., Derenne, S., Sinninghe Damste, J.S., de Leeuw, J.W., 1999. Distribution of aliphatic, nonhydrolyzable biopolymers in marine microalgae. *Organic Geochemistry*, 30, 147-159.

- Gingele, F.x., Zable, M., Kasten, S., Bonn, W.I and Nuernberg, C.C., 1999. Biogenic barium as a proxy for palaeoproductivity: methods and limitations of application. In: Fischer, G. and Wefer, G. (Eds.) Use of proxies in palaeoceanography, pp. 345-364.
- Gliozzi, A., Paoli, G., De Rosa, M., Gambacorta, A., 1983. Effect of isoprenoid cyclization on the transition temperature of lipids in thermophilic archaeobacteria. *Biochimica et Biophysica Acta*, 753, 234-242.
- Goosens, H., de Leeuw, I.W., Schenck, P.A, Brassell, S.C., 1984. Tocopherols as likely precursors of pristane in ancient sediments and crude oils. *Nature*, 312,440-442.
- Goth, K., de Leeuw, I.W., Puttmann, W., Tegelaar, E.W., 1988. Origin of Messel Oil-Shale Kerogen. *Nature* 336, 759-761.
- Grice, K., Gibbison, R., Atkinson, I.E., Schwark, L., Eckardt, C.B., Maxwell, I.R., 1996. Maleimides (1H-pyrrole-2,5-diones) as molecular indicators of anoxygenic photosynthesis in ancient water columns. *Geochimica et Cosmochimica Acta*, 60, 3913-3924.
- Grosse-Damhues, I., Glombitza, K.W., 1984. Isofuhalols, a type of phlorotannins from the brown alga *Chordajilu*. *Phytochemistry*, 23, 2639-2642.
- Hartgers, W.A., Sinninghe I.S., de Leeuw, I.W., 1992. Identification of C₂-C₄ alkylated benzenes in flash pyrolysates of kerogens, coals and asphaltenes. *Journal Of Chromatography*, 606,211-220.
- Hartgers, W.A, Sinninghe Damste, I.S., de Leeuw, I.W., 1994a. Geochemical significance of alkylbenzene distributions in flash pyrolysates of kerogens, coals, and asphaltenes. *Geochimica et Cosmochimica Acta*, 58, 1759-1775.
- Hartgers, W.A, Sinninghe Damste, I.S., Requejo, AG., Allan, J., Hayes, IM., Ling, Y, Xie, T.M., Primack, I., de Leeuw, I.W., 1994b. A molecular and carbon isotopic study towards the origin and diagenetic fate of diaromatic carotenoids. *Organic Geochemistry*, 22, 703-725.
- Hartgers, W.A, Schouten, S., Lopez, J.F., Sinninghe Damste, I.S., Grimalt, I.O., 2000. BC-contents of sedimentary bacterial lipids in a shallow sulfidic monomictic lake (Lake Ciso, Spain). *Organic Geochemistry*, 31, 777-786.
- Hatcher, P.G., Clifford, D.I., 1997. The organic geochemistry of coal: from plant materials to coal. *Organic Geochemistry*, 27,251-274.
- Haywood, AM., Sellwood, B.W., Valdes, P.J., 2000. Regional warming: Pliocene (3 Ma) paleoclimate of Europe and Mediterranean. *Geology*, 28, 1063-1066.
- Herbin, I.P., Magniez-Jannin, F, Miiller, C., 1986. Mesozoic organic rich sediments in the South Atlantic: distribution in time and space. *Mitteilungen aus dem Geologischen-Palaeontologischen Institut der Universitiit Hamburg*, 60,71-97.
- Hershberger, KL., Barns, S.M., Reysenbach, AL., Dawson, S.C., Pace, N.R., 1996. Wide diversity of Crenarchaeota. *Nature*, 384, 420-420.
- Higgs, N.C., Thomson, J., Wilson, T.R.S, Croudace, LW., 1994, Modification and complete removal of eastern Mediterranean sapropels by postdepositional oxidation. *Geology*, 22, 423-426.
- Hilgen, F.I., 1991. Astronomical Calibration of Gauss to Matuyama Sapropels in the Mediterranean and Implication for the Geomagnetic Polarity Time Scale. *Earth and Planetmy Science Letters*, 104, 226-244.
- Hoefs, M.J.L., van Heemst, J.D.H., Gelin, F., Koopmans, M.P., van Kaam-Peters, H.M.E., Schouten, S., de Leeuw, J.W., Sinninghe Damste, I.S., 1995. Alternative biological sources for 1,2,3,4-tetramethylbenzene in flash pyrolysates of kerogens, *Organic Geochemistry*, 23, 975-980.
- Hoefs, M., Sinninghe Damste, J.S., de Lange, GJ, de Leeuw, I.W., 1996. Changes in kerogen composition across an oxidation front in Madeira abyssal plain turbidites as revealed by pyrolysis GC-MS. *Abstract a/papers a/the American Chemical Society*, 21,52-GEOC PartI AUG 25.

- Hoefs, M., Schouten, S., de Leeuw, J.W., King, L.L., Wakeham, S.G., Sinninghe Damste, J.S., 1997. Ether lipids of planktonic archaea in the marine water column. *Applied and Environmental Microbiology*, 63, 3090-3095.
- Hoefs, M., Rijpstra, W.L.C., Sinninghe Damste, J.S., 2002. The influence of oxic degradation on the sedimentary biomarker record I: Evidence from Madeira Abyssal Plain turbidites. *Geochimica et Cosmochimica Acta*. 66, 2719-2735.
- Höld, L.M., Schouten, S., van Kaam-Peters, H.M.E., Sinninghe Damste, J.S., 1998. Recognition of *n*-alkyl and isoprenoid biopolymers in marine sediments by stable carbon isotopic analysis of pyrolysis products of kerogens. *Organic Geochemistry*, 28, 179-195.
- Hollander, D.I., Behar, F., Vandenbroucke, M., Bertrand, P., McKenzie, J.A., 1990. Geochemical alteration of organic matter in eutrophic lake Greifen: implications for the determination of organic facies and the origin of lacustrine source rock. In: Hue, A.Y. (Ed.) Organic facies. AAPG Studies in Geology, 30, pp. 181-193.
- Honjo, S., Hay, B.J., Manganini, S.I., Degens, E.T., Kempe, S., Ittekkot, V., Izdar, E., Konuk, Y.T., Benli, H.A., 1987. Seasonal cyclicity of lithogenic particle fluxes at a southern Black Sea sediment trap station. *Mitteilungen aus dem Geologischen-Palaeontologischen Institut der Universität Hamburg, F.R.G.*, 19-39.
- Hopmans, E.C., Schouten, S., Pancost, R.D., van der Meer, M.T.J., Sinninghe Damste, J.S., 2000. Analysis of intact tetraether lipids in archaeal cell material and sediments by high performance liquid chromatography/atmospheric pressure chemical ionization mass spectrometry. *Rapid Communications in Mass Spectrometry*, 14, 585-589.
- Hopmans, E.C., Rijpstra, W.J.C., Rohling, E.I., Cane, T.R., Sinninghe Damste, J.S., 2003. Photic zone euxinia during S5 sapropel formation in the eastern Mediterranean. *Abstract of the 21th International Meeting on Organic Geochemistry, Krakow, Poland*.
- Huang Y., Street-Perrott, F. A., Metcalfe, S. E., Brenner, M., Moreland, M., Freeman, K. H., 2001. Climate change as the dominant control on glacial-interglacial variations in C₃ and C₄ plant abundance. *Science*, 293, 1647-1651.
- Hue, A.Y., Lallier-Verges, E., Bertrand, P., Carpentier, B. and Hollander, D.I., 1992. Organic matter response to change of depositional environment in Kimmeridgian shales, Dorset, UK. In: J.K. Whelan and J.W. Farrington (Eds.), Productivity, accumulation and preservation of organic matter in recent and ancient sediments. Columbia University Press, New York, pp. 231-263.
- Imhoff, J.F., Triiper, H.G., Pfennig, N., 1984. Rearrangement of the species and genera of the phototrophic 'purple nonsulphur bacteria'. *International Journal of Systematic Bacteriology*, 34, 340-343.
- Ishiwatari, M., Ishiwatari, R., Sakashita, H., Tatsumi, T., Tominaga, H.O., 1991. Pyrolysis of chlorophyll a after preliminary heating at a moderate temperature - implications for the origin of prist-1-ene on kerogen pyrolysis. *Journal of Analytical and Applied Pyrolysis*, 18, 207-218.
- Jeffrey, S.W., Vesk, M. 1997. Introduction to marine phytoplankton and their pigment signatures. In: Jeffrey, S.W., Mantoura, R.F.e., Wright, S.W. (Eds.), *Phytoplankton Pigments in Oceanography*. UNESCO. Paris, 407-428.
- Kampf, C., Pfennig, N., 1986. Chemoautotrophic growth of *Thiocystis violacea*, *Chromatium gracile*, and *C. vinosum* in the dark at various O₂-concentrations. *Journal of Basic Microbiology*, 26, 517-531.
- Karl, D.M., Knauer, G.A 1991. Microbial production and particle flux in the upper 350 m of the Black-Sea. *Deep-Sea Research Part I-Oceanographic Research Papers*, 38, S921-S942.
- Kamer, M.B., de Long, E.F., Karl, D.M., 2001. Archaeal dominance in the mesopelagic zone of the Pacific Ocean. *Nature*, 409, 507-510.

- Katz, B.I., 1983. Limitations of "Rock-Eval" pyrolysis for typing organic matter. *Organic Geochemistry*, 4, 195-199.
- Kemp, A.E.S., Pearce, R.B., Koizumi, I., Pike, I. and Rance, S.J., 1999. The role of mat-forming diatoms in the formation of Mediterranean sapropels. *Nature*, 398, 57-61.
- Kenig, F., Hayes, I.M., Popp, B.N., Summons, R.E., 1994. Isotopic biogeochemistry of the Oxford Clay Formation (Jurassic), UK. *Journal of the Geological Society, London*, 151, 139-152.
- Kidd, R.B., Cita, M.B., Ryan, W.B.F., 1978. Stratigraphy of eastern Mediterranean sapropel sequences recovered during DSDP Leg 42A and their palaeoenvironmental significance. In: *Initial Reports of the Deep Sea Drilling Project. 42A* (Eds. Hsui, K.J., Montadert L., et al.) U.S. Government Printing Office, Washington, 412-443.
- Kimor, B., Berman, T., Schneller, A., 1987. Phytoplankton assemblages in the deep chlorophyll maximum layers off the Mediterranean coast of Israel. *Journal of Plankton Research*, 9, 433-443.
- King, L.L., Pease, T.K., Wakeham, S.G., 1998. Archaea in Black Sea water column particulate matter and sediments - evidence from ether lipid derivatives. *Organic Geochemistry*, 28, 677-688.
- Klok, I., Baas, M., Cox, H.C., de Leeuw, I.W., Schenck, P.A., 1984. Loliolides and dihydroactinidiolide in a recent marine sediment probably indicate a major transformation pathway of carotenoids. *Tetrahedron Letters*, 25, 5577-5580.
- Koga, Y., Nishihara, K., Morii, H., Akagawa-Matsushita, M., 1993. Ether polar lipids of methanogenic bacteria: Structures and comparative aspects, and biosynthesis. *Microbiology Review*, 57, 164-182.
- Koga, Y., Morii, H., Akagawa-Matsushita, M., Ohga, M., 1998. Correlation of polar lipid composition with 16S rRNA phylogeny in methanogens. *Bioscience, Biotechnology and Biochemistry*, 62, 230-236.
- Kok, M.D., Schouten, S., Sinninghe Damste, I.S., 2000. Formation of insoluble, nonhydrolyzable, sulfur-rich macromolecules via incorporation of inorganic sulfur species into algal carbohydrates. *Geochimica et Cosmochimica Acta*, 64, 2689-2699.
- Koopmans, M.P., Koster, I., van Kaam-Peters, H.M.E., Kenig, F., Schouten, S., Hartgers, W.A., de Leeuw, I.W., Sinninghe Damste, I.S., 1996. Diagenetic and catagenetic products of isorenieratene: Molecular indicators for photic zone anoxia. *Geochimica et Cosmochimica Acta*, 60, 4467-4496.
- Krom, M.D., Groom, S., Zohary, T., 2003. The eastern Mediterranean. In: K.D. Black and G. B. Shimmiel (Eds.) *Biogeochemistry of marine systems*, 91-122.
- Kullenberg, B., 1952. On the salinity of the water contained in marine sediments. *Meddel Fr. Oceanogr. Instit. Goteborg*, 21, 1-38.
- Kuypers, M.M.M., Pancost, R.D., Sinninghe Damste, I.S., 1999. A large and abrupt fall in atmospheric CO₂ concentrations during Cretaceous times. *Nature*, 399, 342-345.
- Kuypers, M.M.M., Blokker, P., Erbacher, I., Kinkel, H., Pancost, R.D., Schouten, S., Sinninghe Damste, I.S., 2001. Massive expansion of marine archaea during a mid-Cretaceous oceanic anoxic event. *Science*, 293, 92-94.
- Lafargue, E., Marquis, F., Pillot, D., 1998. Rock-Eval 6 applications in hydrocarbon exploration, production, and soil contamination studies. *Revue De L Institut Francais Du Pétrole*, 53, 421-437.
- Lami, A., Marchetto, A., Lo Bianco, R., Appleby, P.G., Guilizzoni, P., 2000. The last ca. 200 years palaeolimnology of Lake Candia (N. Italy): inorganic geochemistry, fossil pigments and temperature time-series analyses. *Journal of Limnology*, 59, 31-46.
- Larrasoana, I.C., Roberts, A.P., Rohling, E.J., Winkhofer, M., Wehausen, R., 2003. Three million years of monsoon variability over the northern Sahara. *Climate Dynamics*, 21, 689-698.

- Larter, S.R., Horsfield, B., 1993. Determination of structural components of kerogens by the use of analytical pyrolysis methods. In: M.H. Engel and S.A. Macko (Eds.), *Organic Geochemistry*. Plenum press, New York, pp. 271-284.
- Laws, E.A., Popp, B.N., Bigigare, R.R., Kennicutt, M.C. and Macko, S.A., 1995. Dependence of phytoplankton carbon isotopic composition on growth rate and $(CO_2)_{aq}$: Theoretical considerations and experimental results. *Geochimica et Cosmochimica Acta*, 59, 1131-1138.
- Leroy, S.A.G., Dupont, L.M., 1994. Development of vegetation and continental aridity in northwestern Africa during the late Pliocene - the pollen record of ODP Site-658. *Palaeogeography, Palaeoclimatology, Palaeoecology*, 109,295-316.
- Liaaen-Jensen, S., 1978. Chemistry of carotenoid pigments. In: Clayton R.K., Sistrom W.R. (Eds.), *The photosynthetic bacteria*, pp. 233-247.
- Logan, G.A., Smiley, C.J., Eglinton, G., 1995. Preservation of fossil leaf waxes in association with their source tissue, Clarkia, Northern Idaho, USA. *Geochimica et Cosmochimica Acta*, 59, 751-763.
- Lourens, L.J., Hilgen, F.J., Gudjonsson, L., Zachariasse, W.J., 1992. Late Pliocene to Early Pleistocene Astronomically Forced Sea- Surface Productivity and Temperature-Variations in the Mediterranean. *Marine Micropaleontology*, 19, 49-78.
- Lourens, L.J., Antonarakou, A., Hilgen, F.J., van Hoof, A.A.M., Vergnaud-Grazzini, C., Zachariasse, W.J., 1996. Evaluation of the Plio-Pleistocene astronomical timescale. *Paleoceanography*, 11, 391-413.
- Lyons, T.W., 1997. Sulfur isotopic trends and pathways of iron sulphide formation in upper Holocene sediments of the anoxic Black Sea. *Geochimica et Cosmochimica Acta*, 61, 3367-3382.
- Mackenzie, A.S., 1984. Applications of biological markers in petroleum geochemistry. In: J. Brooks and D. Welte (Eds.), *Advances in Petroleum Geochemistry, Volume 1*, Academic press, London, pp. 115-214.
- Mangini, A., Schlosser, P., 1983. The formation of eastern Mediterranean sapropel. *Marine Geology*, 72, 115-124.
- Marlowe, L.T., Green, J.C., Neal, A.C., Brassell, S.C., Eglinton, G., Course, P.A., 1984a. Long-chain (n-C₃₇-C₃₉) alkenones in the Prymnesiophyceae: Distribution of alkenones and other lipids and their taxonomic significance. *British Phycology Journal*, 19, 203-216.
- Marlowe, L.T., Brassell, S.C., Eglinton, G., Green, J.C., 1984b. Long chain unsaturated ketones and esters in living algae and marine sediments. In: P.A. Schenck, J.W. de Leeuw and G.W.M. Lijmbach (Eds.), *Advances in Organic Geochemistry 1983*, Pergamon Press, Oxford, U.K. *Organic Geochemistry*, 6, pp. 135-141.
- Massana, R., Murray, A.E., Preston, C.M., de Long, E.F., 1997. Vertical distribution and phylogenetic characterization of marine planktonic Archaea in the Santa Barbara Channel. *Applied and Environmental Microbiology*, 63, 50-56.
- Massana, R., Taylor, L.J., Murray, A.E., Wu, K.Y., Jeffrey, W.H., de Long, E.F., 1998. Vertical distribution and temporal variation of marine planktonic archaea in the Gerlache Strait, Antarctica, during early spring. *Limnology and Oceanography*, 43, 607-617.
- Matheron, R., Baulaigue, R., 1972. Bacteries photosynthetiques sulfureuses marines. Assimilation des substances organiques et minerales, et influence de la teneur en chlorure de sodium du milieu de culture sur leur developpement. *Archiv für Mikrobiologie*, 86, 291-304.
- McGregor, B.J., Moser, D.P., Aim, E.W., Neilson, K.H., Stahl, D.A., 1997. Crenarchaeota in Michigan sediments. *Applied and Environmental Microbiology*, 63, 1178-1181.
- McKinney, D.E., Hatcher, P.G., 1996. Characterization of peatified and coalified wood by tetramethylammonium hydroxide (TMAH) thermochemolysis. *International Journal of Coal Geology*, 32, 217-228.

- Mercone, D., Thomson, I. and Croudace, I.W., 2000. Duration of S1, the most recent sapropel in the eastern Mediterranean Sea, as indicated by accelerator mass spectrometry radiocarbon and geochemical evidence. *Paleoceanography*, 15,336-347.
- Menzel, D., Hopmans, E.C., van Bergen, P.F., de Leeuw, I.W., Sinninghe Damste, I.S., 2002. Development of photic zone euxinia in the eastern Mediterranean basin during deposition of Pliocene sapropels. *Marine Geology*, 189,215-226.
- Menzel, D., van Bergen, P.F., Schouten, S., Sinninghe Damste, I.S., 2003. Reconstruction of changes in export productivity during Pliocene sapropel deposition: a biomarker approach. *Palaeogeography Palaeoclimatology Palaeoecology*, 190,273-287.
- Menzel, D., Schouten, S., van Bergen, P.F., Sinninghe Damste, I.S., (in press) Higher plant vegetation changes during Pliocene sapropel formation. *Organic Geochemistry*.
- Mudie, P.I., Rochon, A., Aksu, A.E., Gillespie, H. 2002. Dinoflagellate cysts, freshwater algae and fungal spores as salinity indicators in Late Quaternary cores from Marmara and Black seas. *Marine Geology*, 190,203-231.
- Murat, A., 1999. Pliocene-Pleistocene occurrence of sapropels in the western Mediterranean Sea and their relation to eastern Mediterranean sapropels. *Proceedings of the Ocean Drilling Program, Scientific Results*, 161 (Eds. Zahn, R., Comas, M. C. and Klaus, A.), 519-527.
- Murray, I.W., 1991. Hydrographic variability in the Black Sea. In: E. Izdar and I. Murray (Eds.), *Black Sea Oceanography*, pp. 1-15.
- Murray, A.E., Preston, C.M., Massana, R., Taylor, L.T., Blakis, A., Wu, K.Y., de Long, E.F., 1998. Seasonal and spatial variability of bacterial and archaeal assemblages in the coastal waters near Anvers Island, Antarctica. *Applied and Environmental Microbiology*, 64,2585-2595.
- Murray, A.E., Blakis, A., Massana, R., Strawzewski, S., Passow, V., Alldredge, A., de Long, E.F., 1999a. A time series assessment of planktonic archaeal variability in the Santa Barbara Channel. *Aquatic Microbial Ecology*, 20,129-145.
- Murray, A.E., Wu, K.Y., Moyer, C.L., Karl, D.M., de Long, E.F., 1999b. Evidence for circumpolar distribution of planktonic Archaea in the Southern Ocean. *Aquatic Microbial Ecology*, 18, 263-273.
- Nijenhuis, I.A., Schenau, S.I., van der Weijden, C.H., Hilgen, F.I., Lourens, L.J. and Zachariasse, W.I., 1996. On the origin of upper Miocene sapropelites: A case study from the Faneromeni section, Crete (Greece). *Paleoceanography*, 11,633-645.
- Nijenhuis, I.A., Brumsack, H.I., de Lange, G.J., 1998. The trace element budget of the eastern Mediterranean during Pliocene sapropel formation. In: *Proceedings of the Ocean Drilling Program, Scientific Results*, 160 (Eds.: Robertson, A.H.F., Emeis, K.-c., Richter and Camerlenghi, A.), *Ocean Drilling Program, College Station, Texas*, pp. 199-206.
- Nijenhuis, I.A., Bosch, H.I., Sinninghe Damste, I.S., Brumsack, H.I. and de Lange, G.I., 1999. Organic matter and trace metal element rich sapropels and black shales: A geochemical comparison. *Earth and Planetary Science. Letters*, 169,277-290.
- Nijenhuis, I.A., de Lange, G.J., 2000. Geochemical constraints on Pliocene sapropel formation in the eastern Mediterranean. *Marine Geology*, 163,41-63.
- Nip, M., Tegeleaar, E.W., Brinkhuis, H., de Leeuw, I.W., Schenck, P.A., Holloway, P.I., 1986a. Analysis of modern and fossil plant cuticles by Curie-point Py-GC and Curie point Py-GC-MS: Recognition of a new, highly aliphatic and resistant biopolymer. In: D. Leythausen and I. Riillkoetter (Eds.), *Advances in Organic Geochemistry 1985. Organic Geochemistry*, 10, pp. 769-778.
- Nip, M., Tegeleaar, E.W., de Leeuw, J.W., Schenck, P.A., Holloway, P.I., 1986b. A new non-saponifiable highly aliphatic and resistant biopolymer in plant cuticles. Evidence from pyrolysis and ¹³C-NMR analysis of present-day and fossil plants. *Naturwissenschaften*, 73, 579-585.

- Nybakken, J.W., 1993. Plankton and Plankton Communities In: Nybakken, I.W. (Ed.), *Marine Biology, An Ecological Approach*, HarperCollinsCollegePublishers, NY, pp. 37-67.
- Olausson, E., 1961. Studies of deep-sea cores. *Reports of the Swedish Deep-Sea-Expedition 1947-1948*, 336-391.
- Orr, W.L., 1983. Comments on pyrolytic hydrocarbon yields in source-rock evaluation. In: M. Bjoroy *et al.* (Eds.), *Advances in Organic Geochemistry*. Wiley, New York, pp. 775-787.
- Overmann, J., Cypionka, H., Pfennig, N., 1992. An Extremely Low-Light-Adapted Phototrophic Sulfur Bacterium from the Black-Sea. *Limnology and Oceanography*, 37, 150-155.
- Passier, H.F., de.Lange.G.J., 1998. Sedimentary sulphur and iron chemistry in relation to the formation of eastern Mediterranean sapropels. In: Proceedings of the Ocean Drilling Program, Scientific Results, 160 (Eds.: Robertson, A.H.F., Emeis, K-C., Richter and Camerlenghi, A.), Ocean Drilling Program, College Station, Texas, pp. 249-259.
- Passier, H.F., Bosch, H.I., Nijenhuis, L.A., Laurens, L.J., Bottcher, M.E., Leenders, A., Sinninghe Damste, J.S., de Lange, G.J., de Leeuw, J.W., 1999a. Sulphidic Mediterranean surface waters during Pliocene sapropel formation. *Nature*, 397, 146-149.
- Passier, H.F., Middelburg, J.I., de Lange, G.I., Bottcher, M.E., 1999b. Modes of sapropel formation in the eastern Mediterranean: some constraints based on pyrite properties. *Marine Geology*, 199-219.
- Passier, H.F., Bottcher, M.E., de Lange, G.J., 1999c. Sulphur enrichment in organic matter of eastern Mediterranean sapropels: A study of sulphur isotope partitioning. *Aquatic Geochemistry*, 5, 99-118.
- Pearson, A., McNichol, A.P., Benitz-Nelson, B.C., Hayes, J.M., Eglinton, T.I., 2001. Origins of lipid biomarkers in Santa Monica Basin surface sediment: A case study using compound-specific ^{14}C -analysis. *Geochimica et Cosmochimica Acta*, 65, 3123-3137.
- Pedersen, T.F., Calvert, S.E., 1990. Anoxia versus Productivity - What Controls the Formation of Organic-Carbon-Rich Sediments and Sedimentary-Rocks. *AAPG Bulletin-American Association of Petroleum Geologists*, 74,454-466.
- Peters, K.B., 1986. Guidelines for evaluating petroleum source rock using programmed pyrolysis. *The American Association of Petroleum Geologists Bulletin*, 70,318-329.
- Peulve, S., de Leeuw, J.W., Sicre, M.A., Baas, M., Saliot, A., 1996. Characterization of macromolecular organic matter in sediment traps from the northwestern Mediterranean Sea. *Geochimica et Cosmochimica Acta*, 60, 1239-1259.
- Pfennig, N., Markhlam, M.C., Liaaen-Jensen, S., 1968. Carotenoids of Thiorhodaceae. Isolation and characterization of a *Thiothece*, *Lamprocystis* and *Thiodictyon* strain and their carotenoid pigments. *Archiv Mikrobiologie*, 62, 178-191.
- Pfennig, N., 1978. General physiology and ecology of photosynthetic bacteria. In: Clayton R.K., Sistrom W.R. (Eds.), *The photosynthetic bacteria*, New York, Plenum Press, pp. 3-18.
- Pfennig, N., 1989. Ecology of phototrophic purple and green sulphur In: Schlegel, H.G., Bowien, B. (Eds), *Autotrophic bacteria*, Science Technique Publishers, Madison, and Berlin, Heidelberg, New York, pp. 97-116.
- Pfennig, N., Triiper, H.G., 1989. Family Chromatiaceae. In: Staley, I.T., Bryant, M.P., Pfennig, N., Holt, I.G.(Eds.), *Bergey's manual of systematic bacteriology*, Williams and Wilkins, Baltimore, 3, pp. 1637-1654.
- Popp, B.N., Laws, E.A., Bidigare, R.R., Dare, I.E., Hanson, K.L. and Wakeham, S.G., 1998. Effect of phytoplankton cell geometry on carbon isotopic fractionation. *Geochimica et Cosmochimica Acta*, 62, 69-77.
- Poore, R.Z., Sloan, L.C. 1996. Introduction climates and climate variability of the Pliocene. *Marine Micropaleontology*, 27, 1-2.

- Poynter, I.G., Farrimond, P., Brassell, S.C., Eglinton, G., 1989. Aeolian-derived higher plant lipids in the marine sedimentary record: Links with paleoclimate. In: Leinen, M. and Sarthein, M. (Eds.), *Palaeoclimatology and Palaeometeorology: Modern and Past Patterns of Global Atmospheric Transport*, Kluwer, Dordrecht. pp. 435-462.
- Pratt, L.M., 1984. Influence of palaeoenvironmental factors on the preservation of organic matter in Middle Cretaceous Greenhorn Formation, Pueblo, Colorado. *The American Association of Petroleum Geologists Bulletin*, 68, 1146-1159.
- Prell, W.L., Kutzbach, J.E., 1987. Monsoon variability over the past 150,000 years. *Geophysical Research*, 92,8411-8425.
- Rau, G.H., Riebesell, U. and Wolf-Gladrow, D.A., 1996. A model of photosynthetic ^{13}C fractionation by marine phytoplankton based on diffusive molecular CO_2 uptake. *Marine Ecology Progress Series*, 133,275-285.
- Regtop, R.A., Crisp, P.T., Ellis, I., Fookes, C., 1986. I-pristene as a precursor for 2-pristene in pyrolysates of oil shale from Condor, Australia. *Organic Geochemistry*, 19, 351-370.
- Repeta, D., 1993. A high resolution historical record of Holocene anoxygenic primary production in the Black Sea. *Geochimica et Cosmochimica Acta*, 57, 4337-4342.
- Repeta, D.J., Simpson, D.J., Jorgensen, B.B., Jannasch, H.W., 1989. Evidence for anoxygenic photosynthesis from the distribution of bacteriochlorophylls in the Black Sea. *Nature*, 342, 69-72.
- Repeta, D., 1989. Carotenoid diagenesis in recent marine sediments: II. Degradation of fucoxanthin to loliolide. *Geochimica et Cosmochimica Acta*, 53, 699-707
- Riebesell, U., Revill, A.T., Holdsworth, D.G. and Volkman, J.K., 2000. The effects of varying CO_2 concentration on lipid composition and carbon isotope fractionation in *Emiliania huxleyi*. *Geochimica et Cosmochimica Acta*, 64, 4179-4192.
- Rieley, G., Collier, R.J., Jones, D.M., Eglinton, G., Eakin, P.A., Fallick, A.E., 1991. Sources of sedimentary lipids deduced from stable carbon-isotope analyses of individual compounds. *Nature*, 352,425-427.
- Rinna, J., Warning, B., Meyers, P.A., Brumsack, H.J., Rullkötter, J., 2002. Combined organic and inorganic geochemical reconstruction of paleodepositional conditions of a Pliocene sapropel from the eastern Mediterranean Sea. *Geochimica et Cosmochimica Acta*, 66, 1969-1986.
- Rohling, E.J., Gieskes, W.W., 1989. Late Quaternary changes in Mediterranean intermediate water density and formation rate. *Paleoceanography*, 4, 531-545.
- Rohling, E.J., 1991. A simple two-layered model for shoaling of the Eastern Mediterranean pycnocline due to glacio-eustatic sea level lowering. *Paleoceanography*, 6, 537-541.
- Rohling, E.J., 1994. Review and new aspects concerning the formation of eastern Mediterranean sapropels. *Marine Geology*, 122, 1-28.
- Rohling, E.J., Cane, T.R., Cooke, S., Sprovieri, M., Bouloubassi, I., Emeis, K.C., Schiebel, R., Kroon, D., Jorissen, F.J., Lorre, A., Kemp, A.E.S., 2002. African monsoon variability during the previous interglacial maximum. *Earth and Planetary Science Letters*, 202, 61-75.
- Rossignol-Strick, M., Nesteroff, W., Olive, P., Vergnaud-Grazzini, C., 1982. After de deluge: Mediterranean stagnation and sapropel formation. *Nature*, 295, 105-110.
- Rossignol-Strick, M., 1983. African monsoons, an immediate climate response to orbital insolation. *Nature*, 304, 46-49.
- Rossignol-Strick, M., 1985. Mediterranean Quaternary sapropels, an immediate response of the African monsoon to variation of insolation. *Palaeogeography, Palaeoclimatology, Palaeoecology*, 49,237-263.
- Rost, B., Zondervan, I. and Riebesell, U., 2002. Light-dependent carbon isotope fractionation in the coccolithophorid *Emiliania huxleyi*. *Limnology and Oceanography*, 47, 120-128.

- Rullkötter, J., Bouloubassi, I., Meyers, P.A., Doose, H., 1995. Sources and preservation of organic matter in Pliocene-Pleistocene sapropels in the Mediterranean Sea. Leg 160 and 161, Scientific Parties, *EOS, Transactions American Geophysical Union*, 76, F624 (abstract).
- Ryves, D.B., Jones, V.J., Guilizzoni, P., Lami, A., Marchetto, A., Battarbee, R.W., Bettinetti, R., Devoy, E.C., 1996. Late Pleistocene and Holocene environmental changes at Lake Albano and Lake Nemi (central Italy) as indicated by algal remains. In: P. Guilizzoni and F. Oldfield (Guest Editors), *Palaeoenvironmental Analysis of Italian Crater Lake and Adriatic Sediments Mem. Ist. ital. Idrobiol.*, 55, pp. 119-148.
- Sarkanen, K.V., Ludwig, C.H., 1971. *Lignins*. Wiley-Interscience, New York.
- Sasikala, C., Ramana, C.V., 1995. Biotechnological potentials of anoxygenic phototrophic bacteria. I. Production of single-cell protein, vitamins, ubiquinones, hormones, and enzymes and use in waste treatment. *Advances in Applied Microbiology*, 41, 173-226.
- Saunders, V.A., 1978. Genetics of Rhodospirillaceae. *Microbiological Review*, 42, 357-384.
- P., Adam, P., Wehrung, P., Bernasconi, S., Albrecht, P.A., 1997. Molecular and isotopic investigation of free and S-bound lipids from an actual meromictic lake (Lake Cadagno, Switzerland). Abstracts of the 18th International Meeting on Organic Geochemistry, KFA Jillich, 57-58.
- Schefuß, E., Schouten, S., Jansen, J.H.F., Sinninghe Damste, I.S., 2003. African vegetation controlled by tropical sea surface temperatures in the mid-Pleistocene period. *Nature*, 422, 418-421.
- Schenk, P.A., de Leeuw, J.W., van Graas, G., Haverkamp, J., Bouman, M., 1981. Analysis of recent spores and pollen and of thermally altered sporopollenin by flash pyrolysis-mass spectrometry and flash pyrolysis-gas chromatography-mass spectrometry. In: J. Brooks (Ed.), *Organic maturation studies and fossil fuel exploration*. Academic Press, London, pp. 225-237.
- Schouten, S., van Driel, G.B., Sinninghe Damste, J.S., de Leeuw, J.W., 1993. Natural sulphurisation of ketones and aldehydes: key reaction in the formation of organic sulphur compounds. *Geochimica et Cosmochimica Acta*, 57, 5111-5116.
- Schouten, S., Klein Beteler, W., Blokker, P., Schogt, N., Rijpstra, W.I.C., Grice, K. and Baas, M., 1998. Biosynthetic effects on the stable carbon isotopic compositions of algal lipids: Implications for deciphering the carbon isotopic biomarker record. *Geochimica et Cosmochimica Acta*, 62, 1397-1406.
- Schouten, S., Hopmans, E.C., Pancost, R.D., Sinninghe Damste, I.S., 2000. Widespread occurrence of structurally diverse tetraether membrane lipids: Evidence for the ubiquitous presence of low-temperature relatives of hyperthermophiles. *Proceedings of the National Academy of Sciences of the United States of America*, 97, 14421-14426.
- Schouten, S., Hopmans, E.C., Schefuß, E., Sinninghe Damste, I.S., 2002. Distributional variations in marine crenarchaeotal membrane lipids: A new organic proxy for reconstructing ancient sea water temperatures? *Earth and Planetary Science Letters*, 204, 265-274.
- Schouten, S., Hopmans, E.C., Forster, A., van Breugel, Y., Kuypers, M.M.M., Sinninghe Damste, I.S., 2003. Extremely high sea-surface temperatures at low latitudes during the middle Cretaceous as revealed by archaeal membrane lipids. *Geology*, 31, 1069-1072.
- Shaw, H.F., Evans, G., 1984. The nature, distribution and origin of a sapropelic layer in sediments of the Cilicia Basin, northeastern Mediterranean. *Marine Geology*, 61, 1-12.
- Sinninghe Damste, I.S., Kock-van Dalen, A.C., de Leeuw, J.W., Schenck, P.A., 1987. The identification of 2,3-dimethyl-5-(2,6,19-trimethylundecyl)-thiophene, a novel sulphur-containing biological marker. *Geochimica et Cosmochimica Acta*, 53, 873-889.
- Sinninghe Damste, J.S., Kock-van Dalen, A.C., de Leeuw, J.W., Schenck, P.A., 1988. Identification of homologous series of alkylated thiophenes, thiolanes, thianes and benzothiophenes in pyrolysates of sulphur-rich kerogens. *Journal of Chromatography*, 435, 435-452.

- Sinninghe Damste, I.S., Eglinton, T.r., de Leeuw, I.W., Schenck, P.A., 1989. Organic sulphur in macromolecular sedimentary organic matter. r. Structure and origin of sulphur-containing moieties in kerogen, asphaltenes and coal as revealed by flash pyrolysis. *Geochimica et Cosmochimica Acta*, 53, 873-889.
- Sinninghe Damste, I.S., de Leeuw, J.W., 1990. Analysis, structure and geochemical significance of organically-bound sulphur in the geosphere: state of art and future research. *Organic Geochemistry*, 16, 1077-1101.
- Sinninghe Damste, I.S., de las Heras, F.X.C., de Leeuw, I.W., 1992a. Molecular analysis of sulfur-rich brown coals by flash pyrolysis-gas chromatography mass-spectrometry - the type-II-S kerogen. *Journal of Chromatography*, 607,361-376.
- Sinninghe Damste, I.S., Eglinton, T.r., de Leeuw, I.W., 1992b. Alkylpyrroles in a kerogen pyrolysate: evidence for abundant tetrapyrrole pigments. *Geochimica et Cosmochimica Acta*, 56,1743-1751.
- Sinninghe Damste, I.S., Wakeham, S.G., Kohnen, M.E.L., Hayes, J.M., de Leeuw, I.W., 1993a. A 6,000-Year Sedimentary Molecular Record of Chemocline Excursions in the Black-Sea. *Nature*, 362, 827-829.
- Sinninghe Damste, I.S., de las Heras, F.x.C., van Bergen, P.F., de Leeuw, I.W., 1993b. Characterization of Tertiary Catalan lacustrine oil shales: discovery of extremely organic sulfur-rich Type I kerogens. *Geochimica et Cosmochimica Acta*, 57, 389-415.
- Sinninghe Damste, I.S., Koopmans, M.P., 1997. The fate of carotenoids in sediments: An overview. *Pure and Applied Chemistry*, 69, 2067-2074.
- Sinninghe Damste, I.S., Kok, M.D., Koster, I., Schouten, S., 1998. Sulfurized carbohydrates: and important sedimentary sink for organic carbon? *Earth and Planetary Science Letters*, 164, 7-13.
- Sinninghe Damste, I.S., Hopmans, E.C., Schouten, S., van Duin, A.e.T., Geenevasen, I.A.J., 2002a. Crenarchaeol: The characteristic core glycerol dibiphytanyl glycerol tetraether membrane lipid of cosmopolitan pelagic crenarchaeota. *Journal of Lipid Research*, 43, 1641-1651.
- Sinninghe Damste, J.S., Rijpstra, W.r.e., Hopmans, E.e., Prahl, F.G., Schouten, S., 2002b. Distribution of membrane lipids of planktonic crenarchaeota in the Arabian Sea. *Applied and Environmental Microbiology*, 68,2997-3002.
- Sinninghe Damste, I.S., Wakeham, S.G., Kohnen, M.E.L., Hayes, I.M., de Leeuw, I.W., Rijpstra, W.r.e.,Reichard, G.J., 2002c. The influence of oxic degradation on the sedimentary biomarker record II. Evidence from Arabian Sea sediments. *Geochimica et Cosmochimica Acta*, 66,2737-2754.
- Sinninghe Damste, I.S., Kuypers, M.M.M., Schouten, S., Schulte, S., Rullkotter, R., 2003. The lycopane/C₃₁ n-alkane ratio as a proxy to assess palaeoacidity during sediment deposition. *Earth and Planetary Science Letters*, 209, 215-226.
- Slomp, C.P., Thomson, I. and de Lange, G.I., 2002. Enhanced regeneration of phosphorus during formation of the most recent eastern Mediterranean sapropel (SI). *Geochimica et Cosmochimica Acta*, 66, 1171-1184.
- Slomp, C., Thomson, I. and de Lange, G.I., 2004. Controls on phosphorus regeneration and burial during formation of eastern Mediterranean sapropels. *Marine Geology*, 203, 141-159.
- Smittenberg, R.H., Pancost, R., Hopmans, E.C., Paetzel, M., Sinninghe Damste, I.S., 2004. A 400-year record of environmental change in an euxinic fjord as revealed by the sedimentary biomarker record. *Palaeogeography Palaeoclimatology Palaeoecology*, 202, 331-351.
- Stankiewicz, B.A., Briggs, D.E.G., Evershed, R.P., 1997. Chemical composition of Paleozoic and Mesozoic fossil invertebrate cuticles as revealed by pyrolysis-gas chromatography/mass spectrometry. *Energy and Fuels*. 11,515-521.

- Stankiewicz, B.A., Collinson, M.E., Finch, P., Mosle, B., Briggs, D.E.G., Evershed, R.P., 1998. Molecular taphonomy of arthropod and plant cuticles from the Carniferous of North America: implications for the origin of kerogen. *Journal of the Geological Society*, 155,453-462.
- Stankiewicz, B.A., Briggs, D.E.G., Michels, R., Collinson, M.E., Flannery, M.B., Evershed, R.P., 2000. Alternative origin of aliphatic polymer in kerogen. *Geology*, 28, 559-562.
- Staub, O., 1987. Key to Carotenoids. In: Pfander, H., Gerspacher, M., Rychener, M., Schwabe, R. (Eds.) Birkhauser verlag, BasellBoston, pp. 296.
- Struck, D., Emeis, K.C., Voss, M., Krom, M.D. and Rau, G.H., 2001. Biological productivity during S5 formation in the Eastern Mediterranean Sea: Evidence from stable isotopes of nitrogen and carbon. *Geochimica et Cosmochimica Acta*, 65, 3249-3266.
- Strohle, K., and Krom, M.D., 1997. Evidence for the evolution of an oxygen minimum layer at the beginning of S-I sapropel deposition in the eastern Mediterranean. *Marine Geology*, 140, 231-236.
- Summons, R.E., Powell, T.G., 1986. Chlorobiaceae in Palaeozoic seas revealed by biological markers, isotopes and geology. *Nature*, 319, 763-765.
- Sun, M.Y., Aller, R.C., Lee, C., 1991. Early diagenesis of chlorophyll *a* in Long Island Sound sediments: A measure of carbon flux and particle reworking. *Journal of Marine Research*, 49, 379-401.
- Sun, M.Y., Wakeham, S.G., 1994. Molecular evidence of degradation and preservation of organic matter in the anoxic Black Sea basin. *Geochimica et Cosmochimica Acta*, 58, 3395-3406.
- Takahashi, M., Ichimura, S., 1970. Photosynthetic properties and growth of photosynthetic sulphur bacteria in lakes. *Limnology and Oceanography*, 15,929-944.
- Takai, K., Sako, Y., 1999. A molecular view of archaeal diversity in marine and terrestrial hot water environments. *FEMS Microbiology Ecology*, 28, 177-188.
- Tegelaar, E.W., de Leeuw, J.W., Derenne, S., Largeau, C., 1989a. A Reappraisal of kerogen formation. *Geochimica et Cosmochimica Acta*, 53, 3103-3106.
- Tegelaar, E.W., de Leeuw, J.W., Largeau, C., Derenne, S., Schulten, H.R., Miiller, R., Boon, J.J., Nip, M., Sprenkels, J. C. M., 1989b. Scope and limitations of several pyrolysis methods in the structural elucidation of a macromolecular plant constituent in the leaf cuticle of *Agave americana* L.. *Journal of Analytical and Applied Pyrolysis*, 15, 29-54.
- Tegelaar, E.W., HoUmann, G., van der Vegt, P., de Leeuw, J.W., Holloway, P.J., 1995. Chemical characterization of the periderm tissue of some angiosperm species-recognition of an insoluble, non-hydrolyzable, aliphatic biomacro-molecules (suberan). *Organic Geochemistry*, 23, 239-251.
- ten Haven, ILL., Baas, M., de Leeuw, J.W. and Schenck, P.A., 1987a. Late Quaternary Mediterranean sapropels I: On the origin of organic matter in sapropel S7. *Marine Geology*, 75,128-146.
- ten Haven, H.L., Baas, M., de Leeuw, J.W., Schenck, P.A and Brinkhuis, H., 1987b. Late Quaternary Mediterranean sapropels, II. Organic geochemistry and Palynology of S₁ sapropels and associated sediments. *Chemical Geology*, 64, 149-167.
- Ternois, Y., Sicre, M.A., Boireau, A., Marty, J.C., Miquel, J.C., 1996. Production pattern of alkenones in the Mediterranean Sea. *Geophysical Research Letters*, 23, 3171-3174.
- Ternois, Y., Sicre, M.A., Boireau, A., Conte, M.H., Eglinton, G., 1997. Evaluation of long-chain alkenones as paleo-temperature indicators in the Mediterranean Sea. *Deep-Sea Research Part I-Oceanographic Research Papers*, 44, 271-286.
- Thomson, J., Higgs, N.C., Croudace, L.W., Colley, S. and Hydes, D.J., 1993. Redox zonation of elements at an oxic/post-oxic boundary in deep-sea sediments. *Geochimica et Cosmochimica Acta*, 57, 579-595.

- Thomson, J., Mercone, D., de Lange, G.J. and van Santvoort, P.J.M., 1999. Review of recent advances in the interpretation of eastern Mediterranean sapropel S1 from geochemical evidence. *Marine Geology*, 153, 77-89.
- Tissot, B.P., Durand, B., Espitalie, J., Combaz, A., 1974. Influence of nature and diagenesis of organic matter in formation of petroleum. *The American Association of Petroleum Geologists Bulletin*, 58,499-506.
- Tissot, B.P., Espitalie, J., 1975. L'evolution de la matiere organique des simulation mathematique. *Revue De L Institut Francais Du Petrole*, 30, 743-777.
- Tissot, B.P., Welte, D.H., 1984. Petroleum formation and occurrence, 2nd Edition. Springer, Heidelberg.
- Torres, M.E., Brumsack, H.J., Bohrmann, G. and Emeis, K.C., 1996. Barite fronts in continental margin sediments: A new look at barium remobilization in the zone of sulfate reduction and formation of heavy barites in diagenetic fronts. *Chemical Geology*, 127, 125-139.
- Troelstra, S.R., Ganssen, G.M., van der Borg, K. and de Jong, A.F.M., 1991. A late Quaternary stratigraphic framework for eastern Mediterranean sapropel S1 based on AMS ¹⁴C dates and stable oxygen isotopes. *Radiocarbon*, 33,15-21.
- Triiper, H.G., Imhoff, J.F., 1981. The genus *Ectothiorhodospira*. In: Starr, M.P., Stolp, H., Trueper, H.G., Balows, A and Schlegel, H.G. (Eds.), *The Prokaryotes*. Springerverlag, Berlin, pp. 274-278.
- Tyson, R.V., 1995. Sedimentary organic matter: organic facies and palynofacies, Chapman and Hall, London.
- van Bergen, P.F., Collinson, M.E., de Leeuw, J.W., 1993. Chemical composition and ultrastructure of fossil and extant salvinian microspore massulae and megaspores. *Grana (suppl. 1)*, 18-30.
- van Bergen, P.F., Collinson, M.E., Sinninghe Damste, J.S., de Leeuw, J.W., 1994. Chemical and microscopical characterization of inner seed coats of fossil water plants. *Geochimica et Cosmochimica Acta*, 59,231-239.
- van Bergen, P.F., Poole, I., Ogilvie, T.M.A, Caple, C., Evershed, R.P., 2000. Evidence for demethylation of syringyl moieties in archaeological wood using pyrolysis-gas chromatography/mass spectrometry. *Rapid Communications in Mass Spectrometry*, 14, 71-79.
- van Bergen, P.F., Blokker, P., Collinson, M.E., Sinninghe Damste, J.S., de Leeuw, J.W., 2004. Structural biomolecules in plants: what can be learnt from fossil records. In: Alan R. Hemsley and Imogen Poole (Eds.) *The Evolution of Plant Physiology. Linnean Society Symposium Series*, 21, 133-154, Elsevier, Amsterdam.
- van Cappellen, P. and Ingall, E.D., 1994. Benthic phosphorus regeneration, net primary production, and ocean anoxia: A model of the coupled marine biogeochemical cycles of carbon and phosphorus. *Palaeoceanography*, 9, 677-692.
- van de Meent, D., de Leeuw, J.W., Schenck, P.A., 1980a. Chemical characterization of non-volatile organics in suspended matter and sediments of the river Rhine Delta. *Journal of Analytical and Applied Pyrolysis*, 2, 249-263.
- van de Meent, D., de Leeuw, J.W., Schenck, P.A., 1980b. Origin of unsaturated isoprenoid hydrocarbons in pyrolysates of suspended matter and surface sediments. In: A.G. Douglas and J.R. Maxwell (Eds.) *Advances in Organic Geochemistry 1979*. Pergamon Press, pp. 469-474.
- van Heemst J.D.H., van Bergen P.F., Stankiewicz B.A., de Leeuw J.W. 1999. Multiple sources of alkylphenols produced upon pyrolysis of DOM, POM and recent and ancient sediments. *Journal of Analytical and Applied Pyrolysis*. 52, 239-256.
- van Kaam-Peters, H.M.E., Schouten, S., de Leeuw, J.W., Sinninghe Damste, J.S., 1997. A molecular and carbon isotope biogeochemical study of biomarkers and kerogen pyrolysates of the

- Kimmeridge Clay Facies: palaeoenvironmental implications. *Organic Geochemistry*, 27, 399-422.
- van Kaam-Peters, H.M.E., Schouten, S., Koster, J., Sinninghe Damste, J.S., 1998. Controls on the molecular and carbon isotopic composition of organic matter deposited in a Kimmeridgian euxinic shelf sea: Evidence for preservation of carbohydrates through sulfuration. *Geochimica et Cosmochimica Acta*, 62, 3259-3283.
- van Os, B.J.H., Lourens, L.I., Hilgen, F.J., de Lange, G.J., Beaufort, L., 1994. The Formation of Pliocene Sapropels and Carbonate Cycles in the Mediterranean - Diagenesis, Dilution, and Productivity. *Paleoceanography*, 9, 601-617.
- van Santvoort, P.J.M., de Lange, G.J., Thomson, J., Cussen, H., Wilson, T.R.S., Krom, M.D. and Stroehle, K., 1996. Active post-depositional oxidation of the most recent sapropel (S1) in sediments of the eastern Mediterranean Sea. *Geochimica et Cosmochimica Acta*, 60, 4007-4025.
- van Santvoort, P.J.M., de Lange, G.J., Thomson, J., Colley, S., Meysman, F.J.R., Slomp, C.P., 2002. Oxidation and origin of organic matter in surficial eastern Mediterranean hemipelagic sediments. *Aquatic Geochemistry*, 8, 153-175.
- Vergnaud-Grazzini, C., Ryan, W.B.F., Cita, M.B., 1977. Stable isotope fractionation, climatic change and episodic stagnation in the Eastern Mediterranean during the Late Quaternary. *Marine Micropaleontology*, 2, 353-370.
- Vergnaud-Grazzini, C. 1985. Mediterranean late Cenozoic stable isotope record: stratigraphic and paleoclimatic implications. In: Standley, D.J., Wezel, F.C. (Eds.), *Geological Evolution of the Mediterranean Basin*, Springer, New York, pp. 413-451.
- Versteegh, G.J.M., Zonneveld, K.A.F., 2002. Use of selective degradation to separate preservation from productivity. *Geology*, 30, 615-618.
- Volkman, J.K., Eglinton, G., Corner, E.D.S., Forsberg, T.E.V., 1980. Novel unsaturated straight-chain C₃₇-C₃₉ methyl and ethyl ketones in marine sediments and a coccolithophore *Emiliania huxleyi*. In: Douglas, A.G., Maxwell, I.R. (Eds.), *Advances in Organic Geochemistry 1979*. Pergamon, Oxford, pp. 219-228.
- Volkman, J.K., Barrett, S.M., Dunstan, G.A., Jeffrey, S.W., 1992. C₃₀-C₃₂ alkyl diols and unsaturated alcohols in microalgae of the class Eustigmatophyceae. *Organic Geochemistry*, 18, 131-138.
- Volkman, J.K., Barrett, S.M., Dunstan, G.A. and Jeffrey, S.W., 1993. Geochemical significance of the occurrence of dinosterol and other 4-methyl sterols in a marine diatom. *Organic Geochemistry*, 20, 7-15.
- Volkman, J.K., Barrett, S.M. and Blackburn, S.L., 1999. Eustigmatophyte microalgae are potential sources of C₂₉ sterols, C_n-C₂₈ n-alcohols and C₂₈-C_n n-alkyl diols in freshwater environments. *Organic Geochemistry*, 30, 307-318.
- Wakeham, S.G., Lewis, C.M., Hopmans, E.C., Schouten, S., Sinninghe Damste, J.S., 2003. Archaea mediate anaerobic oxidation of methane in deep euxinic waters of the Black Sea. *Geochimica et Cosmochimica Acta*, 67, 1359-1374.
- Ward, D.M., Bateson, M.M., Weller, R., Ruff-Roberts, A.L., 1992. Ribosomal rRNA analysis of microorganisms as they occur in Nature. *Advances in Microbial Ecology*, 12, 219-286.
- Wehausen, R. and Brumsack, H.J., 1999. Cyclic variations in the chemical composition of eastern Mediterranean Pliocene sediments: a key for understanding sapropel formation. *Marine Geology*, 153, 161-176.
- Wehausen, R., Brumsack, H.J., 2000. Chemical cycles in Pliocene sapropel-bearing and sapropel-barren eastern Mediterranean sediments. *Palaeogeography Palaeoclimatology Palaeoecology*, 158, 325-352.
- Whelan, L.X., Thompson-Rizer, C.L., 1993. Chemical methods for assessing kerogen and protokerogen types and maturity. In: M.H. Engel and S.A. Macko (Eds.) *Organic*

- Geochemistry, Principles and applications. Plenum Press, New York and London, pp. 289-346.
- White, F., 1983. The Vegetation of Africa, a Descriptive Memoire to Accompany The UNESCO/AETFATIUNSO Vegetation Map of Africa. UNESCO, Paris.
- Wilkin, R.T., Arthur, M.A. and Dean, W.E., 1997. History of water-column anoxia in the Black Sea indicated by pyrite framboid size distribution. *Earth and Planetary Science Letters*, 148,517-525.
- Woese, c.R., 1987. Bacterial evolution. *Microbiological Review*, 51,221-271.
- Woese, C.R., Kandler, O., Wheelis, M.L., 1990. Towards a natural system of organisms: proposal for the domains Archaea, Bacteria, and Eukarya. *Proceedings of the National Academy of Sciences of the United States of America*, 87,4576-4579.
- Wuchter, C., Schouten, S., Boschker, H.T.S., Sinninghe Damste, I.S., 2003. Bicarbonate uptake by marine Crenarchaeota. *FEMS Microbiology Letters*, 219, 203-207.
- G., 1961. On the vertical circulation of the Mediterranean Sea. *Journal of Geophysical Research-Oceans*, 66, 3261-3271.
- Zaback, D.A., Pratt, L.M., 1992. Isotopic composition and speciation of sulfur in the Miocene Monterey Formation - reevaluation of sulfur reactions during early diagenesis in marine environments. *Geochimica et Cosmochimica Acta*, 56, 763-774.

Summary

The present-day Mediterranean Sea is a nutrient poor and, consequently, low productive marine basin. The sediments are grayish, homogeneous and calcareous, containing low organic carbon (ca. 0.1 %), because the organic matter (OM) produced by primary productivity is mineralized through the water column and at the seafloor by oxic degradation processes. However, a Swedish expedition in 1952 discovered black layers of a few centimeters thick imbedded in these grayish sediments in the entire Mediterranean basin. These black layers are laminated and have a high organic carbon content up to ca. 30 % and are called 'sapropels'.

Sedimentologists found a relationship between the presence of sapropels and the astronomical changes in the solar radiation onto the Earth, known as 'Milankowitch cycles'. The precession cycle (21 ka) showed a strong correlation with the occurrence of Mediterranean sapropels from the late Miocene (5.5 Ma ago) to the Holocene (last 10 ka). Precession minima caused a stronger seasonal contrast of insolation at the Northern Hemisphere, resulting in colder winters and warmer summers. Additionally, the monsoon inflow into low-latitude Africa resulted in an enhanced transport of moisture from the Atlantic to the African continent leading to a northwards shift of the Intertropical Convergence Zone (ITCZ). The substantially increased rainfall caused the enhanced delivery of freshwater and nutrients to the Mediterranean Sea via the river Nile and other rivers. Consequently, enhanced primary productivity may have led to enhanced accumulation rates of OM to the sea floor inducing anoxic bottom waters and eventually the deposition of sapropels. The inflow of freshwater on the top of the more dense seawater may have caused reduced deep water circulation and water stagnation preventing to renew the bottom water with oxygen. Sapropel deposition thus results from a delicate interplay of climatic, biological and physical factors.

In this thesis, three time-equivalent Mediterranean sapropels of the late Pliocene (2.943 Ma ago) spanning an east-west transect of the entire eastern Mediterranean Sea were studied to obtain detailed insight in past climatic and palaeo-environmental conditions, which have caused their deposition. The sediments originate from a depth of about 80 meters below the seafloor and were recovered during Leg 160 of the Ocean Drilling Program (ODP). The sapropels and a few centimeters of sediments above and below the sapropels were investigated using different lipid biomarkers. These lipid biomarkers or so-called molecular fossils are specific biochemicals biosynthesized by a class of organisms or even specific organisms, which are useful tools to reconstruct palaeo-environmental conditions, e.g. changes in terrestrial *versus* marine input, sea surface temperature, phytoplankton assemblage, the presence of photic zone euxinia.

Isorenieratene is a carotenoid, originating from green sulfur bacteria, Chlorobiaceae and is indicative for an overlap of the photic and sulfidic zone. This biomarker was used to study periods of photic zone euxinia during Pliocene sapropel formation (Chapter 2). The amount of intact isorenieratene (summed *all-trans* and *cis* isomers), ranged from non-detectable at the base and top of a sapropel up to 140 sediment in the central parts.

Isorenieratene accumulation rates at the central and western site are remarkably similar and increase sharply to levels of up to $3.0 \text{ mg m}^{-2}\text{yr}^{-1}$ in the central part of the sapropel and then drop to low levels. This pattern indicates an expansion of euxinic conditions reaching into the photic zone, followed by deepening of the chemocline during deposition of this Pliocene sapropel. The sapropel from the easternmost site of the basin, which contains less organic carbon, showed much lower isorenieratene accumulation rates and even absence of isorenieratene in the central part of the sapropel. *BalAl* ratios indicate enhanced palaeoproductivity during sapropel formation, supporting previously proposed models, according to which increased productivity is the driving force for the generation of euxinic conditions.

Besides isorenieratene, a novel unknown carotenoid was found, which showed temporal and spatial differences in relative abundances between the three sites (Chapter 3). Highest relative abundances of the unknown carotenoid were measured at Site 967, located closest to the Nile, and coincided with changes in isorenieratene abundances. Based on its molecular weight, mass spectrum, and its UVVIS absorption maximum this unknown pigment reflects either (i) spheroidenone or (ii) thiothece-474, likely derived from photosynthetic purple nonsulfur bacteria, i.e. the family Rhodospirillaceae. Based on the wide range of physiological adaptations of these Rhodospirillaceae, the palaeo-ecological implication of the presence of these bacteria is uncertain but probably related to the temporal occurrence of shallow photic zone anoxia (i.e. even more shallow than indicated by the presence of pigments of the Chlorobiaceae).

Biomarkers (alkenones, loliolide/isololiolide, dinosterol and C₃₀ 1,15 -dioUketo-ol) representative of four major classes of marine primary producers (haptophytes, diatoms, dinoflagellates, eustigmatophytes, respectively) were studied for changes in phytoplankton export production before, during and after sapropel deposition (Chapter 4). Biomarker contents showed substantial differences between non-sapropelic and sapropelic sediments. In non-sapropelic sediments, small contents are observed, reflecting extensive oxic degradation in oxic pore waters during deposition. In the sapropels, biomarker accumulation rates (ARs) showed a substantial increase from the base to the centre, likely resulting from increased biological productivity since bottom waters were continuously anoxic and preservation conditions are similar. The diatom biomarker, loliolide/isololiolide became distinctly more abundant in the sapropels indicating that the eastern Mediterranean basin was enriched in nutrients. This caused enhanced export production by the major phytoplankton classes leading to periods of sapropel deposition. Alkenone-based SST reconstructions indicated that this change in phytoplankton composition was not influenced by changes in sea surface temperature, but was mainly nutrient-controlled. Compound-specific measurements did not provide additional evidence for substantially increased primary production rates: $\delta^{13}\text{C}$ values of C_{37:2} alkenones and loliolide/isololiolide showed a slight negative shift instead of the anticipated positive shift. This was probably caused by the enrichment of dissolved inorganic carbon in the upper water column, caused by enhanced recycling of respired CO₂ due to the shallow chemocline.

The distribution of glycerol dibiphytanyl glycerol tetraethers (GDGT's), biomarkers of planktonic crenarchaeota showed in both, the homogeneous intervals and sapropels the

dominance of GDGT-O and crenarchaeol among the GDGT's indicating their origin from planktonic crenarchaeota as it was found in many other marine sediments (Chapter 5). In the homogeneous intervals highest GDGT abundances (normalized to TOC) were measured at the easternmost study Site 967 of the eastern Mediterranean Sea and decreased at the central and western Site 969 and 964. Within the three studied sapropels large variations in GDGT abundance was observed. The newly established sea surface temperature (SST) proxy, the TEX₈₆ index, derived from GDGT's of planktonic crenarchaeota was used to estimate past SST. Comparison with previous obtained SST data using the alkenones from haptophyte algae revealed substantial differences. Whereas the U₃₇^{K'}-based SST showed almost constant values of ca. 25°C in both the homogeneous intervals and the sapropels, the TEX₈₆-based SST were 26-29°C in the homogeneous intervals and decreased up to 15-17°C in the sapropels. The TEX₈₆-based SST values outside the sapropel probably reflect summer SST based on a comparison with the present-day Mediterranean Sea. The surprisingly low TEX₈₆-based SST estimates for the sapropels showed similarities with those obtained for the contemporary euxinic Black Sea. The distribution of marine crenarchaeota the modern Black Sea, i.e. thriving at the deeper and colder chemocline, suggests that this leads to a reduction in TEX₈₆, resulting in artificially low SST estimates. A similar situation is inferred for the Pliocene eastern Mediterranean during sapropel deposition since the SST anomaly co-occurs with the build-up of a shallow chemocline.

The δ¹³C values of higher plant wax C₂₇₋₃₃ n-alkanes were determined to study the composition of the vegetation on the continents surrounding the Mediterranean Sea (Chapter 6). A two-end member mixing model transformed the measured δ¹³C values into the contribution of C₄ plants to the terrestrial vegetation. These calculations indicated a high C₄ plant contribution (i.e. 40-50%) in the periods just before and just after sapropel formation. During sapropel deposition the C₄ plant contribution increased by up to 20% at all sites. This is interpreted to record the increased overall plant coverage of the Mediterranean borderlands resulting from the change of formerly barren desert areas into C₄ grass-dominated savannah's as a response to the wetter climate during sapropel deposition. Enhanced accumulation rates (ARs) of long-chain n-alkanes (C₂₇₋₃₃) and n-alkan-1-ols (C₂₆₋₃₀) towards the middle of the sapropel in concert with a decrease in the Ti/Al ratio confirm an increased delivery of terrigenous OM at all sites. These biomarkers were probably predominantly fluvially transported to the Mediterranean Sea, not only by the Nile but also by fossil wadi river systems on the northern African continent.

The OM of the three time-equivalent Pliocene sapropels was characterized as Type II kerogen being dominated by amorphous OM, originating mainly from marine organisms (Chapter 7). This was witnessed by the relatively high abundances of algaenan- and chlorophyll-derived pyrolysis products of the Curie-point pyrolysates of the kerogens of the sapropels. However, a small amount of terrigenous OM was also observed in the form of pollen and spores that most probably yielded the oxygenated aromatic pyrolysis products known to derive from sporopollenin. Lignin pyrolysis products, such as methoxyphenol and catechol (1,2-benzenediol), which are commonly used as unequivocal evidence for contribution of terrestrial higher plants in the form of woody material to the kerogen, were absent in the kerogen pyrolysates of the sapropels. No major spatial and temporal differences

in the kerogen composition of the three time-equivalent sapropels were observed. Palynological studies revealed that the homogeneous intervals, below and above the sapropels, consisted of pollen, spores and amorphous OM. This is confirmed by Curie-point pyrolysis - *GC/MS* results showing a relatively high abundance of algaenan-derived compounds and the presence of oxygenated aromatic pyrolysis products. The differences observed between the kerogen pyrolysates of the sapropels and their homogeneous intervals are suggested to be governed primarily by enhanced preservation conditions, resulting in increased preservation of labile marine OM in the sapropels.

This thesis demonstrates the high potential of using a wide range of biomarkers to reconstruct palaeo-climatic conditions at the time of deposition of Mediterranean sapropels. The data obtained are in general consistent with the idea that the increased run-off from the continent resulted in an increased primary production, which in its turn triggered the deposition of sapropels, but provide unprecedented detailed information with respect to the degree of anoxia and stratification and response of the marine and continental biological communities during this time of rapid climate change.

Samenvatting

De hedendaagse Middellandse Zee bevat relatief lage concentraties aan nutriënten en wordt daarom gekenmerkt door een lage primaire productiviteit. Haar sedimenten zijn grijs gekleurd, homogeen en bevatten een laag gehalte aan organisch koolstof (ca. 0.1 %) omdat de relatief kleine hoeveelheden organisch materiaal (OM) die geproduceerd worden door het phytoplankton tijdens het transport naar de bodem en in het oppervlakesediment zelfvrijwel volledig gemineraliseerd worden. In 1952 werd echter tijdens een Zweedse onderzoek-expeditie gevonden dat er in de gehele Middellandse Zee iets dieper in het sediment zwarte lagen voorkomen. Deze lagen zijn gelamineerd en bevatten veel meer organisch koolstof (tot wel 30%) dan de grijze sedimenten en zij werden sapropelen genoemd.

Sedimentologen hebben een relatie gevonden tussen het voorkomen van sapropelen en de astronomische veranderingen in de instraling van de zon op Aarde bekend als de zogenaamde "Milankowitch" cycli. Van het laat Miocene (5.5 Ma geleden) tot het Holoceen (de afgelopen 10 ka) vertoonde de precessiecyclus (met een periodiciteit van 21 ka) een hoge correlatie met het voorkomen van sapropelen. Minima in de precessiecyclus veroorzaakte een sterker seizoenaal contrast in instraling op het noordelijk halfrond, hetgeen resulteerde in koudere winters en warmere zomers. Bovendien zorgde de passaatwinden voor een verhoogd transport van vocht van de Atlantische Oceaan naar equatoriaal Afrika, hetgeen tot een verschuiving naar het noorden van de Intertropical Convergence Zone (ITCZ) leidde. De grotere neerslag resulteerde in een sterk toegenomen transport van zoetwater rijk aan nutriënten naar de Middellandse Zee via de Nijl en andere rivieren. Hierdoor nam de primaire productie toe en dit resulteerde waarschijnlijk in een toename van de flux van OM naar de zeebodem. Hierdoor werd het bodemwater anoxisch, hetgeen uiteindelijk leidde tot een verbeterde preservatie van OM in het sediment en de afzetting van sapropelen. Daarnaast induceerde de sterke toename van de instroom van zoet water waarschijnlijk een stratificatie van de waterkolom, leidend tot een afname in de circulatie van diep water en een verminderd transport van zuurstof naar het bodemwater. Sapropoelvorming is dus het gevolg van een samenspel van klimatologische, biologische en fysische factoren.

In dit proefschrift wordt de studie beschreven van een laat Pliocene sapropeel (2.943 Ma oud) op drie plaatsen in het oostelijk bekken van de Middellandse Zee die samen een oost-west transect vormen. In deze studie is een gedetailleerd inzicht verkregen in de klimaat- en afzettingscondities die leidde tot afzetting van deze sapropeel, die gekenmerkt wordt door extreem hoge organisch koolstofgehalten (tot 30%). De bestudeerde sedimenten liggen op een ongeveer 80 m diepte vanaf het sediment-water oppervlak en zijn verkregen via Leg 160 van het Ocean Drilling Program (ODP). De sapropeel en de grijs gekleurde, homogene sedimenten afgezet voor en na de periode van sapropeelafzetting zijn bestudeerd met behulp van zogenaamde chemische fossielen. Dit zijn organische componenten waarvan de structuur zo specifiek is dat ze aan bepaalde groepen van organismen of soms zelfs soorten gekoppeld kunnen worden. Zij worden gebruikt om palaeomilieu's te bestuderen en kunnen o.a. inzicht verschaffen in veranderingen in de zeevatertemperatuur, de samenstelling van het

fytoplankton, het voorkomen van anoxische condities in de fotische zone en het transport van plantenmateriaal van het continent naar de zee.

Isorenierateen is een carotenoïde afkomstig van groene zwavelbacterien (Chlorobiaceae) die zowel licht als sulfide nodig hebben. Deze component werd gebruikt om het voorkomen van de overlap van de fotische met de sulfidische zone vast te stellen tijdens sapropeelvorming in het Pliocene (Hoofdstuk 2). De hoeveelheid intact isorenierateen (waarbij de *all-trans* en *cis* isomeren gesommeerd werden) varieerde van niet detecteerbaar in de onder- en bovenkant van de sapropeel tot 140 $\mu\text{g m}^{-2}$ sediment in het midden van de sapropeel. Accumulatiesnelheden van isorenierateen in de centrale en westelijke monsterlocatie zijn heel vergelijkbaar en nemen sterk toe tot waarden van 3.0 mg m^{-2} en dalen dan tot lage waarden. Deze profielen geven een expansie van de sulfidische zone tot in de fotische zone aan, gevolgd door het dieper worden van de chemocline tijdens afzetting van deze Pliocene sapropeel. De sapropeel van de meest oostelijke monsterlocatie (dichter bij de monding van de Nijl) werd gekenmerkt door veel lagere accumulatiesnelheden van isorenierateen en zelfs door een afwezigheid van isorenierateen in het middelste gedeelte van de sapropeel. Ba/Al ratio's geven een toename in de primaire productie tijdens de sapropeelvorming aan. Dit is in overeenstemming met een eerder gepostuleerd model waarbij de toegenomen primaire productie uiteindelijk leidt tot euxinische condities in de waterkolom.

Naast isorenierateen werd nog een ander, onbekend, carotenoïde aangetroffen in de sapropelen (Hoofdstuk 3). De concentraties van dit carotenoïde in de sapropeel vertoonden grote variatie zowel tussen de verschillende monsterlocaties als binnen de sapropeel. De hoogste concentraties werden gevonden in Site 967, dichtbij de monding van de Nijl, en veranderingen in de concentraties waren synchroon met die van isorenierateen. Op basis van het massaspectrum en UVNIS absorptiespectrum werd dit pigment geïdentificeerd als (i) spheroidenon, of (ii) thiotece-474. Het pigment is waarschijnlijk afkomstig van fotosynthetische purperen niet-zwavelbacterien (i.e. de familie Rhodospirillaceae). Omdat deze bacterien zich aan tal van condities kunnen aanpassen is de palaeoecologische interpretatie van het voorkomen van dit carotenoïde onzeker. Meest waarschijnlijk is het echter dat dit geïnterpreteerd moet worden als het tijdelijk voorkomen van een nog grotere overlap van de fotische en euxinische zone (i.e. nog groter dan al aangegeven door het pigment isorenierateen).

Chemische fossielen (alkenonen, loliolide/isololiolide, dinosterol and C₃₀ 1,15 - diol/keto-ol) representatief voor vier belangrijke groepen van fytoplankton (haptofyten, diatomeeën, dinoflagellaten, eustigmatofyten) werden bestudeerd om de verschillen in export productie van deze groepen fytoplankton voor, tijdens en na de afzetting van sapropelen te bestuderen (Hoofdstuk 4). De gehalten aan chemische fossielen vertoonden aanzienlijke verschillen tussen de sapropelen en de grijze, homogene sedimenten. In deze laatste sedimenten werden relatief lage gehalten aangetroffen ten gevolge van de grote mineralisatie in het oxische poriewater. De accumulatiesnelheden van de chemische fossielen in de sapropelen vertoonden een aanzienlijke toename van de onderkant naar het midden van de sapropeel. Dit kan worden geïnterpreteerd als een toename in de biologische productiviteit omdat het bodemwater tijdens afzetting van de sapropeel continue anoxisch geweest is en

condities voor preservatie van OM dus optimaal waren. De chemische fossielen afkomstig van diatomeeën (loliolide/isololiolide) werden relatief meer dominant in de sapropeel. Dit reflecteert vermoedelijk de toegenomen concentratie in nutriënten in het oostelijk bekken van de Middellandse Zee dat resulteerde in sapropeelvorming. Reconstructie van de oppervlakte zeewatertemperaturen m.b.v. alkenonen liet zien dat de verandering in fytoplankton-samenstelling niet beïnvloed werd door veranderingen in de temperatuur van het zeewater maar in belangrijke mate bepaald werd door de nutriëntconcentraties. Component-specifieke $\delta^{13}\text{C}$ metingen verschaften geen additionele ondersteuning voor de toegenomen primaire productie omdat zowel de C_{37:2} alkenoon als loliolide/isololiolide een kleine verandering naar lichtere waarden in plaats van de verwachte toename vertoonden in het midden van de sapropeel. Dit resultaat kan mogelijk verklaard worden door het ondieper worden van de chemocline, waardoor isotopisch licht CO₂ gevormd door afbraak van OM hergebruikt kan worden door het fytoplankton.

De glycerol dibifytanyl glycerol tetraethers (GDGT's), membraanlipiden van crenarchaeota, werden zowel in de homogene intervallen als in de sapropelen gedomineerd door GDGT-O en crenarchaeol (Hoofdstuk 5). Dit indiceerde een herkomst voor de GDGT's van planktonische crenarchaeota zoals voor vele marine sedimenten het geval is. De hoogste concentraties, genormeerd op het totaal organisch koolstof, werden voor de homogene intervallen gemeten in de sedimenten van de meest oostelijke Site 967; de gehalten voor de centrale en meest westelijke monsterlocatie (Site 969 en 964) waren lager. Grote variaties in de GDGT concentraties werden gemeten binnen de sapropelen. De nieuwe proxy voor het bepalen van vroegere oppervlakte zeewatertemperaturen, de TEX₈₆ index, die gebaseerd is op variaties in de GDGT distributies, werd toegepast en deze schattingen werden vergeleken met die gebaseerd op de alkenoon proxy ($U_{37}^{K'}$) en vertoonden aanzienlijke verschillen. Terwijl de schatting voor de zeewatertemperatuur op basis van de $U_{37}^{K'}$ ongeveer 25°C bedroeg en vrijwel geen verandering tussen de homogene sedimenten en sapropeel lieten zien, gaven de TEX₈₆ bepalingen een zeewatertemperatuur van 26-29°C voor de homogene intervallen en 15-17°C voor de sapropelen. De TEX₈₆ schatting buiten de sapropeel geeft waarschijnlijk een schatting voor de zomertemperatuur op basis van een vergelijking met TEX₈₆ waarden van oppervlakte sedimenten in de huidige Middellandse Zee. De verassend lage TEX₈₆ schatting voor de periode tijdens afzetting van de sapropeel vertoont overeenkomsten met die bepaald voor de huidige, sterk gestratificeerde, euxinische Zwarte Zee. De ecologische niche van de planktonische crenarchaeota in de Zwarte Zee (i.e. de diepere en "koude" chemocline) suggereert dat dit leidt tot lagere TEX₈₆ waarden en daarmee een onderschatting van de oppervlakte zeewatertemperaturen. Een vergelijkbare situatie doet zich waarschijnlijk voor in de Pliocene Middellandse Zee omdat de anomalie in de oppervlakte zeewatertemperatuur tegelijkertijd optreedt met de opbouw van een ondiepe chemocline.

De $\delta^{13}\text{C}$ waarden van n-alkanen afkomstig van plantenwassen werden bepaald om veranderingen in de vegetatie van het continent rondom de Middellandse Zee te reconstrueren (Hoofdstuk 6). Met behulp van een eenvoudig mengmodel werden m.b.v. deze waarden de bijdrage van C₄ planten aan de vegetatie berekend. Deze berekeningen gaven een relatief hoog gehalte (i.e. 40-50%) aan C₄ planten in de perioden vlak voor en vlak na de tijd van sapropeelvorming aan. Tijdens de afzetting van sapropelen nam deze bijdrage nog eens met

ongeveer 20% toe voor alledrie onderzochte monsterlocaties. Dit werd waarschijnlijk veroorzaakt door de toegenomen plantenbegroeiing op het continent rondom de Middellandse Zee door transformatie van woestijngebieden in door C_4 grassen gedomineerde savannes ten gevolge van het vochtiger klimaat tijdens de periode van sapropeelvorming. De toename in de accumulatiesnelheden van lange n-alkanen (C_{27-33}) and n-alkan-1-olen (C_{26-30}) van de onderkant naar het midden van de sapropeel samen met een afname in de *TilAl* ratio geeft een toename aan in het transport van terrigeen OM naar de Middellandse Zee tijdens de periode van sapropeelvorming. Deze plantenwassen werden waarschijnlijk voornamelijk fluviatiel getransporteerd, niet alleen door de rivier de Nijl, maar ook door allerlei fossiele wadi systemen op het Noord-Afrikaanse continent.

Het OM van de drie tijdsequivalente sapropelen werd gekarakteriseerd als Type II kerogeen omdat het voornamelijk amorf OM is afkomstig van mariene organismen (Hoofdstuk 7). Deze vaststelling werd ondersteund door het feit dat de Curie-punt pyrolysaten van deze kerogenen gedomineerd werden door pyrolyseproducten afkomstig van algenaan en chlorofyl. Kleine hoeveelheden terrigeen OM werden ook aangetroffen door de pyrolyseproducten van pollen en sporen (geoxygeneerde aromatische producten). Pyrolyseproducten afkomstig van lignine (zoals methoxyfenolen en catechol), die ondubbelzinnig bewijs leveren voor de bijdrage van houtachtig terrestrisch materiaal, werden niet aangetroffen in pyrolysaten van de kerogenen in de sapropelen. De variatie in samenstelling van de pyrolysaten van de sapropelen was relatief gering. Palynologische karakterisering toonde aan dat het OM van de homogene sedimenten vlak onder en boven de sapropelen vooral uit pollen en sporen en amorf OM bestonden. Dit werd bevestigd middels analyses m.b.v. Curie-punt pyrolyse-GC/MS; de pyrolysaten bestonden voornamelijk uit geoxygeneerde aromaten en producten afkomstig van algenaan. De verschillen in de samenstelling van de pyrolysaten van de kerogeen fracties uit de sapropelen enerzijds en die van de homogene sedimenten anderzijds worden vooral veroorzaakt door de verbeterde preservatie condities tijdens afzetting van de sapropelen, die resulteren in een sterk verbeterde preservatie van labiel marien OM.

Het onderzoek beschreven in dit proefschrift laat de potentie van het gebruik van chemische fossielen voor de reconstructie van palaeoklimaat en -milieu tijdens de periode van sapropeelvorming zien. De verkregen gegevens zijn in algemene zin consistent met de hypothese dat de toename in run-off van het continent leidde tot een toename in de primaire productie en dat dit resulteerde in sapropeelvorming, maar geven zeer gedetailleerde informatie met betrekking tot de mate van anoxia en stratificatie en de respons van de mariene en continentale biologische levensgemeenschappen tijdens deze periode van snelle klimaatverandering.

Zusammenfassung

Das heutige Mittelmeer ist ein marines, nährstoffarmes Becken und demzufolge durch geringe Primärproduktion gekennzeichnet. Das Sediment ist grünlich, homogen und kalkreich. Es besitzt einen geringen organischen Kohlenstoffgehalt von ca. 0.1 %, da der vorwiegend von Algen produzierte, geringe Anteil organischen Materials (OM) auf dem Weg durch die Wassersäule und im Sediment durch Bakterien abgebaut wird. Eine schwedische Expedition entdeckte jedoch 1952 im gesamten Mittelmeer schwarze Schichten (von einigen Zentimetern Mächtigkeit), die in das grünliche Sediment eingebettet sind. Diese schwarzen Schichten treten periodisch auf, sind geschichtet und besitzen einen hohen organischen Kohlenstoffgehalt von bis zu 30% gew. und werden 'Sapropel' genannt.

Sedimentologen fanden einen Zusammenhang zwischen der Anwesenheit von Sapropelen und den astronomischen Variationen in der Sonneneinstrahlung zur Erde, bekannt als 'Milankowitch Zyklen'. Besonders der 'Precession' Zyklus (21000 Jahre) zeigte eine positive Korrelation mit dem Vorkommen von Sapropelen im Mittelmeer vom späten Miozän (vor 5.5 Millionen Jahren) bis zum Holozän (die letzten 10000 Jahre). Das 'Precession' Minimum verursacht dabei, durch die veränderte Sonneneinstrahlung auf der nördlichen Halbkugel, einen stärkeren jahreszeitlichen Kontrast, was letztendlich zu kühleren Wintern und wärmeren Sommern führt. Zusätzlich sorgen die Passatwinde für einen erhöhten Transport von Feuchtigkeit vom Atlantik zum nordafrikanischen Kontinent, was zu einer nördlichen Verschiebung der Intertropischen Konvergenzzone (ITCZ) führt. Der daraus resultierende erheblich erhöhte Regenfall verursachte eine erhöhte Zufuhr von Wasser und Nährstoffen vom Nil und anderen Flüssen ins Mittelmeer. Folglich erhöhte sich die Primärproduktion, was wiederum zu erhöhten Akkumulationsraten des OM am Meeresboden geführt haben könnte, woraufhin anoxisches Bodenwasser und damit Sapropelbildung induziert wurden. Außerdem sorgte die Zufuhr von Süßwasser wahrscheinlich zur Reduzierung der Tiefenwasserzirkulation möglicherweise sogar zur Stagnation und somit Stratifizierung der Wassersäule, wodurch die Belüftung des Bodenwassers mit Sauerstoff verhindert wurde. Sapropelbildung ist deshalb das Ergebnis eines Zusammenspiels von klimatischen, biologischen und physikalischen Faktoren.

In dieser Doktorarbeit werden drei Pliozäne Sapropel (2.943 Millionen Jahre alt) von drei verschiedenen Stationen im östlichen Mittelmeerbecken untersucht, die zusammen ein Ost-West-Transect bilden. Diese Studie liefert detaillierte Einsichten über die früheren Klima- und Umweltbedingungen, die schließlich zur Ablagerung der Sapropel führten, die einen extrem hohen organischen Kohlenstoffgehalt besitzen. Das untersuchte Sediment stammt aus einer Tiefe von ca. 80 m unter dem Meeresboden und wurde im Rahmen des Ocean Drilling Program Leg 160 entnommen. Die Sapropel, sowie die grünlich, homogenen Sedimente (homogene Intervalle) wurden mit Hilfe von so genannten Lipid-Biomarkern oder chemischen Fossilien untersucht. Diese Lipid-Biomarker sind organische Verbindungen, deren Struktur so spezifisch ist, dass sie an eine Klasse von Organismen oder sogar eine spezifische Art gekoppelt werden kann. Diese Biomarker können genutzt werden, um frühere Umweltbedingungen zu rekonstruieren, wie z.B. den Transport von terrestrischem

Pflanzenmaterial im das Meer, Änderungen der Oberflächenwassertemperatur, die Algenzusammensetzung, die Anwesenheit von anoxischen Bedingungen in der photischen Zone.

Isorenieratene ist ein Carotenoid, das in grünen Schwefelbakterien der Klasse Chlorobiaceae vorkommt. Chlorobiaceae benötigen für ein optimales Wachstum geringe Lichtintensitäten und Sulfide. Die Anwesenheit von Isorenieratenen im Sediment weist deshalb auf das Überlappen der photischen mit der sulphidischen Zone in der Wassersäule hin. Dieser Biomarker wurde genutzt, um die Perioden der anoxischen/euxinischen Bedingungen in der photischen Zone während der Sapropelbildung zu untersuchen (Kapitel 2). Die Summe der intakten Isorenieratene (summierte *all-trans* und *cis*-isomers) variierte von nicht ermittelbaren Konzentrationen unterhalb und oberhalb des Sapropels bis zu 140 µg/g Sediment im Zentrum des Sapropels. Isorenieratene Akkumulationsraten an der zentralen und westlichen Station waren bemerkenswert ähnlich und zeigten einen deutlichen Anstieg von der Basis des Sapropels bis zu 3.0 mg m⁻² yr⁻¹ im Zentrum des Sapropels und nahmen dann wieder ab. Dieses Muster kennzeichnet die Ausdehnung der euxinischen Bedingungen in die photische Zone. Konzentrationsänderungen im Sapropelprofil spiegeln eine Senkung oder Erhöhung der Chemoklinen während der Ablagerung der Pliocene Sapropel wider. Das Sapropel an der östlichsten Station im Mittelmeerbecken, charakterisiert durch einen geringeren organischen Kohlenstoffgehalt, zeigte im Vergleich zu den anderen zwei Stationen viel geringere Isorenieratene Akkumulationsraten und sogar die Abwesenheit von Isorenieratenen in der Mitte des Sapropels. Ba!Al sind ein Indikator für erhöhte Palaoproductivität während der Sapropelbildung, wodurch ein bereits früher vorgestelltes Modell unterstützt wird, indem die erhöhte Primärproduktivität als der entscheidende Faktor für das Auftreten der euxinischen Bedingungen beschrieben wird.

Neben Isorenieratenen wurde ein neues, unbekanntes Carotenoid entdeckt, das Unterschiede zwischen dem relativen Auftreten der Sapropel der drei Stationen und im individuellen Sapropel selbst anzeigte (Kapitel 3). Die relativen Vorkommen des unbekanntes Carotenoids wurden an der Station 967, am dichtesten am Nil liegend, gemessen. Diese Resultate sind synchron mit den Ergebnissen die auch für Isorenieratene gefunden wurden. Basierend auf dem Molekulargewicht, dem Massenspektrum und seinem UVNIS Absorption Maximum, spiegelt dieses unbekanntes Pigment entweder (1) Spheridone, oder (2) Thiotece-474 wider. Dieses Pigment wird möglicherweise von photosynthetisierenden purpur schwefelfreien Bakterien biosynthetisiert, z.B. von der Familie der Rhodospirillaceae. Aufgrund der breiten physiologischen Adaptation dieser Rhodospirillaceae sind die paläo-ökologischen Auswirkungen dieser Bakterien unsicher. Jedoch konnte man postulieren, dass die Anwesenheit dieses Pigmentes das kurzzeitliche Vorkommen von sulfidischen Bedingungen noch in der photischen Zone (demzufolge als bei der Anwesenheit des Isorenieratenes der Chlorobiaceae) anzeigt.

Biomarker (Alkenone, Loliolide/Isololiolide, Dinosterol und C₃₀ 1,15 -Diol/Keto-ol), kennzeichnend für die vier Hauptklassen der marinen Primärproduzenten (Haptophyten, Diatomeen, Dinoflagellaten, Eustigmatophyten) wurden auf ihre Veränderungen bei der Exportproduktion bevor, und nach der Sapropelbildung untersucht (Kapitel 4). Der Biomarkergehalt zeigte beträchtliche Unterschiede zwischen den nicht-sapropelischen und

sapropelischen Sedimenten. In den nicht-sapropelischen Sedimenten konnten nur kleine Biomarkerkonzentrationen gemessen werden, was den oxidativen Abbau in oxischem Porenwasser während der Ablagerung widerspiegelt. In den Sapropelen, zeigten die Biomarker Akkumulationsraten (AR) einen beträchtlichen Anstieg vom der Basis des Sapropels zur Mitte resultierend aus der biologischen Produktivität in der Zeit, in der das Bodenwasser anoxisch und die Erhaltungsbedingungen optimal waren. Der Diatomeenbiomarker, Loliolide/Isololiolide zeigte in den Sapropelen eine relativ deutliche Dominanz, gegenüber den anderen drei Phytoplanktonklassen, was auf eine Anreicherung von Nährstoffen im östlichen Mittelmeer hinweisen konnte. Diese verursachte eine Exportproduktion der Hauptphytoplanktonklassen was letztendlich zur Ablagerung der Sapropel führte. Die Rekonstruktion der Oberflächentemperatur, die mit Hilfe der Alkenone bestimmt wurde, zeigte dass die Veränderungen in der Phytoplanktonzusammensetzung nicht durch die Veränderungen der Oberflächentemperatur, sondern durch die Nährstoffe beeinflusst wurde. $\delta^{13}\text{C}$ Messungen an den spezifischen Biomarkern zeigten jedoch keinen zusätzlichen Hinweis auf erhöhte Primärproduktion. Im Gegenteil, die $\delta^{13}\text{C}$ Werte der $\text{C}_{37:2}$ Alkenone und Loliolide/Isololiolide zeigten eine geringe negative, statt der erwarteten positiven Verschiebung ihrer $\delta^{13}\text{C}$ Werte. Diese geringe Verschiebung zu niedrigen $\delta^{13}\text{C}$ Werten ist wahrscheinlich durch die Verschiebung der Chemoklinen zur photischen Zone, wodurch das geformte isotopisch leichtere CO_2 durch den Abbau von OM sofort wieder durch das Phytoplankton assimiliert wird, zu erklären.

Die Glycerol Dibiphytanyl Glycerol Tetraethers (GDGTs), Membranlipide der Crenarchaeota zeigte sowohl in den homogenen Intervallen als auch in den Sapropelen die Dominanz von GDGT-O und Crenarchaeol unter den GDGTs. Dieses Resultat ist ein Indikator für die Anwesenheit von planktischen Crenarchaeota in den Sapropelen, wie es auch in vielen anderen marinen Sedimenten gefunden wurde (Kapitel 5). In den homogenen Intervallen, an der östlichen Station 967 des östlichen Mittelmeeres wurden, vergleichbar mit der westlichen und zentralen Station, die höchsten GDGT Konzentrationen (normalisiert auf TOe) gefunden. In den drei untersuchten Sapropelen konnten große Veränderungen in den GDGT Vorkommen beobachtet werden. Das neu entwickelte Proxy zur Rekonstruktion der früheren Oberflächentemperatur (SST), der TEX₈₆ index ist abgeleitet von den Variationen der GDGT Verteilung. Vergleiche der TEX₈₆ Ergebnisse mit dem $U_{37}^{\text{K}'}$, der von den Alkenonen der Haptophyten abgeleitet wird, zeigte große Unterschiede. der $U_{37}^{\text{K}'}$ unveränderte Werte von ca. 25°C, sowohl in den homogenen Intervallen, als auch in den Sapropelen anzeigte, ergaben die TEX₈₆ Werte in den homogenen Intervallen hohe Temperaturen von 26-29°C und in den Sapropelen niedrige Temperaturen von 15-17°C. Die TEX₈₆ Werte in den homogenen Intervallen spiegeln höchst wahrscheinlich die Sommer SST, basierend auf den gemessenen TEX₈₆ Werten des heutigen Mittelmeeres, wider. Die überraschend niedrigen TEX₈₆ Werte in den Sapropelen zeigten im Gegenteil vergleichbare TEX₈₆ Werte, die im heutigen euxinischen, stark stratifizierten Schwarzen Meer gefunden wurden. Die ökologische Nische der marinen Crenarchaeota im heutigen Schwarzen Meer (d.h. in der tieferen und "kühleren" Chemoklinen) konnte die starke Abnahme der TEX₈₆ Werte erklären. Diese Situation wäre vergleichbar für das Mittelmeer während der

Ablagerung des untersuchten Pliocene Sapropel, aufgrund der Anwesenheit einer flachen Chemoklinen, die während der Zeit der Sapropelbildung anwesend war.

Die $\delta^{13}\text{C}$ Werte der C_{27-33} n-alkane, Bestandteil der pflanzenwachse wurden auf die Zusammensetzung der Vegetation auf den Kontinenten rund um das Mittelmeergebiet untersucht (Kapitel 6). Mit Hilfe eines einfachen Mischungsmodells wurden diese gemessenen C_{27-33} Werte in den Anteil der C_4 Pflanzen an der Vegetation berechnet. Diese Berechnung zeigten einen hohen Anteil von 40-50% der C_4 Pflanzen bevor und nach der Sapropelbildung. Während der Sapropelbildung stieg sogar der C_4 Pflanzenanteil an allen drei Stationen auf bis zu 20% an. Dieses Ergebnis wäre zu interpretieren durch die ansteigende Verbreitung der Vegetation. Das dominierende feuchte Klima verursachte die Transformation des Wiistengebietes zu einem Savannengebiet, dass von C_4 Grasem dominierend wurde. Die Akkumulationsraten der langkettigen n-alkanen (C_{27-33}) und n-alkan-I-ols (C_{26-30}) im Zentrum des Sapropels harmonisiert mit der Abnahme der Ti/Al Verhältnisse und bestätigt hiermit die Zunahme der terrigenen Zufuhr an allen Stationen. Diese Pflanzenwachse wurden wahrscheinlich hauptsächlich fluviatil in das Mittelmeer transportiert, aber nicht allein durch den Nil, sondern auch durch die fossilen Wadi-Fluß Systeme, gelegen im nördlichen Teil des afrikanischen Kontinentes.

Das OM der drei zeitgleich abgesetzten Pliocene Sapropelen wurde als Kerogentyp II charakterisiert, aufgrund der Dominanz des amorphen OM, welches hauptsächlich von marinen Organismen abstammt (Kapitel 7). Diese Feststellung wurde durch die relativ hohen Vorkommen der Algaenan - und Chlorophyllabstammenden Pyrolyseprodukte des Kerogens der Sapropelen. Jedoch konnte auch eine kleine Menge des terrigenen OM, in Form von Pollen und Sporen mikroskopisch beobachtet werden. Diese palnologischen Ergebnisse erklären höchst wahrscheinlich auch die oxidierten aromatischen Pyrolyseprodukte, die vom Sporopollenin abgeleitet werden können. Lignin Pyrolyseprodukte, wie Methoxyphenol und Catechol (1,2-benzenediol), die ein eindeutiger Beweis des Eintrages höherer Pflanzen sind, konnten im Kerogenpyrolysat der Sapropelen nicht gefunden werden. Variationen in der Kerogenzusammensetzung zwischen den drei zeitgleich abgesetzten Sapropelen waren gering. Palynologische Untersuchungen zeigten in den homogenen Intervallen, also bevor und nach der Sapropelbildung, die Anwesenheit von Pollen, Sporen und auch amorphen OM. Diese Ergebnisse wurden auch im Kerogenpyrolysat wiedergefunden in Form der Algaenan und oxidierten aromatischen Pyrolyseprodukte. Die Unterschiede im Kerogenpyrolysat zwischen den Sapropelen und den homogenen Intervallen ist wahrscheinlich auf die vorherrschenden verbesserten Erhaltungsbedingungen und damit die Erhaltung von labilem marinen OM in den Sapropelen

Diese Doktorarbeit demonstriert das hohe Potential der Nutzung einer Vielzahl von Biomarkern in der Rekonstruktion Klima- und Umweltbedingungen, die zur Bildung der Sapropelen im Mittelmeer haben. Diese Ergebnisse stimmen im Allgemeinen mit der Hypothese, dass der Süßwasserzufluss, hauptsächlich des Nils, zur Verstärkung der Primärproduktivität hat, was ausschlaggebend für die Ablagerung der Sapropelen war. Zusätzlich liefert diese Arbeit beispiellose, detaillierte Informationen das Ausmaß von Euxinia und Wassererstratifikation sowie der Anwesenheit mariner und kontinentaler biologischer Gemeinschaften während der Zeit eines rapiden Klimawechsels.

Dankwoord

Ik wil hier graag alle mensen bedanken die tijdens mijn tijd als AIO aan de Universiteit Utrecht het tot stand komen van dit proefschrift mede mogelijk gemaakt hebben.

Ten eerste wil ik Jan de Leeuw, Jaap Sinninghe Damste en Pim van Bergen eervol vermelden. Zij hebben mij de mogelijkheid gegeven om, komende van de mariene biologie, de organische geochemie in te duiken.

Het was een geweldige tijd samen met Pim toen hij nog mijn dagelijkse begeleider was binnen onze kleine sectie. Pim was niet alleen een enthousiaste en stimulerende wetenschapper, van wie ik veel kon leren, maar hij werd ook een vriend. Des te triester vond ik het, toen hij toch besloot naar Shell te gaan. Gelukkig was ik toen al over de helft van mijn AIO periode.

Jaap, mijn begeleider van het NIOZ (Texel) en promotor, probeerde mij altijd op het juiste pad te houden/sturen, wat mij als afgestudeerd bioloog vooral in het begin van het onderzoek een iets zekerder bestaan in het voor mij nieuwe vakgebied geochemie gaf. Na het vertrek van Pim kreeg ik van Jaap heel veel steun bij het afronden van mijn proefschrift. Vooral na het bericht van mij in oktober 2003 dat ik in verwachting was, werd het tijdschema strakker aangetrokken. Ik wil Jaap hier dan ook een groot compliment maken voor zijn steun. Hij had altijd oog voor de beperkte tijd om het promotie-onderzoek tot een goed einde te brengen. Ook heb ik van onze wetenschappelijke discussies genoten.

Jan, bedankt voor jouw opbeurende interesse in de voortgang van mijn onderzoek en het bediscussieren van resultaten.

Enkele malen per jaar ging ik mijn "biomarker"-collega's op Texel "bezoeken". Het was prettig om in de groep van de Mariene Biogeochemie en Toxicologie (MBT) te werken. Niet alleen om werkresultaten uit te wisselen, maar ook omdat ik altijd het gevoel had dat ik meer bij deze groep hoorde en niet op het organisch-geochemische eilandje "Utrecht". Wat betreft het werk bij MBT wil ik vooral Ellen, Stefan (beiden inclusief wetenschappelijke samenwerking) en Michiel ontzettend bedanken voor de hulp bij het gebruiken van de HPLC-MS en de IRM-GC-MS. Verder wil ik ook graag voor alle nodige en/of onnodige vragen en hulp in het lab Marianne en Irene bedanken. Bovendien had ik af en toe ook een logeerplekje in Den Helder nodig, als ik dinsdagavond naar de acrobatisch R'n'R training in Alkmaar moest en ik de laatste boot terug naar Texel niet meer kon pakken. [ik wil daarvoor Ellen, Rienk en Yvonne bedanken.

Zoals boven reeds beschreven, voelde ik mij soms op een onbewoond eiland in Utrecht wat betreft mijn onderzoeksonderwerp. Maar ik geniet nog steeds van de gezelligheid binnen de vakgroep geochemie. Ik wil hiervoor graag Andy, Anke, Andreas, Annet, Arnold, Caroline, Celine, Christelle, Christian, Christof, Claudette, David, Dineke, Elise, Freek, Gernot, Gert, Gert-Jan, Gijs, Guus, Helen, Imogen, Jaqueline, Jeffrey, Johan, Mariette, Martin, Parisa, Pien, Pierre, Pieter, Ralf, Rick, Rinske, Sandra, Steeve, Sanella, Thilo, Vincent en Yvonne bedanken. Mijn excuses als ik iemand ben vergeten! Philippe, bedankt voor jouw beiangstelling voor mijn onderzoek. [var wil ik bedanken voor data en medewerking. Jammer, Niels, dat je naar Canada vertrokken bent. Ik mis gewoon je dikke

knuffels. Anke & Anja, haht Dank für eure immer Hilfe, wenn ich sie brauchte!
Gert-Jan, fijn dat jouw deur altijd open stond vom het bediscussieren van resultaten und
manchen Witz! Bovendien ben ik jou, maar zeker ook Imogen, Andy en Jeffrey dankbaar
voor het corrigeren van mijn Engelse teksten.

Het lab hebben wij met TNO-NITG gedeeld. Vooral door Kathrin's aanwezigheid
was het er leuk werken. Mijn kamergenoten Dennis en Johan wil ik bedanken voor de
gezellige sfeer. Wat betreft computerproblemen kon ik altijd bij Johan om hulp vragen. Voor
het oplossen van technische problemen bij ons op het lab wil ik graag Ton en Bart bedanken.

Naast het werk trainde ik op wedstrijdniveau acrobatisch R'n'R. Acrobatisch R'n'R
heeft mij de nodige balans in en afleiding van de (niet-)vorderende wetenschap gegeven.
Voor de leuke trainingstijd tijdens mijn promotieperiode wil ik hier graag onze R'n'R groep
Razzel Dazzel noemen, met Jaqueline & Erwin, & Edwin, Mariska & Joost, Nina &
Erik, Marleen & Richard, Kirsten & Richard, Martin & Wilma en Joop & Mareike.

Verder wil ik ook mijn vrienden en familie in Nederland en Duitsland danken voor de
afleiding en hun belangstelling voor mijn promotie-onderzoek. Vor aHem danke ich Biggi
und Jana, die die Hohen und Tiefen bis zu diesem Tag gefolgt und mich unterstüzt haben.
Uta, wir haben's geschafft!

Bovenaan staan natuurlijk mijn twee mannen, Justus en Daniel.

Curriculum Vitae

Diana Menzel werd op 2 april 1968 in Woldegk geboren. Van 1974 tot 1984 bezocht ze de Polytechnischen Oberschule "Arthur Becker" in Strasburg. Van 1984 tot 1987 volgde ze een pedagogische opleiding aan de Medische Fachschule in Prenzlau. Van 1987 tot 1991 werkte ze in de kinderopvang in Strasburg. In oktober 1991 begon ze met de studie biologie aan de Rostock, waar zij in september 1994 het Vordiplom behaalde. Vervolgens legde ze zich primair toe op de mariene biologie, met stages bij het PML (Plymouth, Engeland) en de Universiteit van Amsterdam (vakgroep microbiële ecologie), en Diplomarbeit bij het IOW (Institut für Ostseeforschung, W Rostock). De studie biologie werd in april 1999 afgesloten. Per september 1999 werd zij door het IPPU bij de Universiteit Utrecht aangesteld als Assistent in Opleiding. In deze functie verrichtte ze organisch-geochemisch onderzoek aan sedimenten uit de Middellandse Zee. Na beëindiging van het dienstverband in februari 2004, werd het onderzoek afgerond, resulterend in deze dissertatie.